NASA CR-120852

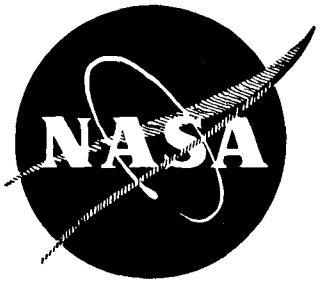

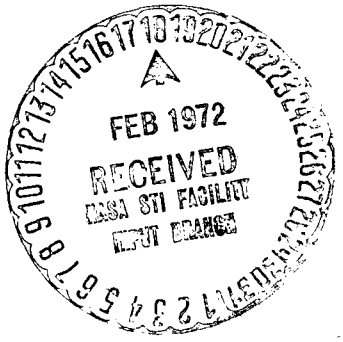

Alloyed Coatings for Dispersion Strengthened Alloys

by

F. R. Wermuth and A. R. Stetson

SOLAR DIVISION OF INTERNATIONAL HARVESTER COMPANY

SAN DIEGO, CALIFORNIA 92112

prepared for

NATIONAL AERONAUTICS AND SPACE ADMINISTRATION

NASA LEWIS RESEARCH CENTER
CONTRACT NAS 3-14312
John P. Merutka, Project Manager

NOTICE

This report was prepared as an account of government-sponsored work. Neither the United States, nor the National Aeronautics and Space Administration (NASA), nor any person acting on behalf of NASA:

A.) Makes any warranty or representation, expressed or implied, with respect to the accuracy, completeness, or usefulness of the information contained in this report, or that the use of any information, apparatus, method, or process disclosed in this report may not infringe privately owned rights; or

B.) Assumes any liabilities with respect to the use of, or for damages resulting from the use of any information, apparatus, method or process disclosed in this report.

As used above, "person acting on behalf of NASA" includes any employee or contractor of NASA, or employee of such contractor, to the extent that such employee or contractor of NASA, or employee of such contractor prepares, disseminates, or provides access to, any information pursuant to his employment or contract with NASA, or his employment with such contractor.

1. Report No.	2. Government Accession No.	3. Recipient's Catalog No.
CR-120852		

4. Title and Subtitle	5. Report Date
ALLOYED COATINGS FOR DISPERSION STRENGTHENED ALLOYS	September 1971
	6. Performing Organization Code
7. Author(s)	8. Performing Organization Report No.
F. R. Wermuth and A. R. Stetson	RDR-1686-3
	10. Work Unit No.
9. Performing Organization Name and Address	11. Contract or Grant No.
Solar Division of International Harvester Company 2200 Pacific Highway San Diego, California 92112	NAS3-14312
	13. Type of Report and Period Covered
12. Sponsoring Agency Name and Address	Contractor Report
National Aeronautics and Space Administration Washington, D.C. 20546	14. Sponsoring Agency Code

15. Supplementary Notes

Project Manager, John P. Merutka, NASA Lewis Research Center, Cleveland, Ohio

16. Abstract

Processing techniques were developed for applying several diffusion barriers to TD-Ni and TD-NiCr. Barrier coated specimens of both substrates were clad with Ni-Cr-Al and Fe-Cr-Al alloys and diffusion annealed in argon. Measurement of the aluminum distribution after annealing showed that, of the readily applicable diffusion barriers, a slurry applied tungsten barrier most effectively inhibited the diffusion of aluminum from the Ni-Cr-Al clad into the TD-alloy substrates. No barrier effectively limited interdiffusion of the Fe-Cr-Al clad with the substrates. A duplex process was then developed for applying Ni-Cr-Al coating compositions to the tungsten barrier coated substrates. A Ni-(16 to 32)Cr-3Si modifier was applied by slurry spraying and firing in vacuum, and was then aluminized by a fusion slurry process. Cyclic oxidation tests at 2300° F (1533° K) resulted in early coating failure due to inadequate edge coverage and areas of coating porosity. EMP analysis showed that oxidation had consumed 70 to 80 percent of the aluminum in the coating in less than 50 hours (1.8×10^5 sec).

17. Key Words (Suggested by Author(s))	18. Distribution Statement
Diffusion barrier Dispersion strengthened nickel alloys Nickel-chromium-aluminum coatings	Unclassified - unlimited

19. Security Classif. (of this report)	20. Security Classif. (of this page)	21. No. of Pages	22. Price*
Unclassified	Unclassified	90	$3.00

* For sale by the National Technical Information Service, Springfield, Virginia 22151

FOREWORD

This is the Final Technical Report on NASA-Lewis Research Center Contract NAS3-14312 and covers all experimental work performed on the program.

This contract was initiated between NASA-Lewis Research Center and the Solar Division of International Harvester Company for the development of coatings and diffusion barriers for the protection of TD-Ni and TD-NiCr. Technical direction was supplied by Mr. John P. Merutka, NASA-LeRC, Cleveland, Ohio. Responsible Solar personnel were Forrest R. Wermuth, principal investigator, and Alvin R. Stetson, technical program director.

Other Solar personnel contributing to the program were H. A. Cook, support engineer, coating application and equipment modification; R. Hutting, metallography; and M. E. Gulden, electron microprobe analysis.

Solar internal report number is RDR 1686-3.

ABSTRACT

Processing techniques were developed for applying several diffusion barriers to TD-Ni and TD-NiCr. Barrier coated specimens of both substrates were clad with Ni-Cr-Al and Fe-Cr-Al alloys and diffusion annealed in argon. Measurement of the aluminum distribution after annealing showed that, of the readily applicable diffusion barriers, a slurry applied tungsten barrier most effectively inhibited the diffusion of aluminum from the Ni-Cr-Al clad into the TD-alloy substrates. No barrier effectively limited interdiffusion of the Fe-Cr-Al clad with the substrates. A duplex process was then developed for applying Ni-Cr-Al coating compositions to the tungsten barrier coated substrates. A Ni-(16 to 32)Cr-3Si modifier was applied by slurry spraying and firing in vacuum, and was then aluminized by a fusion slurry process. Cyclic oxidation tests at 2300° F (1533° K) resulted in early coating failure due to inadequate edge coverage and areas of coating porosity. EMP analysis showed that oxidation had consumed 70 to 80 percent of the aluminum in the coating in less than 50 hours (1.8×10^5 sec).

CONTENTS

ILLUSTRATIONS

ILLUSTRATIONS (Cont)

ILLUSTRATIONS (Cont)

TABLES

1

SUMMARY

Previous investigations had shown that the depletion of aluminum from duplex applied chromium-aluminum coatings and nickel-chromium-aluminum coatings by oxidation and inward diffusion was a limiting factor in the protective life of the coatings. The basic objective of this program was to increase coating life by limiting the diffusion of aluminum from the coating into the substrate. To achieve this goal, the program was divided into two basic tasks: first, the development and evaluation of several diffusion barriers; and second, the development and evaluation of coating systems consisting of the best diffusion barrier and various Ni-Cr-Al coating compositions.

In the first task, application processes were developed for applying nine different diffusion barriers to TD-Ni and TD-NiCr. The barriers were evaluated by measuring their relative effectiveness in limiting aluminum diffusion from Ni-Cr-Al and Fe-Cr-Al clads into the TD-alloy substrates during a high-temperature anneal. With the Ni-Cr-Al clad, tungsten foil was the most effective barrier. However, a slurry applied tungsten barrier was selected for further use because it was readily applicable, while the tungsten foil was not. No barrier was effective with the Fe-Cr-Al clad.

In the second task, a fusion slurry process was developed for applying Ni-(16 to 32)Cr-3Si modifiers to both substrates over the slurry tungsten barrier. A fusion slurry process was then used to aluminize the modifiers, resulting in a final coating composition (excluding the tungsten barrier) of Ni-(14 to 30)Cr-(5 to 8)Al-3Si.

Coated tensile specimens were tested in cyclic oxidation at 2300° F (1533° K). Coating failure had occurred on all specimens within 44 hours (1.4×10^5 sec). Analysis of the specimens after test indicated that the failures had occurred prematurely because of thin coating on the edges and localized areas of porosity. Inward diffusion of aluminum had been limited, but oxidation had consumed most of the original aluminum. Tensile tests at RT and 2000° F showed that the coatings had slightly reduced room temperature ductility, but, in all other respects, coated specimens were equal to or better than uncoated specimens.

The principal conclusions were as follows:

- Thin edge coverage and porosity limited the 2300° F (1533° K) cyclic oxidation life of the coatings to 44 hours (1.4×10^5 sec) or less.

- Rapid consumption of the aluminum by oxidation indicated that the Ni-Cr-Al coatings were less oxidation resistant than a previous investigation had shown.

- The slurry applied tungsten barrier showed the potential to limit aluminum diffusion from coating to substrate.

- Within the scope of this investigation no diffusion barrier was found that could effectively retard the diffusion of aluminum from an Fe-Cr-Al clad into the TD-alloy substrate.

2

INTRODUCTION

Above 1900° F (1313° K) the dispersion-strengthened alloys, TD-Ni and TD-NiCr, are superior to other superalloys in creep resistance, stress rupture and thermal stability. They are thus candidate materials for use in gas turbines and other typical superalloy applications. However, both alloys oxidize rapidly above 1900° F (1313° K) in the oxidation-erosion environments which are encountered in most of the potential turbomachinery or aerospace applications.

A considerable amount of work has been performed in developing coatings capable of protecting these alloys in oxidizing environments (Refs. 1 through 8). Two coatings systems have been found equally effective: a duplex Cr-Al coating, in which a nickel aluminide (usually β-NiAl) is formed, and a duplex-applied Ni-Cr-Al gamma solid-solution coating. In both cases, the formation of an Al_2O_3 scale is the primary mechanism of protection.

The initiation of failure in both coatings is associated with the depletion of aluminum from the coating. The aluminum is lost by oxide formation and by diffusion into the substrate. Below a certain aluminum concentration (~0.1 to 0.3 wt % at 2200° F), the Al_2O_3 scale loses its self-healing ability. Cracks in the oxide scale caused by thermal cycling are no longer repaired by formation of additional Al_2O_3. Instead, Cr_2O_3 and/or NiO begin to form, and the rate of oxidation increases greatly.

An increase in the life of the aluminum "reservoir" would result directly in an increase in coating life. Simply increasing the quantity of aluminum initially present can extend coating life only to a certain point. Beyond this point, developing a means for slowing aluminum diffusion into the substrate is the most direct way to significantly improve the protective life of state-of-the-art coatings.

The goal of this program was to improve coating life by limiting the diffusion of aluminum from the coating into the substrate. To achieve this goal, the program was divided into two technical tasks. In the first task, processing techniques were developed for applying several diffusion barriers to the TD-alloy substrates. The barriers investigated included an oxide (Al_2O_3), carbides ($Cr_{23}C_6$, TaC), refractory metals (Cr, Ta, Mo, W), an intermetallic (YNi_4), and a combination oxide-refractory metal (Al_2O_3 + Ta). The application processes used were slurry techniques, a pack process, fused salt plating, and cladding. For evalution, barrier coated substrates

were diffusion bonded to Ni-22Cr-3.5Al and Fe-22Cr-5.5Al-0.5Co clads and diffusion annealed in argon for 100 hours (3.6×10^5 sec) at 2300° F (1533° K). Metallographic and electron microprobe (EMP) analyses of as-bonded and annealed specimens were used to determine which barrier was most effective in limiting aluminum diffusion.

In the second task, processing techniques were developed for applying Ni-(15 to 30)Cr-(5 to 8)Al coatings to both substrates over the best diffusion barrier. Both vacuum sintering and vacuum fusion techniques were investigated for applying a Ni-(16 to 32)Cr modifier. The modifier was then aluminized by a fusion slurry process to develop the desired coating composition. The duplex coatings were applied to tensile specimens of both substrate alloys. Cyclic oxidation tests at 2300° F (1533° K) and tensile tests at room temperature and 2000° F (1366° K) were performed on coated and uncoated specimens to determine the best coating.

3

EXPERIMENTAL PROGRAM

The experimental work described herein was aimed at developing a composite protective coating consisting of two distinct layers, a highly oxidation-resistant outer layer and a diffusion inhibiting inner layer. Approximately the first half of the program was devoted to diffusion barrier development and evaluation and the second half to coating development and evaluation.

3.1 MATERIALS

The substrate materials used in the program consisted of sheet stock of TD-Ni (Ni-2ThO_2) and TD-NiCr (Ni-20Cr-2ThO_2). The chemical compositions and mechanical properties of these materials are given in Table I. The chemical compositions of the principal materials used in the diffusion barriers and coatings are given in Table II.

3.2 DIFFUSION BARRIER DEVELOPMENT

Previous coating development on TD-Ni and TD-NiCr (Refs. 1 through 8) had yielded the following results: the best coatings were based on an Al_2O_3 protective scale; failure of these coatings was associated with aluminum depletion; and aluminum was depleted from the coatings by oxide formation and inward diffusion. It was concluded that maintaining the aluminum concentration in the coatings for a longer time was the best approach to increase coating life. Two alternatives were possible to extend the life of the aluminum reservoir: increasing the amount of aluminum in the coating, or inhibiting inward diffusion of aluminum. Previous work had shown, however, that the amount of aluminum cannot be increased much without forming extensive diffusional (Kirkendall) voids which cause massive coating spalling and premature failure. The logical alternative, then, was to prevent or inhibit the inward diffusion of aluminum from the coating into the substrate by the use of a barrier. The basic approach of the program was to explore this alternative as a means for increasing coating life. Primary emphasis was therefore placed on the development of a diffusion barrier which was capable of limiting aluminum diffusion and could be reproducibly applied to the substrates. In this section, the diffusion barrier concepts are discussed and the development of the application processes is described.

TABLE I

COMPOSITION AND PROPERTIES OF PROGRAM ALLOYS

Alloy	Heat No.	Thickness (inch)	Composition (Wt %) C	N	S	Cu	Ti	Co	Fe	Cr	ThO_2	Ni
TD-Ni	1218*	0.033	0.0015	---	0.0012	<0.001	<0.001	<0.01	<0.01	<0.01	2.5	Bal.
TD-Ni	3088**	0.060	0.0108	---	0.0025	0.005	0.001	0.080	0.010	0.004	2.41	Bal.
TD-NiCr	2697-A*	0.040	0.0241	0.004	0.0061	---	---	---	---	19.38	1.9	Bal.
TD-NiCr	3266**	0.060	0.0102	---	0.0042	0.002	---	0.030	---	19.96	1.96	Bal.

Transverse Mechanical Properties

Alloy	Heat No.	Test Temp. (° F)	U.T.S. (ksi)	Y.S. (ksi)	Elong. (% in 1")	2000° F Stress Rupture Stress (ksi)	Life (hrs)	Elong. (% in 1")	105° Bend Radius
TD-Ni	1218*	RT	68.1	51.4	13.5				1T
		2000	15.1	13.9	3.0	5.5	>20	3.2	
TD-Ni	3088**	RT	62.4	46.5	19.3				1T
		2000	15.6	15.5	4.1	5.5	>20	4.4	
TD-NiCr	2697-A*	RT	127.7	85.9	19.5				1.5T
		2000	16.4	15.9	3.6	4.0	>20	10.8	
TD-NiCr	3266**	RT	118.9	76.4	27.5				2T
		2000	18.8	17.6	7.5	5.5	>20	7.6	

* DuPont material used in diffusion barrier development.

** Fansteel material used in the remainder of the program.

TABLE II

MATERIALS USED IN DIFFUSION BARRIERS AND COATINGS - SOURCE AND CHEMICAL ANALYSIS

MATERIAL AND SOURCE	CHEMICAL ANALYSIS (w/o)													
CHROMIUM	Cr	Al	Fe	C	N	P	Si	S						
Union Carbide Corporation	99.6	.03	.23	.01	.04	.006	.01	.03						
NICKEL	Ni	Co	C	Si	S	Fe								
Glidden-Durkee	99.47	.15	.048	.30	.006	.03								
SILICON	Si	Ca	Al	Fe										
Foote Mineral	98.6	.03	.33	.64										
YTTRIUM	Eu	Tb	Dy	Y	Sm	Si	Fe	Mg	Ca	Al	La	Lu	Gd	Nd
Research Chemicals	-	<.01	<.01	Bal	<.01	<.01	<.01	<.01	<.02	<.01	-	<.002	.02	-
MATERIAL AND SOURCE	CHEMICAL ANALYSIS (ppm)													
	Al	Ca	Si	Fe	Cr	Ni	Cu	W	Mn	Mg	Sn	C	O	Mo
TUNGSTEN	6	15	9	9	4	6	3	Bal	6	3	6	10	375	88
MOLYBDENUM	8	15	13	47	8	7	6	123	10	10	12	12	1456	Bal
General Electric														
TANTALUM	Al	C	Cb	Cu	Cr	Fe	H	Mg	Mn	N	Ni	O	Sn	Zr
Wah Chang Albany Corp.	<20	<10	310	<10	<10	<20	6	<5	<10	27	<20	49	<10	<50

3.2.1 Diffusion Barrier Concepts

In selecting candidate materials for evaluation as a diffusion barrier, there were two primary requirements: first, a low diffusion rate of aluminum in the barrier; and second, a low interdiffusion rate of barrier/substrate and barrier/coating. The diffusion barriers evaluated under this program were selected because of their potential for meeting these requirements. The following is a more detailed discussion of the rationale for selection of the individual diffusion barriers:

- Yttrium-Nickel (YNi_4). Yttrium has negligible solid solubility for nickel, aluminum, and chromium (forming a series of intermetallic compounds) and, because of its large atomic diameter, is relatively immobile. It has the potential, therefore, to significantly limit inward diffusion of coating elements.

- Chromium (Cr). Chromium was selected primarily as a baseline barrier. Its extensive use as part of the duplex Cr-Al coating system qualifies it as such. For other diffusion barriers to be considered effective, they should at least surpass chromium in inhibiting diffusion, particularly in view of the fact that chromium improves oxidation resistance while most of the other barriers do not.

- Carbides (TaC, $Cr_{23}C_6$). Selection of the carbides was based on experimental evidence obtained at Solar on Contract NAS3-9401 (Ref. 9). It was observed that a thin, continuous layer of chromium carbide formed between an aluminide coating and the X-40 alloy substrate and that the carbide was effective in inhibiting aluminum diffusion into the substrate. Tantalum carbide is another very stable carbide and should be a similarly effective diffusion barrier.

- Aluminum Oxide (Al_2O_3). Diffusion rates of the coating and substrate elements in aluminum oxide are very low and the mobility of the oxide is also low. It is potentially an excellent diffusion barrier, either as a continuous layer or as a non-continuous layer which in effect reduces the interface area.

- Refractory Metals (Ta, Mo, W). Tantalum, molybdenum, and tungsten are refractory metals with high melting points and relatively low interdiffusion rates with nickel, chromium, and aluminum. They thus warrant evaluation as diffusion barrier materials.

3.2.2 Application Process Development

In developing the application processes for the diffusion barriers, the goal was to deposit a uniform and dense barrier layer 0.0005 to 0.001 inch (1.3×10^{-5} to 2.5×10^{-5} m) thick. Test specimens used in the application process development were 1/2 x 1/2 inch (0.013 x 0.013 m) or 1/2 x 3/4 inch (0.013 x 0.019 m) coupons of TD-Ni and TD-NiCr.

Yttrium-Nickel (YNi_4)

The application process for yttrium-nickel was designed to form a uniform YNi_4 surface layer by applying YNi_2 in slurry form and reacting it with the substrate in a fusion firing.

Using pure yttrium (99.0+%) and electrolytic nickel (99.9%), the alloy YNi_2 (60Ni-40Y by weight) was inert gas arc melted. A total of 0.20 kg was melted, two 0.05 kg buttons and one 0.10 kg button. A slurry was prepared from the YNi_2 ingots by crushing them in liquid nitrogen, then placing the resulting coarse powder in an ethyl cellulose-xylene vehicle and ball milling for 4 hours (1.4×10^4 sec). The slurry was sprayed on TD-Ni and TD-NiCr specimens, with the dry bisque weights ranging from 7 to 40 mg/cm^2 (0.07 to 0.40 kg/m^2), and the specimens were fired in vacuum ($<10^{-4}$ Torr, <0.013 N/m^2) at 2300°F (1533°K) for 10 minutes (600 sec). On each specimen, a significant amount of bisque did not melt and was removed by wire brushing, leaving non-uniform deposits of zero to 30 mg/cm^2 (0.00 to 0.30 kg/m^2) with unacceptably rough surfaces.

It was felt that the use of a flux might result in more complete melting and thus provide a controlled deposit and a smooth surface; therefore, two preliminary firing runs were made in argon at 2300°F (1533°K) using a $67CaF_2$-33LiF (m.p. = 2000°F = 1366°K) flux overcoat. The barriers applied in these runs were acceptably smooth and uniform on a macroscopic scale, but, on a microscopic scale, there was incomplete bonding to the substrate and some porosity, primarily on TD-NiCr. It was suspected that the problems were due to inclusion of flux in the barrier. A third run with a flux overcoat, fired in argon at 2300°F (1533°K) for 30 minutes (1.8×10^3 sec), confirmed this suspicion. An excessive amount of flux, 3 to 5 mg/cm^2 (0.3 to 0.5 kg/m^2), remained after firing (this is equivalent to 25 to 40 volume percent of the diffusion barrier). The flux method was then abandoned pending the results of further vacuum runs.

A new slurry with a finer YNi_2 particle size (milled 16 hours (5.8×10^4 sec)) was applied to specimens (8 to 11 mg/cm^2 (0.08 to 0.11 kg/m^2) dry bisque weight) and fired at $<10^{-4}$ Torr (<0.013 N/m^2) as follows: 2400°F (1589°K) for 10 minutes (600 sec) plus 2000°F (1366°K) for 1 hour (3.6×10^3 sec). After wire brushing, an

acceptably uniform and dense barrier of 6 to 10 mg/cm^2 (0.06 to 0.10 kg/m^2) remained (Fig. 1). It is likely that the higher firing temperature, rather than finer particle size, made the difference. The presence of Y_2O_3 probably raised the flow point of the alloy to near 2400°F (1589°K), well above the theoretical melting point of YNi_2, 2040°F (1389°K). In any case, the 2400°F (1589°K) vacuum firing process was selected for application of the YNi_4 diffusion barrier.

Chromium (Cr)

Past experience at Solar and elsewhere had shown the pack process to be a reliable method for depositing chromium. Therefore, atmospheric pressure and vacuum pack processes were investigated for chromizing the TD-alloy substrates.

Two standard chromizing pack runs (Solar pack H2-56B) were made in argon at 2000°F (1366°K) for 64 hours (2.3 x 10^5 sec), in each case depositing approximately 20 mg/cm^2 (0.20 kg/m^2) on TD-Ni and 16 mg/cm^2 (0.16 kg/m^2) on TD-NiCr. The H2-56B pack consists of chromium, Al_2O_3, and halide activator powders. As can be seen in Figure 2, the deposit was smooth, uniform and non-porous. The barely visible outer layer is believed to be alpha-chromium.

An attempt was made to chromize the TD-Ni and TD-NiCr using a pure chromium pack (-100 mesh) in vacuum. Sixteen-hour firings at $<10^{-4}$ Torr (0.013 N/m^2) were made at 2100 and 2000°F (1422 and 1366°K) using an unsealed columbium retort to contain the chromium powder and specimens. While the amount of chromium deposited was in the acceptable range, 10 to 20 mg/cm^2 (0.10 to 0.20 kg/m^2), there was significant pack sintering in each case. Based on the results of a previous investigation (Ref. 2), coarser particle size would probably have eliminated the sintering problem. However, the lack of coarse powder on hand and the success of the atmospheric pack dictated that the standard pack process be selected to apply the chromium barrier.

Tantalum (Ta)

The fused salt plating technique was used to apply tantalum to TD-Ni and TD-NiCr specimens. The fused salt cell was operated under a high purity argon atmosphere. A 3.5-inch (0.038 m) diameter by 15-inch (0.38 m) high cylindrical nickel crucible was used to contain both the salt bath and a 3-inch (0.076 m) diameter by 10-inch (0.25 m) high cylindrical tantalum anode.

The composition of the salt bath used was as follows: 0.413 kg of LiF, 1.024 kg of KF, 0.146 kg of NaF, and 0.237 kg of K_2TaF_7. All salts were vacuum dried at 250°F (394°K) for about 16 hours (5.8 x 10^4 sec) before being used. All

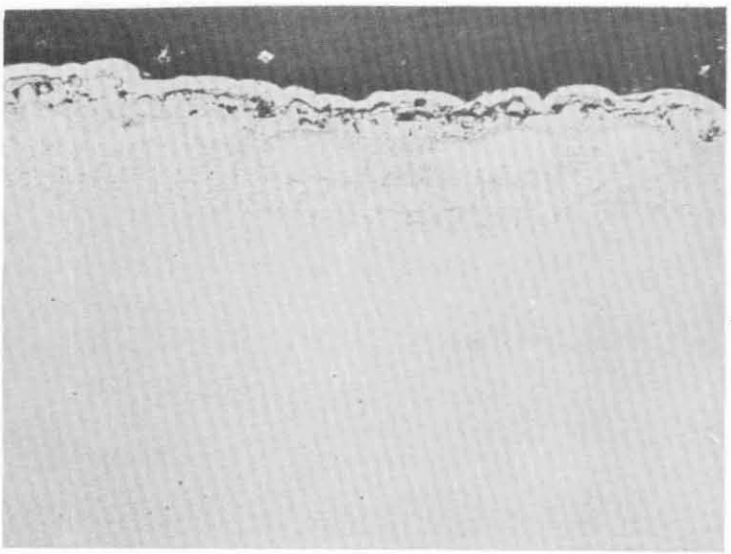

Ni Plating

Yttrium-Rich Diffusion Barrier

TD-Ni Substrate

Barrier Deposit: 9 mg/cm^2

Unetched

Magnification: 250X

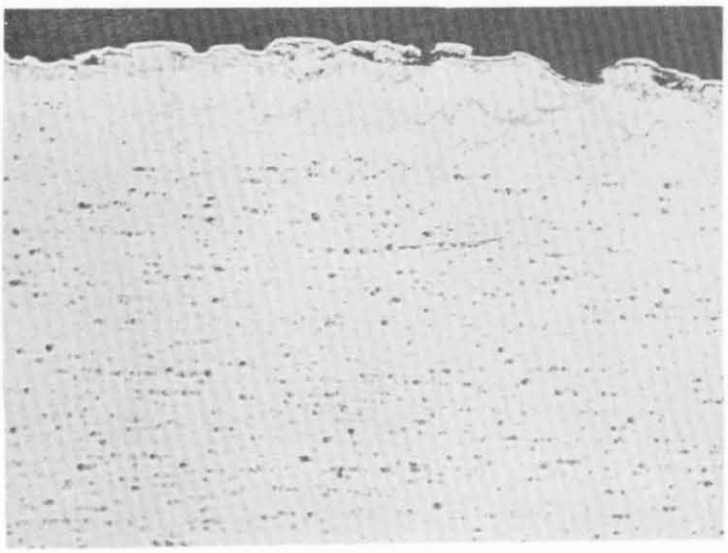

Ni Plating

Yttrium-Rich Diffusion Barrier

TD-NiCr Substrate
(with dispersed Cr_2O_3 particles)

Barrier Deposit: 7 mg/cm^2

Unetched

FIGURE 1. YNi_4 DIFFUSION BARRIER ON TD-Ni AND TD-NiCr; Fired in Vacuum for 10 Minutes at 2400°F Plus 1 Hour at 2000°F

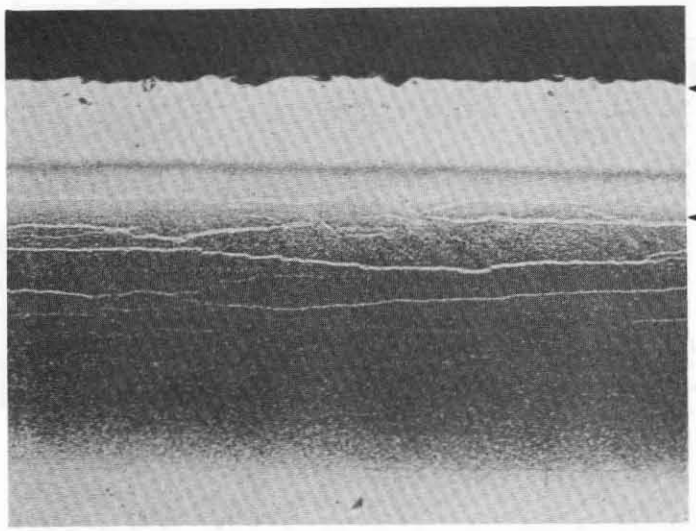

Probable α-Cr Layer

Cr-Rich TD-Ni Substrate

(Etching varies with Cr concentration; etch lines are due to modification of substructure)

Barrier Deposit: 21 mg/cm^2

Etchant: Oxalic Acid-Electrolytic

Magnification: 250X

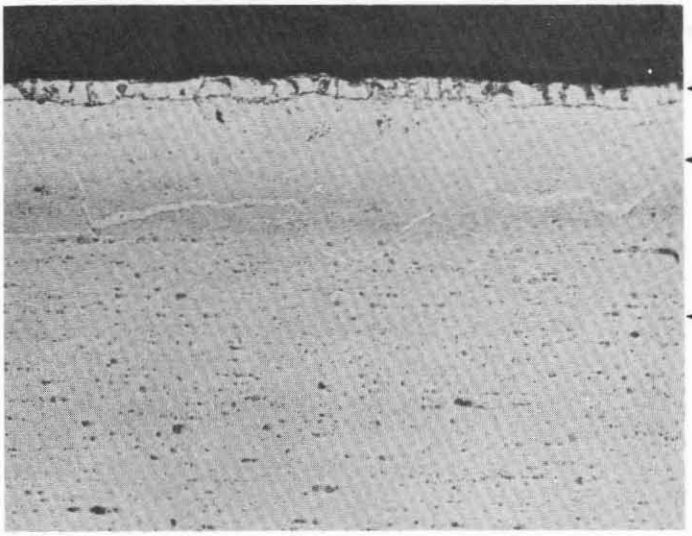

Probable α-Cr Layer

Cr-Rich TD-NiCr Substrate

Unaffected Substrate
(with dispersed Cr_2O_3 particles)

Barrier Deposit: 16 mg/cm^2

Etchant: Oxalic Acid-Electrolytic

FIGURE 2. Cr DIFFUSION BARRIER ON TD-Ni AND TD-NiCr; Solar Standard Atmospheric Pack H2-56B Fired at 2000°F for 64 Hours

salts except the K_2TaF_7 were placed in the cell, purged with argon, and heated to 1400 to 1500°F (1033 to 1089°K) for 16 hours (5.8×10^4 sec). The K_2TaF_7 was then added.

Test plating runs were made with copper samples at a temperature of 1480°F (1077°K) and a current density of 0.015 amp/cm^2 (150 amp/m^2). Plating runs were continued until a defect-free tantalum plate was obtained. The program evaluation specimens were then plated four at a time while held by support wires through 3/32-inch (0.0024 m) diameter holes in the specimen corners. The specimens were first brought to thermal equilibrium with the bath at 1480°F (1077°K) and "rinsed" by slow vertical movement in and out of the bath. The power was then turned on. The plating cycle consisted of 1 hour (3.6×10^3 sec) at the 1480°F (1077°K) operating temperature using a current density of approximately 0.05 amp/cm^2 (500 amp/m^2). The amount of tantalum deposited ranged from 16 mg/cm^2 (0.16 kg/m^2) to 30 mg/cm^2 (0.30 kg/m^2).

The tantalum diffusion barrier can be seen in Figure 3. It was dense, uniform, and consisted of two distinct layers. It is likely that the outer (darker) layer was tantalum, while the inner layer was a nickel-tantalum intermetallic compound.

Chromium Carbide ($Cr_{23}C_6$)

Initially, solid-state carburization using vacuum pack techniques was investigated. TD-Ni and TD-NiCr specimens which had previously been atmospheric pack chromized were fired at $<10^{-4}$ Torr (0.013 N/m^2) in a carburizing pack consisting of graphite powder in a graphite retort for 16 hours (5.8×10^4 sec) at 2100°F (1422°K), 2175°F (1464°K), and 2300°F (1533°K). Specimens fired at 2300°F (1533°K) exhibited surface degradation, more extreme on TD-Ni than on TD-NiCr. This degradation can probably be attributed to a low melting eutectic in the Ni-Cr-C system. Specimens fired at 2175°F (1464°K) and 2100°F (1422°K) exhibited lesser degrees of surface roughness, but even the 2100°F (1422°K) specimens were found to have unacceptable surface roughness and porosity.

Because solid-state carburization in vacuum pack was found unsatisfactory, a gas carburization method was developed for use on chromized TD-Ni and TD-NiCr. The specimens used had been previously chromized with Solar atmospheric pack H2-56B, described above. The gas carburization took place in a welded Inconel retort using an argon-methane gas mixture flowing at about 16 cfh (1.2×10^{-4} m^3/sec). The first run was made at 2000°F (1366°K) for 30 minutes using a mixture of 80Ar-20CH_4 (by volume). An excessive amount of carbon, 2 to 3 mg/cm^2 (0.02 to 0.03 kg/m^2) was deposited on the surface of the specimens.

A second run was made at 1800°F (1255°K) for 1 hour (3.6×10^3 sec) using 94Ar-6CH_4, with a negligible amount of carbon deposited. A third run, made at

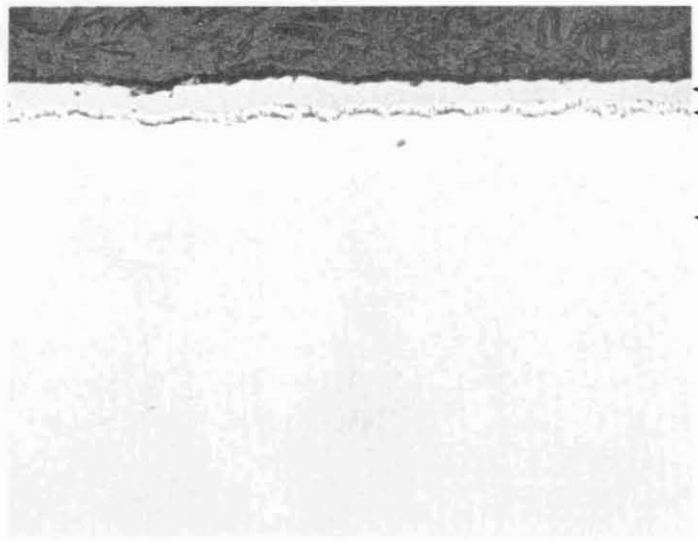

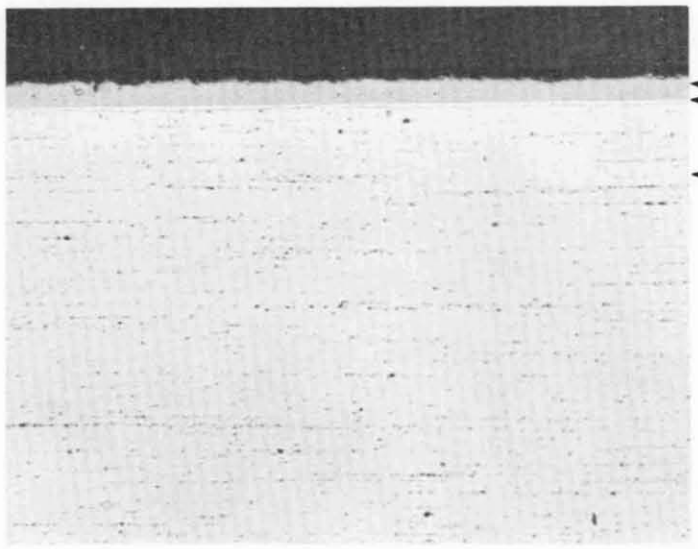

FIGURE 3. Ta DIFFUSION BARRIER ON TD-Ni AND TD-NiCr; Applied by Fused Salt Plating

1900°F (1311°K) for 1 hour (3.6×10^3 sec) using 94Ar-6CH_4, resulted in a carbon pickup of 0.1 to 0.3 mg/cm^2 (0.001 to 0.003 kg/m^2). This is equivalent to a 0.0001 to 0.0003 inch (2.5×10^{-6} to 7.6×10^{-6} m) continuous layer of $Cr_{23}C_6$. Metallographic examination revealed a somewhat dispersed, semi-continuous carbide phase within what is probably an alpha chromium layer on TD-Ni, and a continuous carbide phase on the surface of this same layer on TD-NiCr (Fig. 4). Microhardness traverses showed that carbon penetration was limited to about 0.0005 inch (1.26×10^{-5} m). The 1900°F (1311°K), 1 hour (3.6×10^3 sec) gas carburization yielded the desired amount of chromium carbide and was selected to prepare the evaluation specimens.

Tantalum Carbide (TaC)

The approach taken in developing the TaC barrier was the same as for the $Cr_{23}C_6$ barrier, i.e., investigating carburization by both pack and gas techniques. Because the tantalum anode material for fused salt plating was not received early in the program, 0.005-inch (1.3×10^{-4} m) tantalum foil specimens were used for preliminary carburization studies.

To determine if tantalum could be pack carburized, the tantalum foil specimens were run in the 2300°F (1533°K) carburizing pack described above. Chemical analysis showed that the carbon content went from 0.0017 weight percent before firing to 0.056 weight percent after firing. Considering that the actual thickness of tantalum to be carburized would be only 0.0005 to 0.001 inch (1.26×10^{-5} to 2.5×10^{-5} m) and that the firing temperature could be raised to 2400°F (1529°K), it appeared that the pack method could be used for carburizing tantalum coated specimens.

Tantalum foil specimens were also run in the preliminary gas carburization cycles along with the chromized specimens. There was no measurable weight gain at 1800°F (1255°K) or 1900°F (1311°K), but the 2000°F (1366°K) cycle resulted in a carbon deposit of 0.2 to 0.5 mg/cm^2 (0.002 to 0.005 kg/m^2). Based on these tests, it appeared that sufficient TaC could be formed at 2000°F (1366°K) in 1 to 3 hours (3.6×10^3 to 1.1×10^4 sec) using the gas method. This offered an advantage over pack carburization which, as shown by previous testing, required higher temperature, 2300 to 2400°F (1533 to 1580°K), and longer times (about 16 hours (5.8×10^4 sec)).

When tantalum plated TD-Ni and TD-NiCr specimens became available, two gas carburizing runs were made, both at 1950 to 2000°F (1339 to 1366°K) for 1 hour (3.6×10^3 sec) in 94Ar-6CH_4. The amount of carbon deposited ranged from about 0.2 to 0.6 mg/cm^2 (0.002 to 0.006 kg/m^2). The barrier, shown in Figure 5, consisted of a very thin carbide layer on the surface and probably an additional 3 atomic percent carbon dissolved in the tantalum (Ref. 10). This barrier configuration appeared to be acceptable, and the 2000°F (1366°K) gas carburization cycle was selected for preparation of the evaluation specimens.

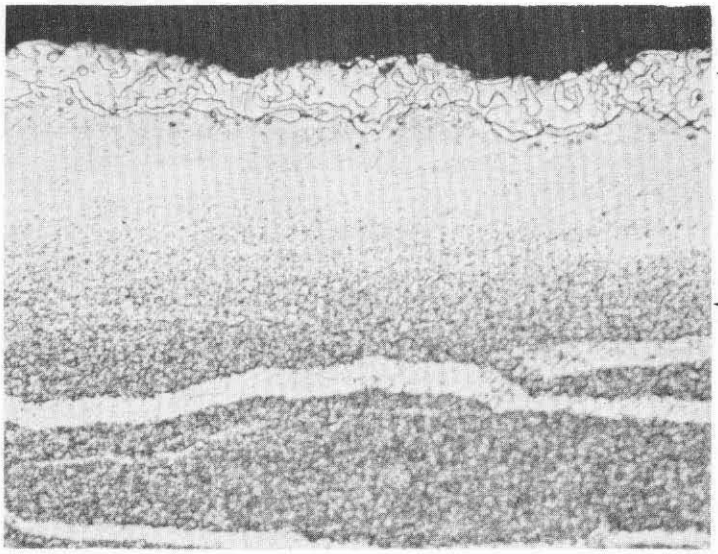

α-Cr Layer With Cr_xC_y Dispersed Phase

Cr-Rich TD-Ni Substrate

C Deposit: 0.2 mg/cm^2

Etchant: HCl - Electrolytic

Magnification: 1000X

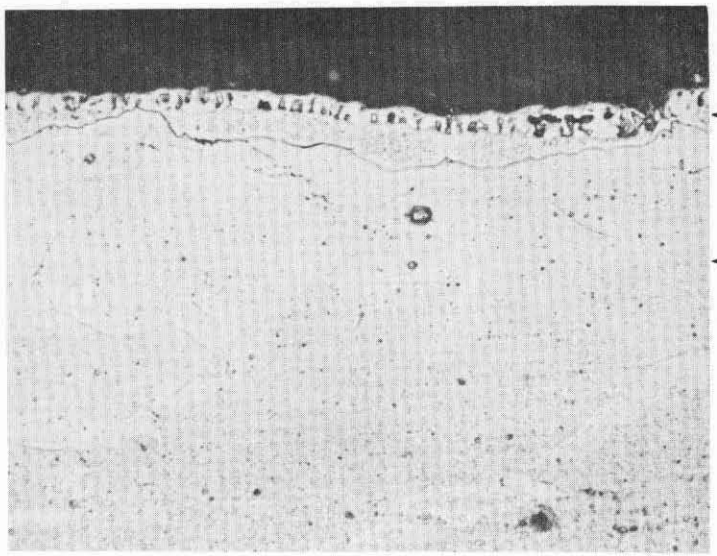

α-Cr With Cr_xC_y Dispersed Phase

Cr-Rich TD-NiCr Substrate

C Deposit: 0.3 mg/cm^2

Etchant: Oxalic Acid - Electrolytic

FIGURE 4. Cr-C DIFFUSION BARRIER ON TD-Ni AND TD-NiCr; Solar H2-56B Pack Chromized Plus Gas Carburized in 94Ar-6CH_4 for 1 Hour at 1900°F

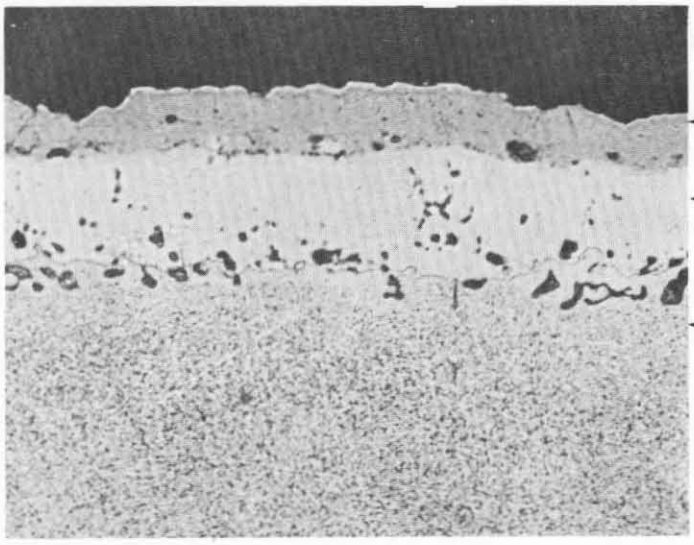

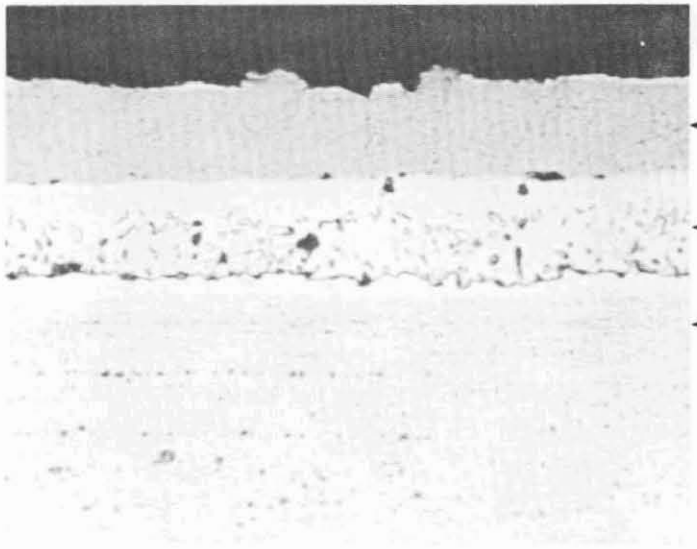

FIGURE 5. TaC DIFFUSION BARRIER ON TD-Ni AND TD-NiCr; Fused Salt Ta Plated Plus Gas Carburized in 94Ar-6CH_4 for 1 Hour at 2000°F

Aluminum Oxide (Al_2O_3)

Continuous Al_2O_3. In applying a continuous aluminum layer for subsequent oxidation, two standard slurry techniques were used. An S8100 aluminizing slurry (essentially aluminum and flux) was sprayed and fired in argon at 1250°F (950°K) for 5 minutes (300 sec), resulting in a uniform deposit of 0.6 to 0.9 mg/cm^2 (0.006 to 0.009 kg/m^2) of aluminum. Two firings were made using an S13-53C slurry (vapor transport slurry consisting mainly of iron and aluminum). The first, with a 0.007-inch (1.8 x 10^{-4} m) bisque fired at 1950°F (1339°K) for 2-1/2 hours (9 x 10^3 sec), resulted in far too heavy a deposit, 5 to 7 mg/cm^2 (0.05 to 0.07 kg/m^2); the second, using a 0.001-inch (2.5 x 10^{-5} m) bisque and fired at 1940°F (1339°K) for 1 hour resulted in the undesirable codeposition of a significant amount of iron. The S8100 slurry was thus chosen for pure aluminum deposition.

Two controlled oxidation runs were then made using aluminized TD-Ni and TD-NiCr specimens: 1800°F (1255°K) for 2 hours (7.2 x 10^3 sec) and 1900°F (1311°K) for 2 hours (7.2 x 10^3 sec), both at a pressure of 10^{-4} Torr (0.013 N/m^2) or less. The amount of oxide present could not be detected by normal metallography (Fig. 6). It should be noted that the variation in thickness of the aluminide layer was due to processing problems encountered in applying an extremely small quantity of aluminum. An unsuccessful attempt was made to determine surface oxide thickness by examination of a surface replica on the electron microscope. The 1900°F (1311°K) oxidation cycle was selected to ensure that the oxide formed would definitely be alpha-Al_2O_3, which becomes stable above approximately 1800°F (1255°K).

Discontinuous Al_2O_3. A nickel coated Al_2O_3 powder was initially proposed for sintering onto the surface of TD-Ni and TD-NiCr to provide a discontinuous Al_2O_3 diffusion barrier. However, because a source for nickel coated Al_2O_3 could not be located, a mixture of Al_2O_3 and nickel powder was substituted. Several mixtures of -325 mesh nickel and Al_2O_3 powders, with Ni/Al_2O_3 weight ratios of 60/40, 80/20, and 90/10, were suspended in an ethyl cellulose-xylene vehicle, sprayed on TD-Ni and TD-NiCr specimens and fired in vacuum for 16 hours (5.8 x 10^4 sec) at 2200 to 2300°F (1477 to 1533°K). The 60/40 barrier failed to adhere to the substrate at all. There was apparent adherence of about half of the 80/20 and 90/10 barriers, but subsequent microscopic examination revealed poor bonding to the substrate and extensive porosity.

Two slurries were then made up with compositions of 88Ni-10Al_2O_3-2Si and 78Ni-20Al_2O_3-2Si, both in an ethyl cellulose-xylene vehicle. The silicon was added to promote liquid phase sintering. All specimens were fired in vacuum as follows: 2400°F (1589°K) for 10 minutes (600 sec), plus 2000°F (1366°K) for 1 hour (3.6 x 10^3 sec). The dry bisque weights ranged from 9 to 16 mg/cm^2 (0.09 to 0.17 kg/m^2). After firing, the 20 weight percent Al_2O_3 specimens lost about 30 to 50 percent of the

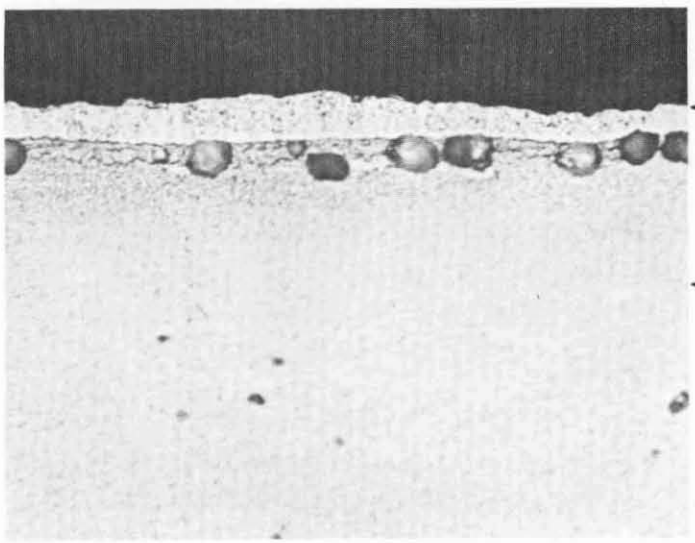

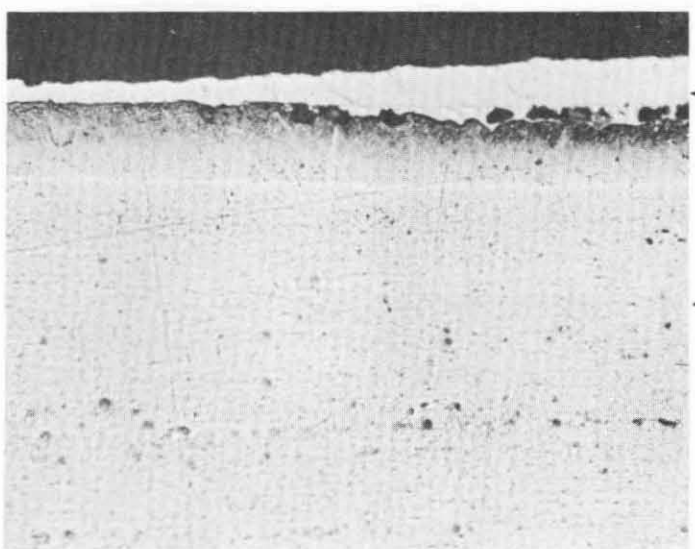

FIGURE 6. CONTINUOUS Al_2O_3 DIFFUSION BARRIER ON TD-Ni AND TD-NiCr; Solar S8100 Fusion Slurry Aluminized Plus Controlled Oxidation in 10^{-4} Torr Air at 1900° F for 1 Hour

barrier when wire brushed, indicating incomplete sintering. The 10 weight percent Al_2O_3 composition adhered better but was not uniform across the surface. A subsequent firing at 2200° F (1477° K) for 4 hours (1.4×10^4 sec) resulted in reasonably good adherence, uniformity, and barrier density (Fig. 7). Very few Al_2O_3 particles were observed in the barrier after firing. However, it is possible that particles which had been present after firing were removed during polishing. Further development work on this barrier was not considered practical; therefore the 10 percent Al_2O_3 slurry, fired at 2200° F (1477° K) for 4 hours (1.4×10^4 sec), was selected for evaluation.

Aluminum Oxide Plus Tantalum (Al_2O_3 + Ta)

This diffusion barrier was a combination of two barriers previously developed. The discontinuous Al_2O_3 was first applied to TD-Ni and TD-NiCr specimens as described above. The fired Ni-Al_2O_3-Si deposit ranged from 8 to 12 mg/cm^2 (0.27 to 0.12 kg/m^2). This coating was then plated with tantalum to a level of 27 to 45 mg/cm^2 (0.27 to 0.45 kg/m^2). The diffusion barrier is shown in Figure 8. Some of the previously vacant areas in the discontinuous Al_2O_3 barrier were now filled. Apparently, these areas had been voids rather than Al_2O_3 particles, indicating that the Al_2O_3 density in the original discontinuous oxide barrier was low.

Tungsten (W)

Tungsten was first evaluated in the form of diffusion bonded foil. Its excellent performance (Sec. 3.3) necessitated the development of a practical slurry application process.

Eleven different slurries (see Table III for compositions) were applied to both TD-Ni and TD-NiCr substrates. Nickel was used as the primary additive because it has been found useful in enhancing the sintering of tungsten and is compatible with the nickel-base substrate and coating. Titanium and silicon were used to form eutectics with nickel and thus promote liquid phase sintering. Chromium was added after noting that the W-1 through W-3 barriers all adhered better to the TD-NiCr than to the TD-Ni. W-7, W-8 and W-11 were prepared so that the effect of higher nickel additive levels (up to 25 volume percent) on diffusion barrier effectiveness could be subsequently evaluated.

The application process used for W-1 through W-8, W-10 and W-11 was as follows: elemental powders were mixed in an ethyl cellulose-xylene vehicle and ball milled for 8 hours. The slurry was sprayed on both substrates with a bisque weight of 40 to 50 mg/cm^2 (0.40 to 0.59 kg/m^2) and fired at 2300° F (1533° K) for 3 hours (1.1×10^4 sec) at $\leq 10^{-4}$ Torr (<0.013 N/m^2). In general, the barriers adhered to the TD-NiCr substrate better than to the TD-Ni substrate. The 100W barrier (W-1)

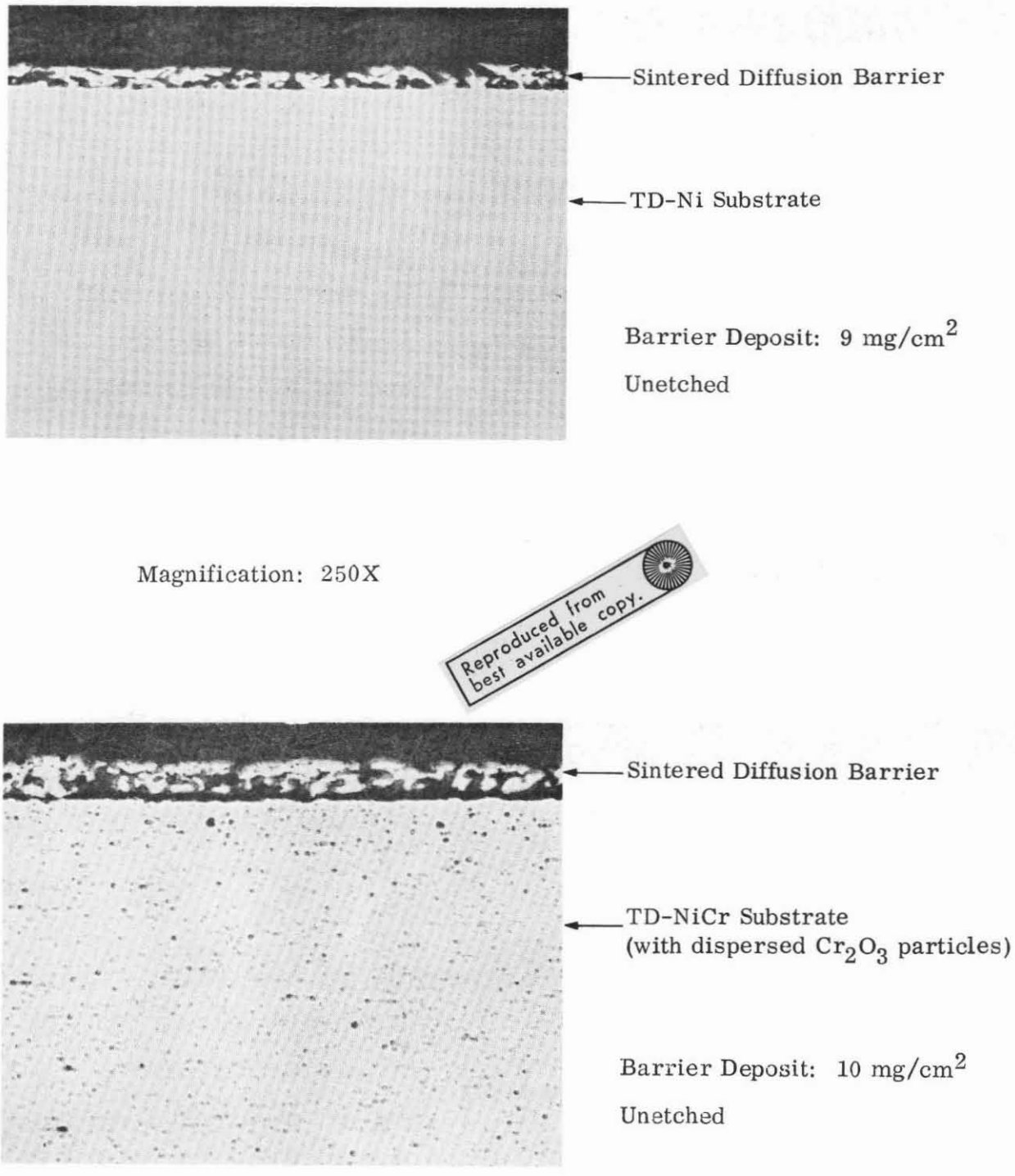

FIGURE 7. DISCONTINUOUS Al_2O_3 DIFFUSION BARRIER ON TD-Ni AND TD-NiCr; 88Ni-10Al_2O_3-2Si Fired in Vacuum at 2200°F for 4 Hours

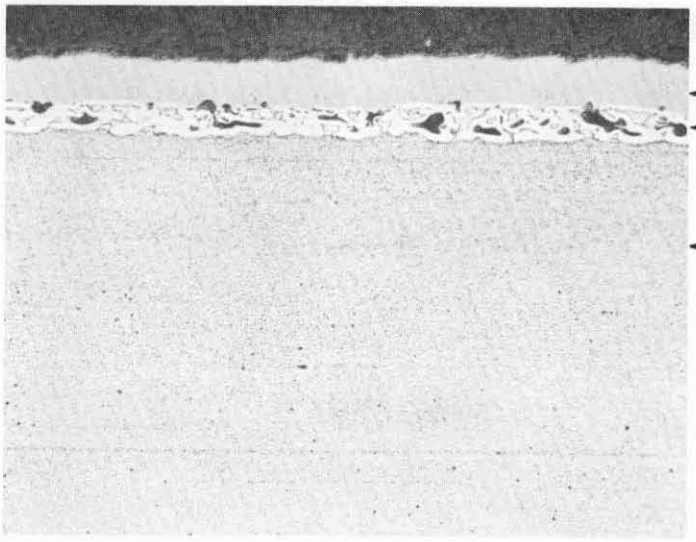

Magnification: 250X

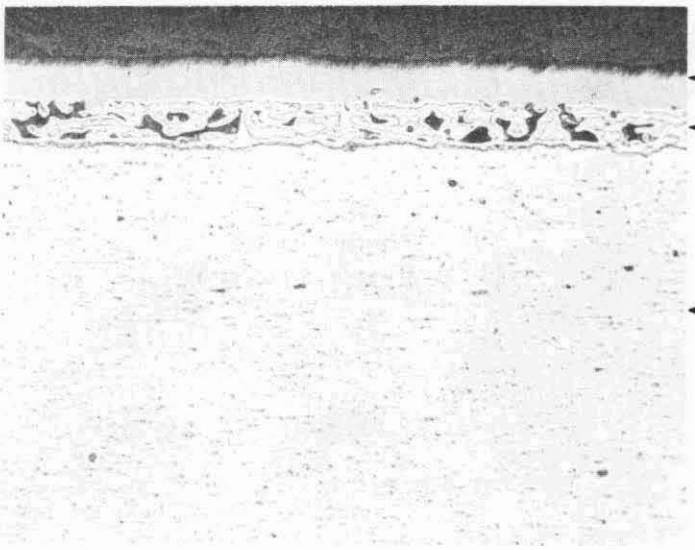

FIGURE 8. Al_2O_3 + Ta DIFFUSION BARRIER ON TD-Ni AND TD-NiCr; Discontinuous Al_2O_3 + Fused Salt Ta Plated

TABLE III

SLURRY TUNGSTEN DIFFUSION BARRIER COMPOSITIONS

Barrier Designation	Barrier Composition (wt%)					
	Ni	Cr	Ti	Si	W	Other
W-1	--	--	--	--	100	--
W-2	0.5	--	1	--	Bal.	--
W-3	1.0	--	--	0.5	Bal.	--
W-4	--	2	--	--	Bal.	--
W-5	0.5	1	1	--	Bal.	--
W-6	2.0	2	--	--	Bal.	--
W-7	9.0	--	--	--	Bal.	--
W-8	13.0	--	--	--	Bal.	--
W-9	0.25	--	--	--	Bal.	--
W-10	5.0	--	--	3.0	Bal.	3MgO
W-11	10.0	3	--	--	Bal.	--

could be easily removed from the TD-Ni after firing, but partially adhered to the TD-NiCr substrate. The W-2 and W-3 barriers, with Ni-Ti and Ni-Si eutectic compositions, formed apparently strong and dense layers but separated extensively along the interface with TD-Ni. W-4 and W-5 adhered well to TD-NiCr and, although there was still some edge separation, the presence of chromium definitely had improved the adherence to TD-Ni when compared to similar compositions without chromium (W-1 and W-2). The W-6 through W-8 barriers and W-11 adhered well to both substrates. W-10, with the 3 MgO addition, did not adhere well. All diffusion barriers except W-1, W-2, and W-10 were sufficiently dense after firing that they could not be removed by wire brushing.

The microstructures typically observed for the as-fired diffusion barriers are shown in Figure 9. Because of particle pull-out which occurred during polishing, these microstructures were not representative of the actual barrier layers. To permit a more critical examination of the barriers, a Ni-28Cr-3Si coating was prepared and applied to both substrates which had been previously coated with the W-6 barrier. The coating was applied by slurry spraying and firing at 2400° F (1589° K) for 15 minutes (90 sec) at $\leq 10^{-4}$ Torr (< 0.013 N/m^2). The coating used was similar in composition

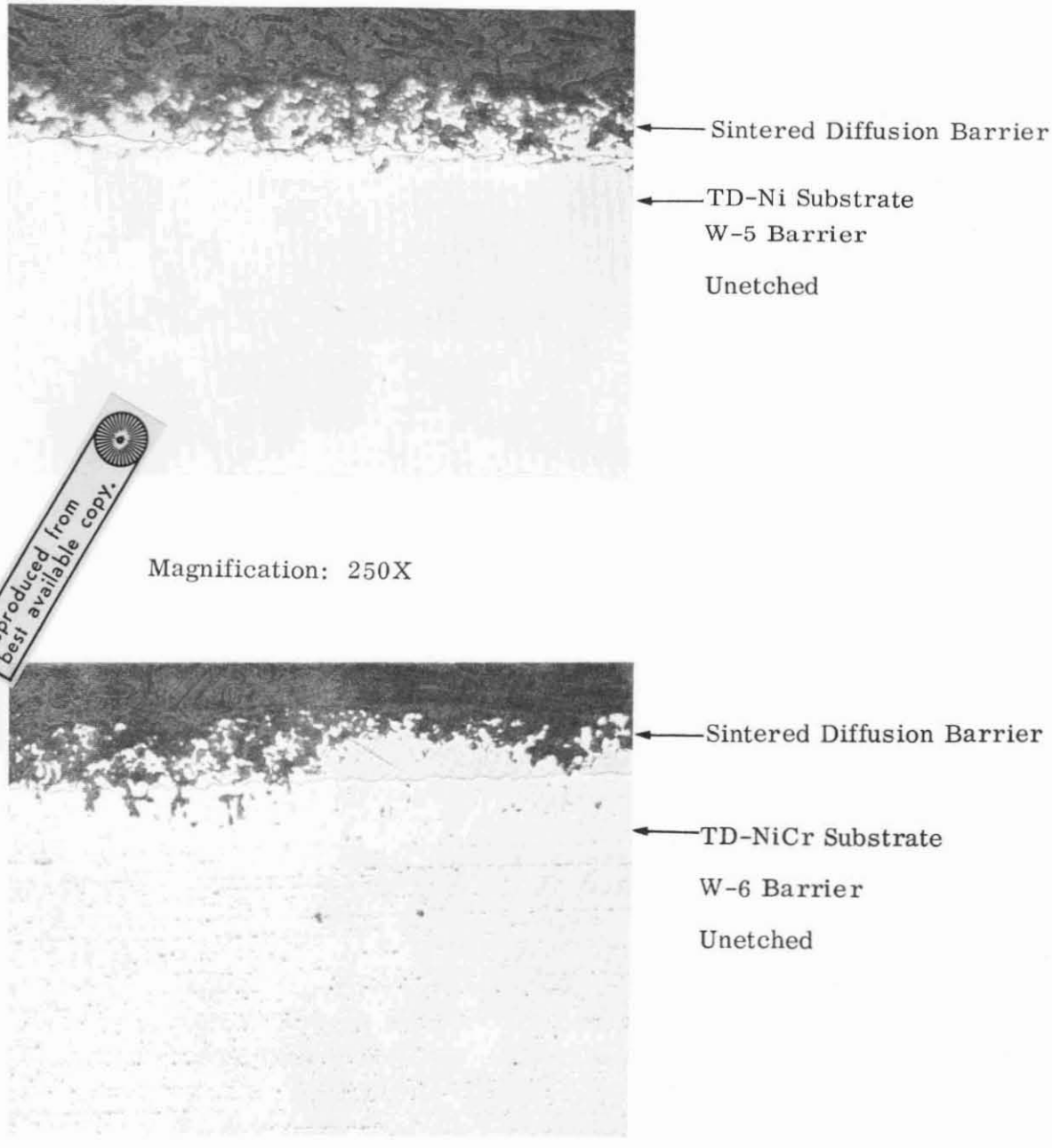

FIGURE 9. SLURRY TUNGSTEN DIFFUSION BARRIERS ON TD-Ni AND TD-NiCr; Fired in Vacuum at 2300° F for 3 Hours

to the first-step coatings (see Table VI on page 50). The resulting microstructure is shown in Figure 10. The diffusion barrier appeared to be a 70 to 80 percent (by volume) semi-continuous tungsten layer about 0.001-inch (2.5×10^{-5} m) thick, with the tungsten particles surrounded by a nickel-base matrix. The presence of the tungsten particles and the nickel-tungsten gamma solid solution should inhibit aluminum diffusion. The gamma solid solution matrix should also alleviate the problem of the difference in thermal expansion between the substrate and the tungsten barrier.

The W-9 barrier was applied by a method similar to that described in Reference 11. A water-base slurry of pre-milled tungsten and nickel nitrate was prepared, sprayed on the TD-alloy substrates, dried in vacuum for 16 hours (5.8×10^4 sec) at 250°F (394°K) and fired in both hydrogen and vacuum at 2100°F (1422°K) for 3 hours. The purpose of this procedure was to uniformly deposit nickel on the surface of the tungsten particles by decomposing the nickel nitrate and to provide enhanced diffusion of tungsten in this nickel layer. The barriers applied by this method were dense but sheared extensively on TD-Ni.

3.2.3 Summary of Application Processes

Table IV is a summary of both the diffusion barriers investigated and the application processes used to deposit the barriers on TD-Ni and TD-NiCr.

3.3 DIFFUSION BARRIER EVALUATION

The purpose of the evaluation was to determine the ability of each diffusion barrier to inhibit the diffusion of aluminum from a typical coating into the TD-alloy substrates. To ensure that the composition of the coating layer remained constant and to facilitate specimen preparation, cladding alloys were applied to the TD-alloys over previously deposited diffusion barriers. Nickel- and iron-base alloys, similar in composition to the proposed coating compositions (see Sec. 3.4.1), were used for this purpose. A diffusion anneal in argon and subsequent metallographic and electron microprobe analyses were used to determine barrier effectiveness.

3.3.1 Specimen Preparation

TD-Ni and TD-NiCr specimens, 0.060 x 1/2 x 1/2 inch (0.0015 x 0.013 x 0.013 m), were prepared as follows: first, each diffusion barrier was applied to four specimens of each substrate alloy using the techniques previously developed; then 1/2 x 1/2 inch (0.013 x 0.013 m) pieces of each of the two clads (Fe-Cr-Al and Ni-Cr-Al) were diffusion bonded to two specimens of each barrier/substrate combination. A test specimen ready for evaluation is shown schematically in Figure 11. Clad preparation and the diffusion bonding process are described below.

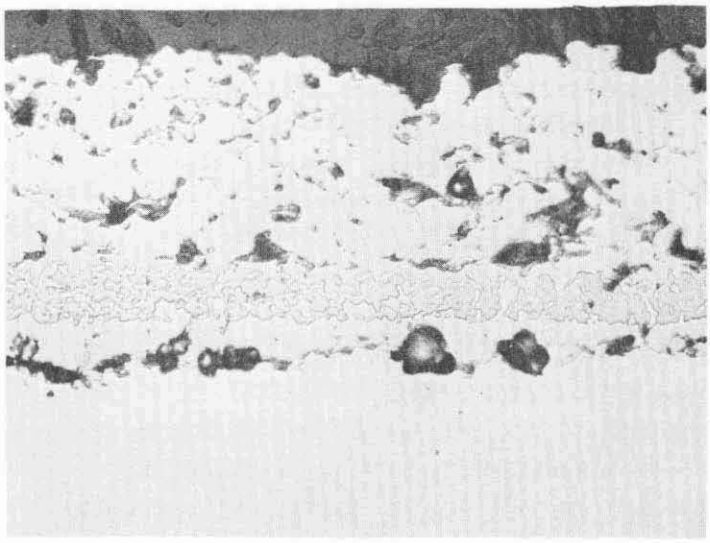

Magnification: 250X

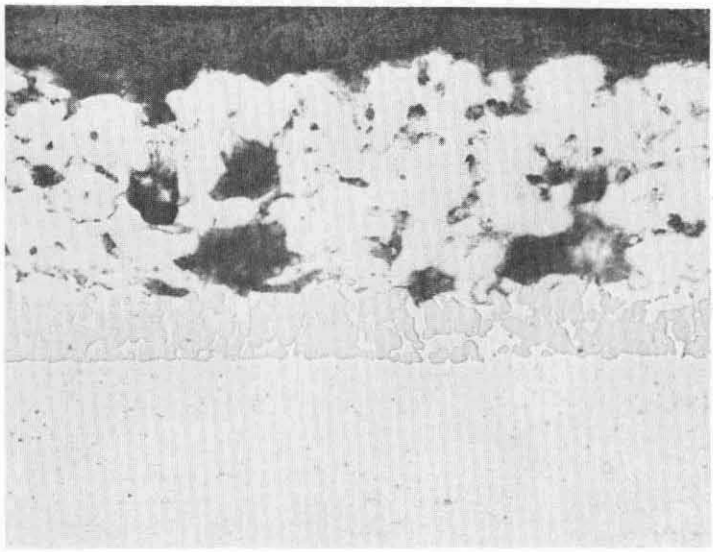

FIGURE 10. SLURRY TUNGSTEN DIFFUSION BARRIER AND Ni-28Cr-3Si FIRST-STEP COATING ON TD-Ni AND TD-NiCr

TABLE IV

DIFFUSION BARRIERS INVESTIGATED

Diffusion Barrier	Application Process
Yttrium-Nickel Intermetallic (YNi_4)	Fusion Slurry ($YNi_2 \longrightarrow YNi_4$)
Chromium (Cr)	Chromizing Pack
Tantalum (Ta)	Fused Salt Plating
Tantalum Carbide (TaC)	Ta Plating + Gas Carburizing
Chromium Carbide ($Cr_{23}C_6$)	Chromizing + Gas Carburizing
Aluminum Oxide (Al_2O_3)	a. Sintered Slurry ($Ni + Al_2O_3$) b. Fusion Slurry (Al)+ Controlled Oxidation
Al_2O_3 + Ta	Sintered Slurry + Ta Plating
Molybdenum (Mo)	Diffusion Bonding of Mo Foil (for evaluation only)
Tungsten (W)	a. Diffusion Bonding of W Foil (for evaluation only) b. Sintered Slurry

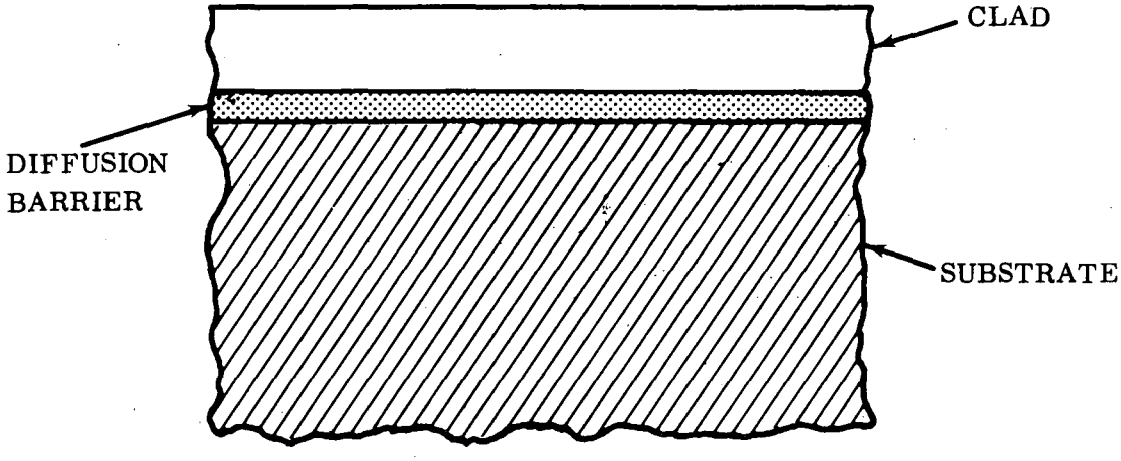

FIGURE 11. SCHEMATIC OF MICROSECTION ON TYPICAL DIFFUSION BARRIER EVALUATION SPECIMEN

Cladding Alloys

Ni-Cr-Al. Two starting compositions were arc melted in inert gas, 71Ni-22Cr-7Al and 74Ni-22Cr-4Al. The 7 percent aluminum composition was the initial choice for the cladding alloy; however, it cracked extensively when rolled either hot or cold. The 4 percent aluminum alloy, a more ductile composition, was then prepared. After a homogenization anneal of 16 hours (5.8×10^4 sec) at 2200° F (1477° K) in air and subsequent descaling, the alloy was easily cold rolled from about 0.35 to 0.013 inch (0.009 to 3.4×10^{-4} m) with one intermediate anneal at 2150° F (1450° K) for 15 minutes (900 sec). A wet chemical analysis was made on the rolled strip and the aluminum content was determined to be 3.5 weight percent. This was adequate for the purposes of the diffusion barrier evaluation.

Fe-Cr-Al. A commonly used electrical resistance alloy, Kanthal A-1, was selected for use as the iron-base clad because its composition (Fe-22Cr-5.5Al-0.5Co) was acceptably close to the composition originally proposed (Fe-25Cr-5Al). The Kanthal was purchased as 0.100 x 1.0 inch (0.0025 x 0.025 m) strip and thus needed reduction to the desired thickness. An attempt was made to cold roll the strip after annealing it at 2150° F (1450° K) for 20 minutes (1200 sec). Severe edge cracking occurred at a thickness reduction of less than 30 percent. Hot rolling was found satisfactory, however. The metal was heated to 2150° F (1450° K) for 3 to 5 minutes (180 to 300 sec) between each pass. A final thickness of 0.012 inch (3.1×10^{-4} m) was achieved with only slight edge cracking. The very adherent oxide scale present after rolling was removed by glass bead blasting.

Diffusion Bonding

The Solar yield strength diffusion bonding (YSDB) facility was used to bond the clads to the TD-Ni and TD-NiCr test samples. Preliminary tests were made by bonding the clads to bare TD-Ni and TD-NiCr (i.e., with no diffusion barrier). Because it was anticipated that bonding to the substrates with diffusion barriers on the surface would be difficult, the preliminary runs were used to establish the maximum time, temperature and pressure which could be used without causing cracking or excessive deformation of the cladding or substrate alloys. Based on these preliminary runs, the following parameters were selected for use in preparing the evaluation specimens: for TD-Ni, the cycle was 2100° F (1422° K) for 30 seconds at a stress level of 12 ksi (8.3×10^7 N/m^2); for TD-NiCr, the cycle consisted of 2200° F (1477° K) for 30 seconds at a stress level of 12 ksi (8.3×10^7 N/m^2).

The sequence of events during a diffusion bonding cycle was as follows: (1) apply the proper load to the specimen; (2) resistance heat the specimen to temperature (heatup time = 10 to 20 seconds); (3) soak at the bonding temperature for the

desired length of time; (4) cool the sample; (5) remove the load. All bonding was performed in an argon atmosphere using 0.002-inch (5×10^{-4} m) molybdenum foil to separate the top and bottom of the sample from the tungsten mandrels. The mandrels used were 3/8 inch (0.009 m) wide by 2-1/2 inches (0.063 m) long and thus provided a bond area of approximately 3/8 x 1/2 inch (0.009 x 0.013 m). Each separator sheet/TD-alloy/clad/separator sheet sandwich was prepared prior to bonding by spot tacking (outside the bond area).

Using the selected bonding cycles, the Fe-Cr-Al and Ni-Cr-Al clads were bonded to TD-Ni and TD-NiCr specimens. Judging by the adherence of substrate and clad, there was apparent bonding on all samples. This was later substantiated by metallography (Figs. 12 thru 14). The micrographs of the as-bonded specimens show that good metallurgical bonds were obtained on all samples. There were intermittent pores or included particles observed on the chromized samples, but they covered only about 15 percent of the interface area and thus did not prevent evaluation. The dark area along the interface on YNi_4 coated samples was a preferentially etched YNi_4 phase rather than porosity.

In some cases, the molybdenum separator foil stuck to the substrate and/or the clad, but it could be peeled off with relative ease in most cases. As observed on the preliminary samples, there was slight edge cracking on about one-third of the TD-NiCr samples. There was also discoloration noted on the edges of the TD-NiCr samples, probably due to the presence of small quantities of water or oxygen in the argon atmosphere.

On samples with the tantalum, TaC and Al_2O_3+Ta diffusion barriers there was apparent liquid formation during bonding, as evidenced by smooth metal deposits which had been extruded out from between the substrate and clad during bonding. It is likely that this liquid is of a Ta-Cr-Ni eutectic composition. Ternary alloys in this system have been found to melt as low as 2150°F (1450°K) (Ref. 12). A continuous tantalum layer remained after bonding, however.

3.3.2 Diffusion Anneal

The high-temperature cycle which had been selected to test diffusion barrier effectiveness was 2300°F (1533°K) for 100 hours (3.6×10^5 sec) in argon. A total of three 100-hour (3.6×10^5 sec) annealing runs were made. One specimen of each clad/barrier/substrate and clad/(bare) substrate combination was subjected to the anneal cycle.

A cylindrical Inconel 600 retort, 1/8 inch (0.003 m) thick by 4 inches (0.10 m) in diameter by 18 inches (0.45 m) long, was used to contain the specimens. Within the retort, the specimens rested on a strip of molybdenum foil which was spot welded to an Inconel sheet. A single gas line (1/2 inch (0.013 m) diameter tubing) was run in

one end of the retort. The end plates and gas line, both Inconel 600, were welded in place. After all welding had been completed, the retort outer surfaces were sand-blasted and sprayed with an aluminizing coating. The retort was then evacuated and backfilled with titanium gettered argon several times, placed in the furnace at 2300° F (1533° K) and held at temperature for 100 hours (3.6×10^5 sec). A positive argon pressure of 1 inch Hg (3.4×10^3 N/m^2) was maintained during the run.

When the specimens were removed from the furnace, the TD-Ni and TD-NiCr surfaces were bright, as were the Inconel surfaces. In the first two runs, a white scale was found on the surfaces of the Ni-Cr-Al clads; and on the Fe-Cr-Al clads, a light gray scale was observed. It is likely that both were Al_2O_3, which is thermodynamically stable at 2300° F (1533° K) for any partial oxygen pressure above 10^{-25} Torr (1.3×10^{-27} N/m^2). After the third run, which included only specimens with slurry applied tungsten barriers, no oxide was observed on the clad surfaces. This was probably the result of a slightly lower oxygen partial pressure during the run which slowed the rate of oxide formation enough so that no visible scale was present after 100 hours (3.6×10^5 sec).

3.3.3 Metallographic Examination

Two specimens of each clad/barrier/substrate combination, one as-bonded and one annealed, were sectioned, mounted and examined metallographically. Examples of as-bonded and annealed microstructures are shown in Figures 12 through 15.

The extent of apparent interdiffusion after annealing was greater for specimens with the Fe-Cr-Al clad than for those with the Ni-Cr-Al clad. Similar results were obtained in a previous investigation (Ref. 5) and were not unexpected. There was very little driving force for nickel to diffuse from the Ni-Cr-Al clad into the substrate or vice versa, because the nickel concentration gradient across the interface was small. On the other hand, the iron-base clad on the nickel-base substrate created very large nickel and iron concentration gradients in opposite directions and resulted in more extensive interdiffusion. Also, the extent of obvious interdiffusion was greater on TD-Ni specimens than on comparable TD-NiCr specimens. This may be the result of lower diffusion rates in TD-NiCr and/or the absence of a significant chromium concentration gradient between the two clad alloys and the TD-NiCr, all of which contain 20 to 25 weight percent chromium.

The extent of penetration of the clad alloy elements (iron, chromium, aluminum) into the substrate was very difficult to determine from metallography alone. The elements diffusing into the substrate went into solid solution in the gamma-nickel without forming any significant amount of identifiable second phase which could be used to

(text continued on page 35)

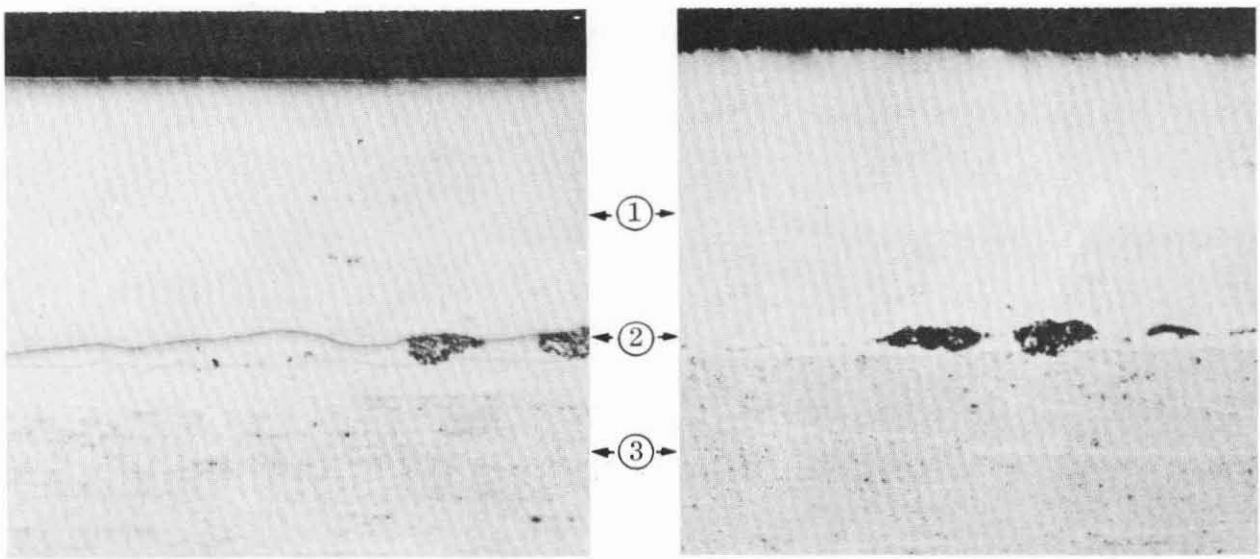

NiCrAl Clad - As Bonded NiCrAl Clad - Annealed

Legend: ① Clad
② Cr Diffusion Barrier (black particles are Al_2O_3 from pack process)
③ TD-NiCr Substrate
④ Al_2O_3 Internal Oxide Particles in Annealed FeCrAl Clad

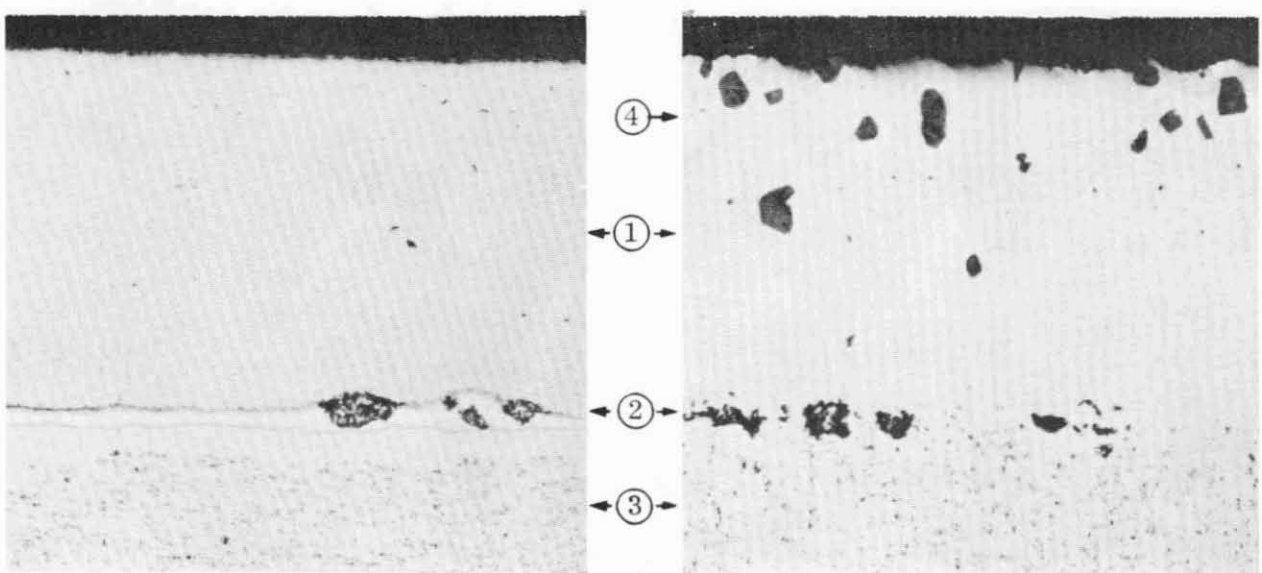

FeCrAl Clad - As Bonded FeCrAl Clad - Annealed

Magnification: 150X

FIGURE 12. TD-NiCr WITH Cr DIFFUSION BARRIER AND CLAD ALLOYS; As-Bonded and After Annealing at 2300° F for 100 Hours in Argon

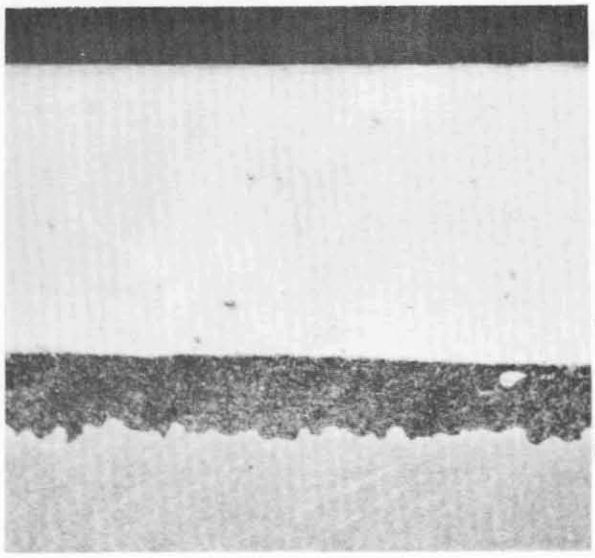

NiCrAl Clad - As Bonded

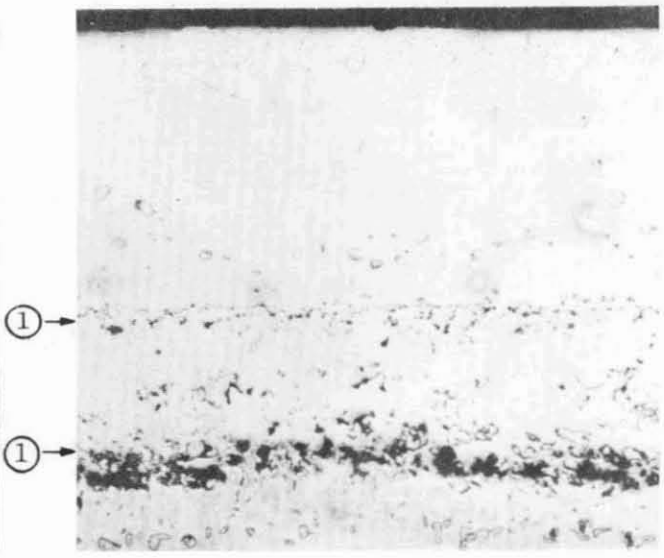

NiCrAl Clad - Annealed

① Apparent Kirkendall Voids

Magnification: 150X

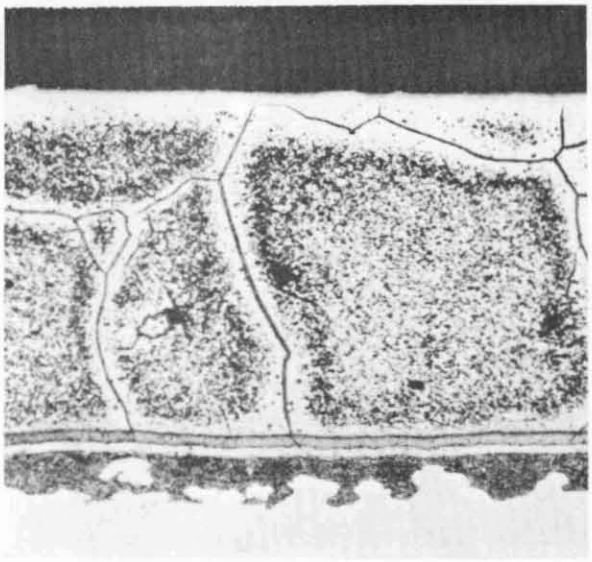

FeCrAl Clad - As Bonded

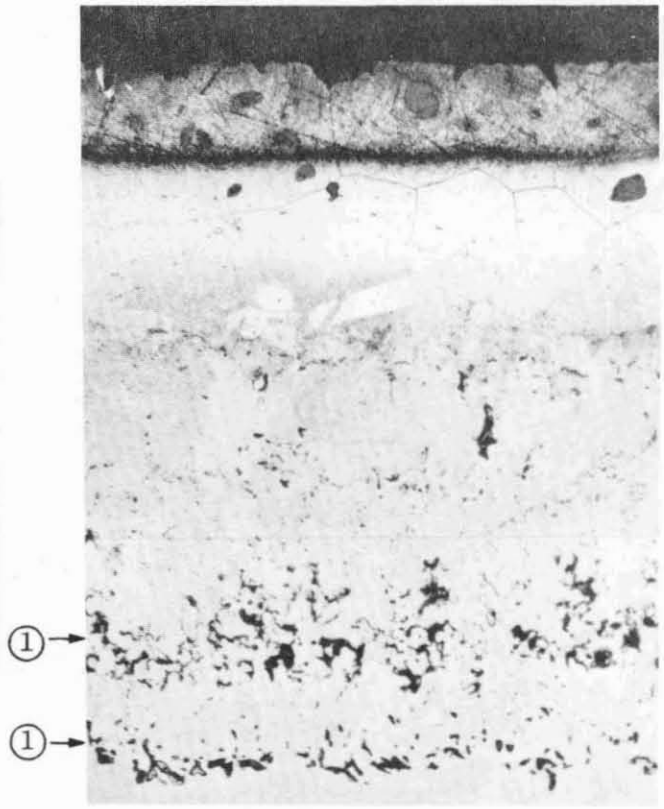

FeCrAl Clad - Annealed

FIGURE 13. TD-Ni WITH YNi_4 DIFFUSION BARRIER AND CLAD ALLOYS; As-Bonded and After Annealing at 2300° F for 100 Hours in Argon

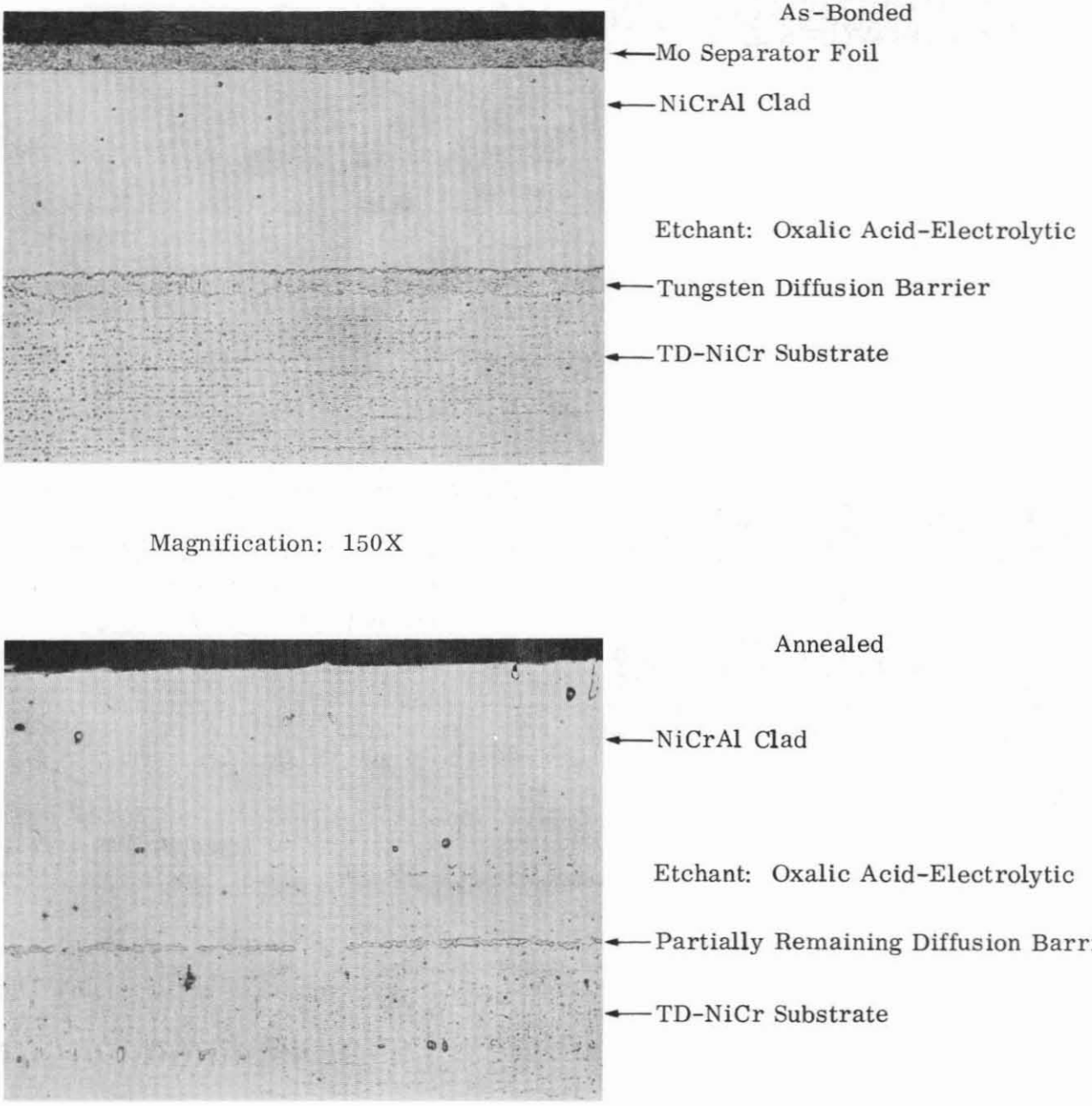

FIGURE 14. TD-NiCr WITH W-8 DIFFUSION BARRIER AND NiCrAl CLAD; As-Bonded and After Annealing at 2300°F for 100 Hours in Argon

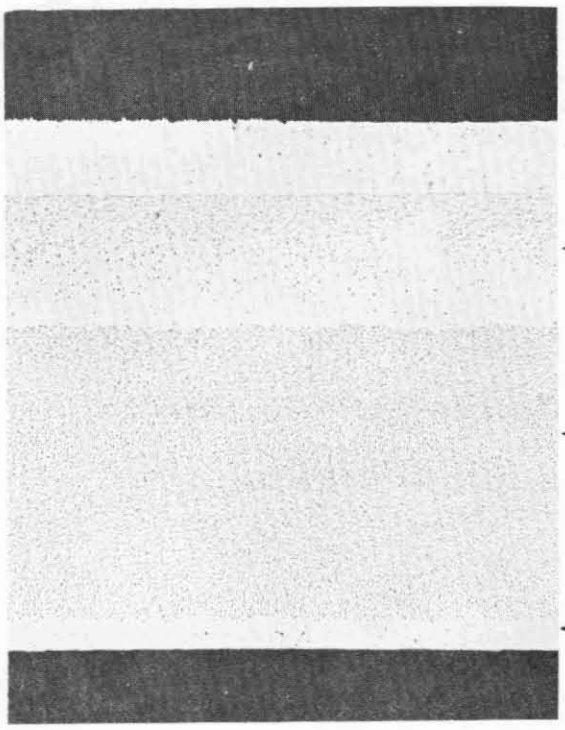

←NiCrAl Clad (One Side Only)

←Al Diffusion Zone in Substrate

←Unaffected TD-NiCr Substrate

←Cr_2O_3 Depleted Zone on Specimen Backside

Note: The zones of reduced particle (Cr_2O_3) density observed on these specimens are typical for all clad TD-NiCr specimens after annealing.

Magnification: 40X

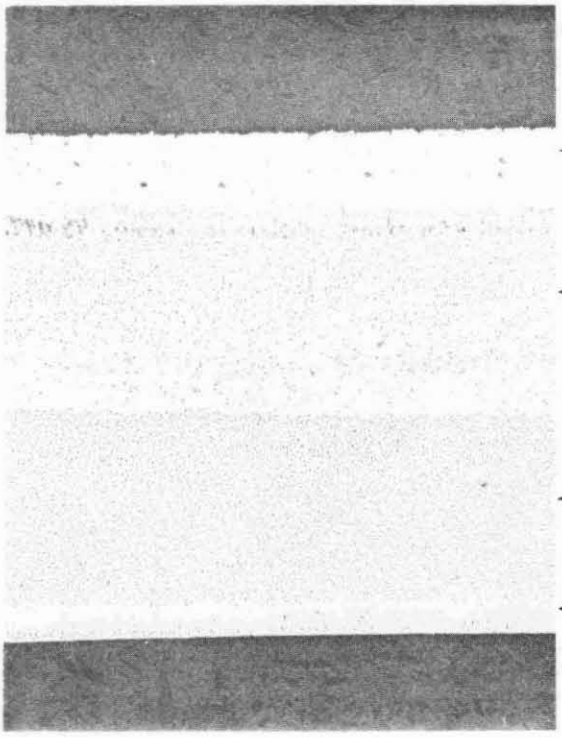

←FeCrAl Clad (One Side Only)

←Al Diffusion Zone in Substrate

←Unaffected TD-NiCr Substrate

←Cr_2O_3 Depleted Zone on Specimen Backside

FIGURE 15. CLAD TD-NiCr AFTER ANNEALING AT 2300° F FOR 100 HOURS

estimate extent of penetration. On many annealed specimens, porosity was observed at the approximate location of the original interface and extended over a range of 0.001 to 0.004 inch (2.5×10^{-5} to 1.0×10^{-4} m). The amount of porosity in these cases varied, but did not appear to be extensive enough to cause spalling nor deep enough to degrade substrate mechanical properties by itself. From the standpoint of interface and substrate porosity, the annealed specimens with the YNi_4 diffusion barrier suffered the greatest degradation. On the annealed Fe-Cr-Al/YNi_4/TD-Ni specimen, significant porosity extended about 0.012 inch (0.1×10^{-4} m) into the substrate, as measured from the original interface (Fig. 13).

Large inclusions (dark second-phase particles) were found in the Fe-Cr-Al clads after annealing (Figs. 12 and 13). These particles were subsequently identified as Al_2O_3 by electron microprobe analysis.

On the TD-NiCr samples, there was a reduction in density of the commonly observed dark particles in the substrate (believed to be Cr_2O_3 not reduced during alloy production) to a certain depth after annealing (see Fig. 15). This depth of reduced particle density was consistently found to be about 0.018 inch (4.5×10^{-4} m) on samples with the Ni-Cr-Al clad and about 0.025 inch (6.6×10^{-4} m) on samples with the Fe-Cr-Al clad. A zone of Cr_2O_3 depletion about 0.003 inch (7.6×10^{-5} m) deep was also observed on the edges and sides opposite the clad on all annealed TD-NiCr specimens (see Sec. 3.3.4).

A significant amount of tungsten was observed at the clad/substrate interface on annealed TD-NiCr specimens (Fig. 14). Virtually no visible barrier phase remained at this interface on any other specimens after annealing. The interdiffusion of tungsten with the Ni-Cr-Al clad and TD-NiCr obviously took place very slowly. As previously noted, this low mobility is one of the requirements for an effective diffusion barrier. The interdiffusion of tungsten and TD-Ni was apparently more rapid, resulting in a tungsten-nickel solid solution at the original barrier location.

The metallographic examination of the annealed test specimens yielded several interesting results (summarized below). However, the extent of aluminum diffusion from the clad into the TD-alloy substrates, the most critical factor in diffusion barrier evaluation, remained to be determined by electron microprobe analysis. The metallographic observations can be summarized as follows:

- Interdiffusion was more extensive on specimens with Fe-Cr-Al clads than on those with Ni-Cr-Al clads.
- Interdiffusion was more extensive on TD-Ni than on TD-NiCr.
- The extent of porosity along the original interface varied from sample-to-sample but did not appear to be extensive enough to cause spalling.

- Large oxide inclusions were observed in the Fe-Cr-Al clads after annealing due to internal oxidation.

- A zone of reduced Cr_2O_3 particle density was observed in all annealed TD-NiCr samples (Fig. 15). (Discussed in Sec. 3.3.4).

- Tungsten was the only diffusion barrier which remained at least partially in place after annealing (Fig. 14).

3.3.4 Electron Microprobe Analysis

All as-bonded and annealed test specimens were evaluated by electron microprobe scan analysis. Elemental scans were made for aluminum on all specimens, starting from the clad outer surface, traversing the clad and scanning an additional 0.030 to 0.040 inch (7.6×10^{-4} to 1.0×10^{-5} m) in the substrate. On most TD-Ni specimens, scans were also made for chromium. On many specimens with the Fe-Cr-Al clads, scans were made for iron. Selective scans were also made for nickel and elements comprising the diffusion barriers. The scanning rate was 0.005 inch/minute (2.0×10^{-6} m/sec). In addition to scans, spot readings were made for individual elements at points of interest.

Pure elemental standards were included in the metallographic mounts; however, to minimize the influence of other elements present on the test results, the concentration of aluminum, iron, chromium and nickel in the as-bonded clads were used as standards. The concentration of an element in an annealed specimen was calculated using the following formula:

$$C = \frac{R}{R_o} C_o$$

where C = Concentration in the annealed specimen (weight percent)

C_o = Known concentration in the as-bonded clad or pure elemental standard (weight percent)

R = Reading in the annealed specimen (counts/sec)

R_o = Reading in the as-bonded clad or pure elemental standard (counts/sec)

This is an approximation which does not take into account the analytical errors which vary with the composition of the matrix. It also neglects scattering of the electron beam caused by variation in surface topography resulting from etching, particle pull-out and porosity. Data generated in this manner thus lacks accuracy on an absolute basis. However, it is very valuable on a relative basis, i.e., for comparing the shape of the composition versus depth curves for the various diffusion barriers.

Figures 16 through 19 show the distribution of aluminum, chromium, and iron in the annealed specimens and present the diffusion data for the individual diffusion barriers in tabular form. Composite curves were made where appropriate (i.e., where individual curves were similar in shape and close enough to each other to be within the accuracy limits of the measurements).

Diffusion of Aluminum

For the Ni-Cr-Al clad on each alloy, four curves are shown: one for the specimen with no barrier, one which is a composite curve for the specimens with diffusion barriers except tungsten, and one for the specimen with a slurry applied tungsten barrier, and one for the tungsten foil barrier. The data and curves given for the W-8 barrier are typical of those obtained with the other slurry applied tungsten barriers.

The total aluminum remaining (area under the curve) varied from curve-to-curve on specimens with the Ni-Cr-Al clad because of differences in vaporization losses (discussed below) and experimental error at the low concentration levels. Thus, the depth of penetration and the aluminum concentration in the clad could not be used as a basis for comparing the diffusion barriers. There were two aspects of the curve shapes, however, which could be used to compare barriers: the fraction of the remaining aluminum which was in the clad area, and the slope of the curve across the clad/substrate interface. In both respects, the slurry applied tungsten barrier was clearly superior to the other barriers and to no barrier. It appeared to be capable of extending the life of the aluminum "reservoir" and thus prolonging coating life. As expected, the slurry applied barrier was not as effective as the continuous tungsten barrier (diffusion bonded tungsten foil). The slurry applied barrier provided some Ni-W solid solution paths through the barrier, and aluminum diffusion along these paths was more rapid than it was through the pure tungsten foil.

The results of the scans on specimens with the slurry applied tungsten barrier were, on first analysis, somewhat ambiguous. On any given specimen, in some areas the total aluminum remaining in both clad and substrate after annealing was very low (about 30 percent of the original aluminum content), and the aluminum concentration in the clad area was correspondingly low (about 1/2 weight percent compared to an initial concentration of 3.5 weight percent). But in other areas, the remaining aluminum content was high (70 percent of the original content), and the aluminum concentration in the clad was high (2 weight percent). Metallographic examination of the areas scanned showed that the high aluminum readings were taken where molybdenum separator foil (used in diffusion bonding) remained on the surface of the clad, and low aluminum readings were taken in areas with no molybdenum foil. Apparently, more than half of the aluminum (in areas with no foil) had been lost by vaporization during annealing. However, all previously analyzed samples had been scanned in areas with no foil on the surface, and the loss of aluminum by vaporization had been limited to

(Text continued on page 41)

Substrate	Barrier	Clad	Aluminum Concentration (wt%) at Various Distances From Surface - Inch (10^{-4} m)							Depth of Penetration Inch (10^{-4} m)
			Surface	.005 (1.3)	.010 (2.5)	.015 (3.8)	.020 (5.1)	.030 (7.6)	.040 (10.2)	
TD-Ni	None	NiCrAl	0.4	0.7	0.8	0.8	0.7	0.3	0	0.038 (9.6)
"	YNi_4	"	0.7	1.5	1.5	1.3	0.8	0.3	0	0.039 (9.9)
"	Cr	"	1.2	1.2	1.2	1.1	0.8	0.3	0	0.040 (10.2)
"	Ta	"	1.0	1.2	1.2	1.1	0.9	0.3	0	0.038 (9.6)
"	TaC	"	0.8	0.9	1.0	1.0	0.8	0.3	0	0.039 (9.9)
"	Al_2O_3*	"	0.7	0.8	1.0	1.0	0.9	0.4	0	0.040 (10.2)
"	Al_2O_3**	"	1.1	1.2	1.2	1.2	1.0	0.4	0	0.040 (10.2)
"	Al_2O_3 + Ta	"	1.2	1.3	1.2	0.9	0.7	0.1	0	0.036 (9.1)
"	W (Foil)	"	3.1	3.3	3.2	0.1	0	0	0	0.018 (4.6)
"	W-13Ni(slurry)	"	1.5	1.8	1.9	1.3	0.9	0.3	0	0.040 (10.2)
"	Mo	"	1.2	1.2	1.1	1.0	0.8	0.3	0	0.040 (10.2)
TD-Ni	None	FeCrAl	0	0.2	0.4	0.5	0.8	0.9	0.3	0.050 (12.7)
"	YNi_4	"	0.2	0.4	0.5	0.7	1.0	0.9	0.2	0.049 (12.4)
"	Cr	"	0.2	0.2	0.2	0.4	0.8	0.9	0.3	0.048 (12.1)
"	Cr_xC_y	"	0.2	0.3	0.3	0.5	0.8	0.6	0.1	0.046 (11.6)
"	Ta	"	0.3	0.3	0.3	0.7	1.0	1.0	0.3	0.049 (12.4)
"	TaC	"	0.3	0.2	0.4	0.7	1.0	0.9	0.3	0.046 (11.6)
"	Al_2O_3*	"	0.2	0.3	0.4	0.6	1.0	0.9	0.2	0.050 (12.7)
"	Al_2O_3**	"	0.2	0.3	0.4	0.6	1.0	0.9	0.2	0.048 (12.1)
"	Al_2O_3 + Ta	"	0.2	0.2	0.4	0.9	1.3	0.9	0.2	0.047 (11.9)
"	W (Foil)	"	0.6	0.5	0.5	0.5	0.5	0.1	0	0.037 (9.4)
"	Mo	"	0.3	0.2	0.4	0.8	1.2	1.0	0.2	0.047 (11.9)

* Continuous Al_2O_3

** Discontinuous Al_2O_3

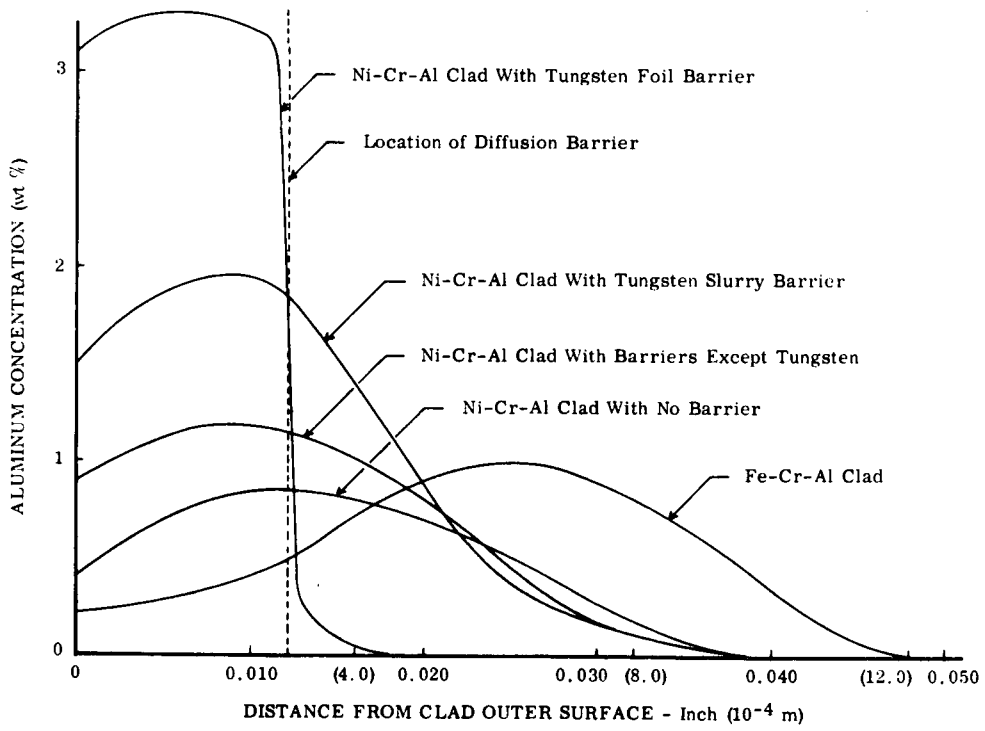

FIGURE 16. ALUMINUM DISTRIBUTION IN TD-Ni AFTER ANNEALING (2300° F for 100 Hours in Argon)

Substrate	Barrier	Clad	Aluminum Concentration (wt%) at Various Distances From Surface - Inch (10^{-4} m)							Depth of Penetration Inch (10^{-4} m)
			Surface	.005 (1.3)	.010 (2.5)	.015 (3.8)	.020 (5.1)	.030 (7.6)	.040 (10.1)	
TD-NiCr	None	NiCrAl	0.5	0.8	0.9	0.9	0.9	0.4	0	0.033 (8.4)
"	YNi_4	"	1.4	1.5	1.3	1.0	0.8	0	0	0.030 (7.6)
"	Cr	"	1.6	1.6	1.4	1.3	1.0	0	0	0.030 (7.6)
"	Cr_xC_y	"	2.0	1.8	1.6	1.3	0.8	0	0	0.027 (6.9)
"	Ta	"	1.0	1.1	1.1	0.8	0.4	0	0	0.026 (6.6)
"	TaC	"	0.9	1.0	1.2	1.1	0.7	0	0	0.027 (6.9)
"	Al_2O_3*	"	0.7	0.9	1.1	1.0	0.7	0.1	0	0.031 (7.9)
"	Al_2O_3**	"	1.5	1.5	1.4	1.1	0.8	0	0	0.030 (7.6)
"	Al_2O_3 + Ta	"	1.4	1.2	1.0	0.7	0.4	0	0	0.026 (6.6)
"	W (Foil)	"	3.1	3.2	3.1	0	0	0	0	0.013 (3.3)
"	W-13Ni(slurry)	"	2.0	2.1	2.0	1.3	0.6	0	0	0.030 (7.6)
"	Mo	"	1.2	1.3	1.4	1.0	0.6	0	0	0.027 (6.9)
TD-NiCr	None	FeCrAl	0	0.2	0.4	1.0	1.2	1.0	0.2	0.042 (10.7)
"	YNi_4	"	0.2	0.5	0.8	1.3	1.4	0.6	0	0.037 (9.4)
"	Cr	"	0.2	0.2	0.4	0.9	1.3	1.1	0.1	0.041 (10.4)
"	Cr_xC_y	"	0.4	0.4	0.5	1.0	1.2	0.8	0	0.038 (9.6)
"	Ta	"	0.4	0.3	0.4	1.3	1.6	1.1	0	0.040 (10.2)
"	TaC	"	0.2	0.3	0.5	1.2	1.3	0.8	0	0.039 (9.9)
"	Al_2O_3*	"	0	0.2	0.5	1.1	1.3	0.7	0	0.040 (10.2)
"	Al_2O_3**	"	0.2	0.2	0.4	1.0	1.4	0.8	0	0.040 (10.2)
"	Al_2O_3 + Ta	"	0.3	0.2	0.3	1.0	1.4	1.0	0	0.040 (10.2)
"	W (Foil)	"	0.5	0.4	0.3	0.7	0.6	0	0	0.027 (6.9)
"	Mo	"	0.3	0.3	0.5	1.1	1.4	1.0	0	0.040 (10.2)

* Continuous Al_2O_3

** Discontinuous Al_2O_3

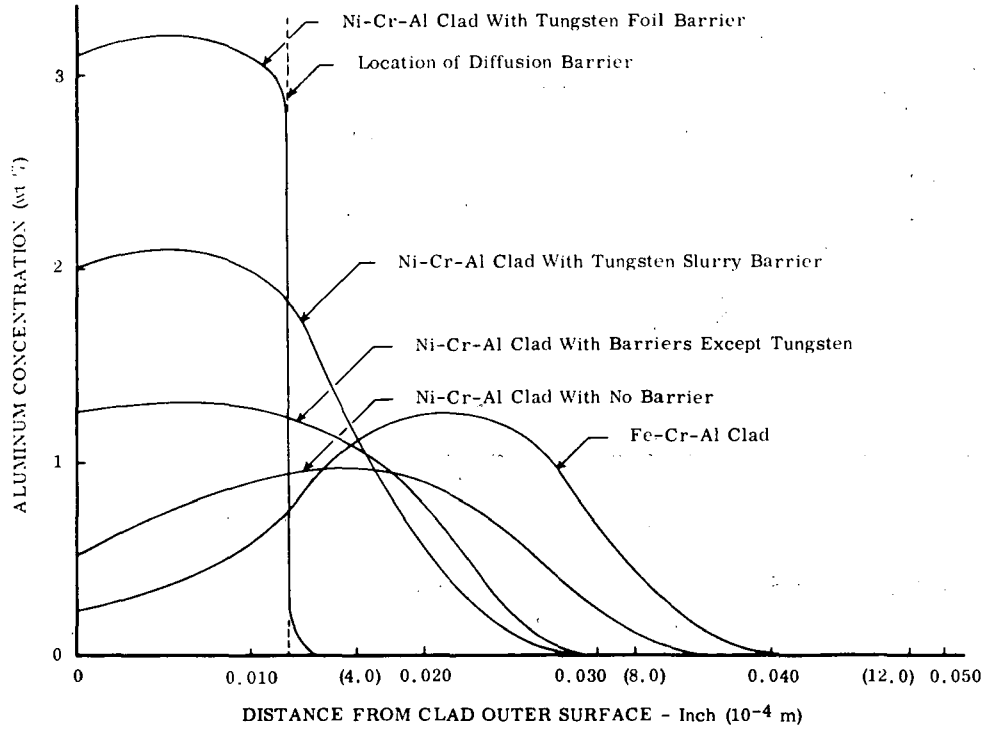

FIGURE 17. ALUMINUM DISTRIBUTION IN TD-NiCr AFTER ANNEALING (2300° F for 100 Hours in Argon)

Substrate	Barrier	Clad	Chromium Concentration (wt%) at Various Distances From Surface - Inch (10^{-4} m)							Depth of Penetration Inch (10^{-4} m)
			Surface	.005 (1.3)	.010 (2.5)	.015 (3.8)	.020 (5.1)	.030 (7.6)	.040 (10.2)	
TD-Ni	None	NiCrAl	16	13	11	7	4	0.5	0	0.036 (9.1)
"	YNi_4	"	17	16	14	10	7	0.5	0	0.034 (8.6)
"	Cr	"	19	18	16	11	6	1	0	0.038 (9.6)
"	Ta	"	15	13	8	3	1	0	0	0.026 (6.6)
"	TaC	"	17	15	11	6	3	0.5	0	0.034 (8.6)
"	Al_2O_3*	"	16	15	12	8	7	1	0	0.037 (9.4)
"	Al_2O_3**	"	18	17	15	10	6	1	0	0.036 (9.1)
"	Al_2O_3 + Ta	"	16	13	8	4	2	0	0	0.028 (7.1)
"	W (Foil)	"	18	19	1	0	0	0	0	0.017 (4.3)
"	Mo	"	18	18	14	7	3	1	0	0.035 (8.9)
TD-Ni	None	FeCrAl	23	17	10	7	4	1	0	0.036 (9.1)
"	YNi_4	"	24	19	11	7	4	1	0	0.035 (8.9)
"	Cr	"	27	26	16	10	7	1	0	0.040 (10.2)
"	Cr_xC_y	"	24	21	13	8	5	1	0	0.040 (10.2)
"	Ta	"	21	19	9	2	1	0	0	0.027 (6.9)
"	TaC	"	24	18	11	7	4	1	0	0.036 (9.1)
"	Al_2O_3*	"	23	18	12	7	5	1	0	0.026 (6.6)
"	Al_2O_3**	"	21	17	10	6	4	1	0	0.040 (10.2)
"	Al_2O_3 + Ta	"	22	23	19	5	2	1	0	0.032 (8.1)
"	W (Foil)	"	19	20	15	6	3	1	0	0.035 (8.8)
"	Mo	"	16	15	9	6	4	1	0	0.040 (10.2)

* Continuous Al_2O_3

** Discontinuous Al_2O_3

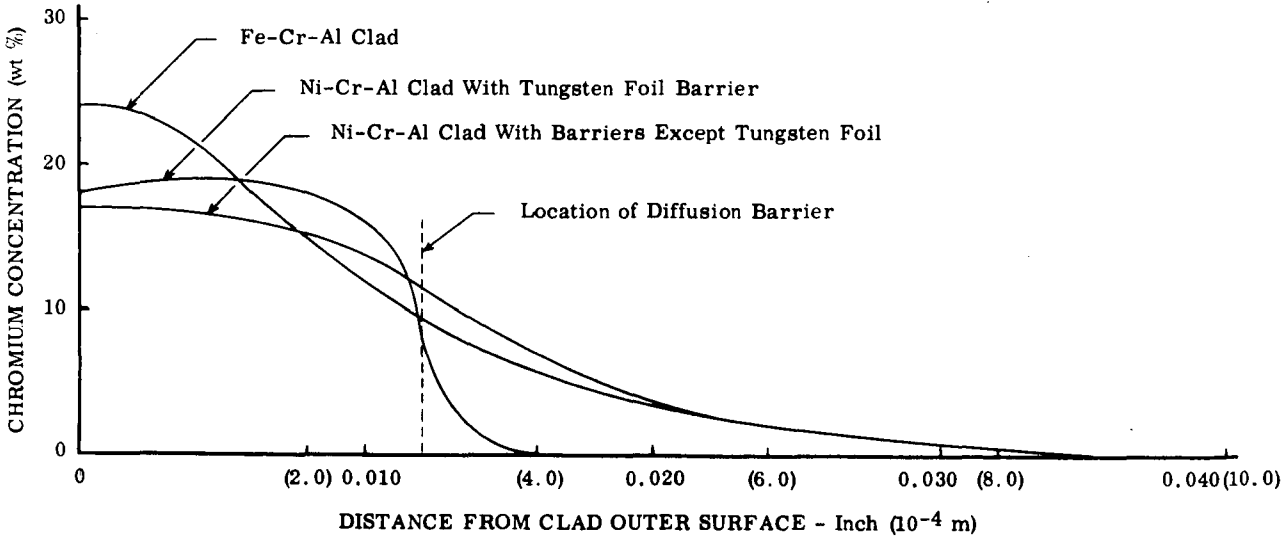

FIGURE 18. CHROMIUM DISTRIBUTION IN TD-Ni AFTER ANNEALING (2300° F for 100 Hours in Argon)

Substrate	Barrier	Clad	Iron Concentration (wt %) at Various Distances -Inch, (10^{-4} m) from Surface							Depth of Penetration Inch (10^{-4} m)
			Surface	.005 (1.3)	.010 (2.5)	.015 (3.8)	.020 (5.1)	.030 (7.6)	.040 (10.2)	
TDNi	None	FeCrAl	72	63	31	17	9	1	0	0.034 (8.6)
"	YNi_4	"	72	62	43	27	17	4	0.5	0.041 (10.4)
"	Cr	"	77	75	51	28	16	3	0	0.038 (9.6)
"	Cr_xC_y	"	74	74	56	30	17	3	0	0.037 (9.4)
"	Ta	"	70	72	51	18	8	1	0	0.034 (8.6)
"	TaC	"	72	68	43	26	15	3	0	0.038 (9.6)
TDNiCr	None	FeCrAl	74	67	45	26	15	2	0	0.038 (9.6)
"	YNi_4	"	68	59	36	20	11	1	0	0.034 (8.6)
"	Cr	"	60	60	50	26	15	2	0	0.038 (9.6)
"	Cr_xC_y	"	69	68	49	28	13	1	0	0.036 (9.1)
"	Ta	"	64	64	46	22	10	1	0	0.034 (8.6)
"	TaC	"	69	66	49	28	16	2	0	0.038 (9.6)

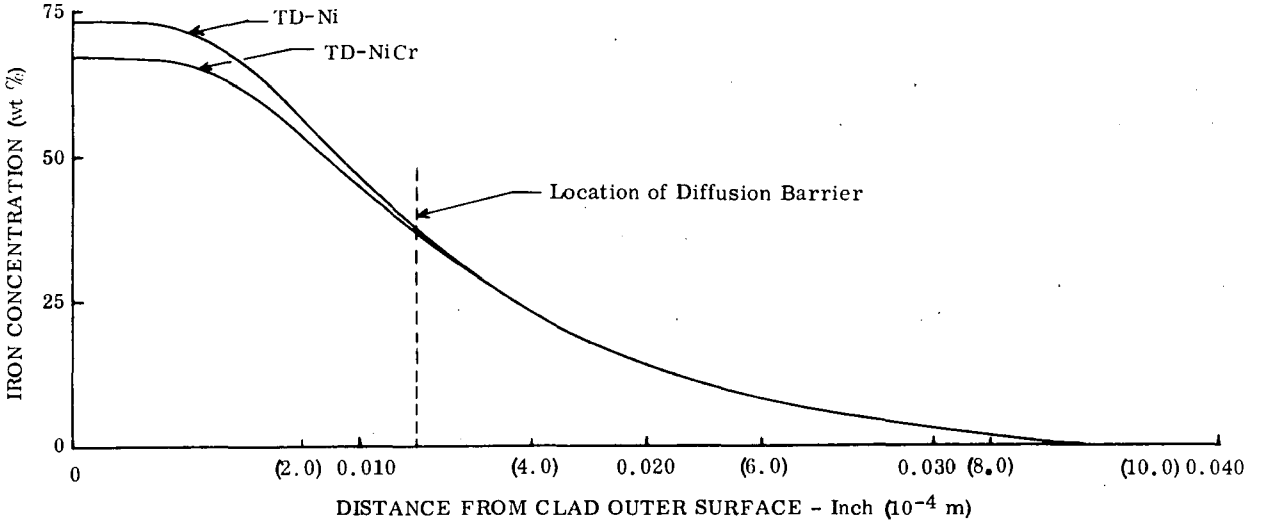

FIGURE 19. IRON DISTRIBUTION IN TD-Ni AND TD-NiCr AFTER ANNEALING (2300° F for 100 Hours in Argon)

about 30 percent. Visual examination of the clad surfaces of annealed specimens revealed the presence of a clearly visible oxide (Al_2O_3) on all previously annealed specimens but no visible oxide on the specimens with the slurry tungsten barriers. It was concluded that the surface oxide had prevented aluminum vaporization in previous annealing runs, and that the lack of a significant oxide scale during the most recent run (due to a cleaner argon atmosphere) permitted the loss of at least half of the aluminum by vaporization in areas not protected by molybdenum foil. The effects of the Al_2O_3 scale and the molybdenum foil were apparently similar in preventing vaporization. Therefore, the curves shown for the tungsten barrier were taken from the areas with molybdenum foil.

Only one curve is given for the Fe-Cr-Al clad on each substrate because there was virtually no difference between the sample with no barrier and those with barriers. The shape of the curves was somewhat unusual. There was almost no aluminum in the clad (approximately 0.3 weight percent), and the peak of the curve (~1 weight percent) was 0.010 to 0.020 inch (2.5×10^{-4} to 5.0×10^{-4} m) into the substrate. Also, the depth of penetration was about 0.010 inch (2.5×10^{-4} m) greater than for the Ni-Cr-Al clad. There was a much higher diffusion rate for aluminum in a gamma Fe-Ni solid solution than in gamma Ni-Cr solid solution; also, $\Delta \bar{F}$ Ni (Al)$\ll$ $\Delta \bar{F}$ Fe(Al). The difference in free energies was equivalent to a chemical activity gradient which caused "uphill" diffusion of aluminum from the alpha Fe into the gamma Ni.

A second feature to be noted on the aluminum distribution curves for specimens with the Fe-Cr-Al clad is that a significant amount of aluminum was "lost" during annealing. In fact, the areas under the aluminum curves for Ni-Cr-Al and Fe-Cr-Al clads were approximately the same after annealing, in spite of the fact that the original aluminum concentration in the Ni-Cr-Al clad was 3.5 weight percent, as compared to 5.5 weight percent in the Fe-Cr-Al clad. This apparent anomaly can be explained as follows: the inclusions observed in the Fe-Cr-Al clad after annealing were identified as Al_2O_3 particles (high aluminum, low nickel, chromium and iron) by spot analysis. This internal oxide was not observed on samples with the Ni-Cr-Al clad. The amount of aluminum in the oxide particles was calculated to be 20 to 30 percent of the aluminum originally contained in the Fe-Cr-Al clad, which accounts for the low aluminum remaining in solution in the clad and substrate after annealing.

The microprobe data verified that aluminum diffusion was more rapid in TD-Ni than in TD-NiCr. The total depth of aluminum penetration into the substrate was about 0.008 inch (2.0×10^{-4} m) greater for TD-Ni than for TD-NiCr.

The zones of reduced Cr_2O_3 particle density on annealed TD-NiCr samples have been noted previously. Electron microprobe analysis showed that the depth of these zones corresponded exactly to the depth of aluminum penetration. It is likely that Cr_2O_3 was reduced and that Al_2O_3 was formed (Al_2O_3 being much more thermodynamically stable than Cr_2O_3). The precise mechanism may have been a direct reaction between Al in solution and the Cr_2O_3 particles. It is more probable, however, that the simultaneous reaction of Al with dissolved oxygen and dissociation of Cr_2O_3 took place. The equilibrium concentration of dissolved oxygen should be much lower for Al_2O_3 than for the less stable Cr_2O_3. The Al_2O_3 would, therefore, continue to form until the dissolved oxygen concentration had dropped far below the level at which Cr_2O_3 is stable, causing the Cr_2O_3 to dissociate. The end point of the reaction would be reached when Al_2O_3 was in equilibrium with dissolved oxygen (at a very low concentration) and when virtually all Cr_2O_3 had dissolved. As seen in Figure 15, there is a distribution gradient in the density of particles found in the aluminum diffusion zone after annealing, with the particle density being the greatest near the original clad/substrate interface. The particles observed in this zone are probably Al_2O_3. The

reason for the gradient in particle density is apparently related to the time required for the nucleation and growth of Al_2O_3 particles large enough to be visible. The more limited zones of Cr_2O_3 depletion observed on the specimen edges and the side opposite the barrier and clad were probably caused by vaporization losses (either direct vaporization of Cr_2O_3 or formation and vaporization of CrO_3). EMP analysis did not show any aluminum in these areas.

Diffusion of Chromium

Scans for chromium were made on many TD-Ni samples and on one TD-NiCr/Fe-Cr-Al sample. Figure 18 shows the diffusion data and typical curves for chromium diffusion in TD-Ni. The diffusion of chromium was slower than the diffusion of aluminum. Approximately 75 percent of the original chromium remained in the clad. With the exception of the tantalum barrier, very little difference was noted between samples with and without diffusion barriers. On both TD-Ni samples with the tantalum diffusion barrier, the total amount of chromium remaining after annealing (area under chromium content versus distance curve) was significantly lower than for the other samples (see tabular data). It is possible that the "lost" chromium can be accounted for by the melting previously noted on tantalum plated samples (Ref. 9). If, in the area scanned, a significant reduction in original clad thickness had occurred by melting and extrusion during diffusion bonding, the total amount of chromium would be reduced accordingly.

The chromium concentration at the surface of the Fe-Cr-Al clad on annealed specimens was higher than at the surface of the Ni-Cr-Al clad after annealing and also higher than the original chromium concentration (22 weight percent) in the as-bonded Fe-Cr-Al clad. This difference was apparently due to a lower partial molar free energy of solution of chromium in alpha Fe than in gamma Ni. A scan for chromium on the annealed TD-NiCr/Cr/Fe-Cr-Al specimen verified this tendency. After annealing, the chromium concentration in a 0.005-inch (1.3×10^{-4} m) thick alpha Fe surface layer had risen from 22 to 27 percent, while the chromium in the TD-NiCr substrate was slightly depleted near the interface.

Diffusion of Iron

The data for iron diffusion from the Fe-Cr-Al clad into TD-Ni and TD-NiCr are presented graphically and tabularly in Figure 19. There was little difference in iron diffusion on samples with barriers and those without. Approximately 70 percent of the iron remained in the clad after annealing. The slightly lower iron concentration at the surface of the clad on TD-NiCr corresponded to the higher surface chromium content on TD-NiCr noted in the previous paragraph.

Diffusion of Nickel

Scans for nickel, made in several cases, were used primarily to check the accuracy of the concentration values measured for other elements. The total concentration was calculated by adding aluminum, chromium, nickel, and iron (where applicable) concentrations and was within 10 percent of 100 weight percent in each case. This is quite accurate for data obtained by scan analysis uncorrected for compositional effects.

Diffusion of Other Elements

Scans were made for yttrium, tantalum, and tungsten to determine the extent of diffusion of the diffusion barrier elements into the substrate and clad. After annealing, yttrium was found within 0.008 inch (2.0×10^{-4} m) of the original barrier location as a series of small peaks. It was probably present in the form of a Y-Ni intermetallic compound and as Y_2O_3. A typical distribution curve was observed for tantalum after annealing, with a maximum at approximately the original interface and a depth of penetration into the substrate of 0.013 to 0.023 inch (3.4×10^{-4} to 5.7×10^{-4} m). The concentration of both yttrium and tantalum was low at the original barrier location after annealing in comparison with the concentration before annealing.

Scans were made for tungsten only on annealed TD-NiCr specimens and only for specimens with the foil (continuous) tungsten barrier. Results showed that tungsten had interdiffused more rapidly with the Fe-Cr-Al clad than with the Ni-Cr-Al clad (Fig. 20), leaving a Ni-Fe-(30 to 50)W layer between the Fe-Cr-Al clad and the substrate, while an essentially 100 percent tungsten layer remained between the Ni-Cr-Al clad and the substrate.

Summary of Diffusion Data

The behavior of the diffusion barriers as determined by microprobe analysis is summarized below.

- All barriers at least marginally improved aluminum retention in the Ni-Cr-Al clad. The slurry applied tungsten barrier was superior to all other barriers except tungsten foil in this respect.
- No barrier was effective in retaining aluminum in the Fe-Cr-Al clad.
- The barriers did not affect chromium retention in either clad (the chromium concentration was acceptable on all annealed specimens).
- The zone of Cr_2O_3 particle depletion observed on annealed TD-NiCr specimens corresponded to the zone of aluminum penetration.

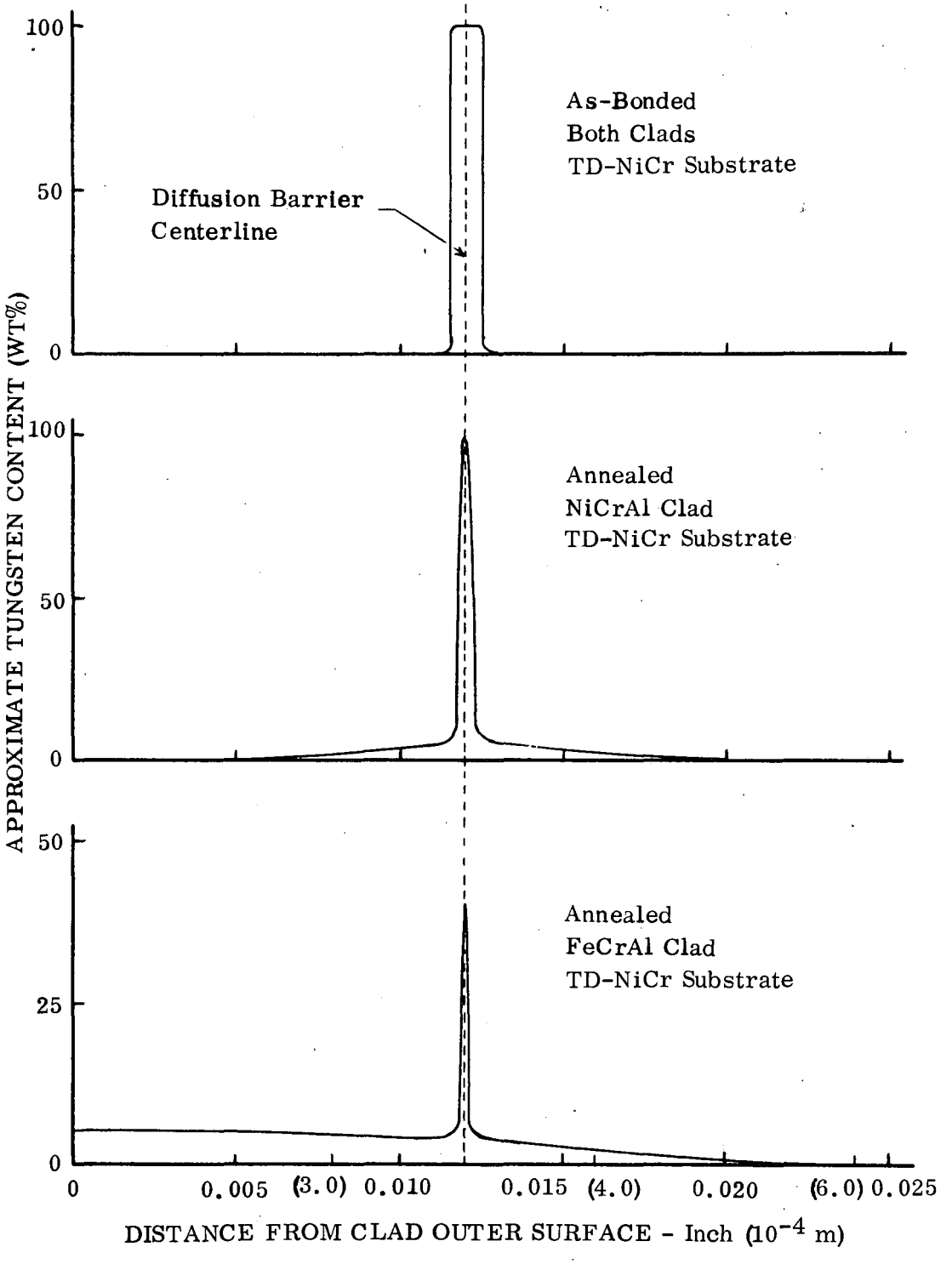

FIGURE 20. INTERDIFFUSION OF FOIL TUNGSTEN BARRIER WITH CLAD AND SUBSTRATE DURING ANNEALING (2300° F for 100 Hours in Argon)

3.3.5 Further Testing of Tungsten Barrier

The tungsten diffusion barrier had shown promise of reducing aluminum diffusion and thus increasing coating life. However, it was felt that two possible problem areas associated with the use of a tungsten barrier needed further investigation. First, there was the possibility of shearing between the barrier and substrate because of differential thermal expansion. Second, there was the possibility that rapid or even catastrophic oxidation might take place along the barrier if it was exposed to the oxidizing atmosphere. To examine these possibilities, samples of each substrate with tungsten barriers (diffusion bonded tungsten foil and slurry applied W-13Ni) and Ni-Cr-Al clads were cycled four times in air at 2100°F (1422°K) for a total of 100 hours (3.6×10^5 sec). Prior to oxidation a slot was cut through the clad and barrier into the substrate so that the diffusion barrier layer was exposed to the atmosphere. After exposure, the specimens with the slurry applied barrier were intact (no clad/substrate separation had taken place) and metallographic examination revealed only slightly accelerated oxidation at the site of the exposed barrier (see Fig. 21). It should be noted, however, that almost any metallic diffusion barrier would be expected to oxidize more rapidly than the highly oxidation resistant Ni-Cr-Al clad. On almost all specimens with the tungsten foil barrier (continuous), at least partial clad/substrate separation had taken place and oxide penetration at the location of the exposed barrier was somewhat more extensive (Fig. 21). The difference in the behavior of the two types of tungsten barrier can be explained in terms of physical configuration. The tungsten-nickel slurry applied barrier, after overcoating or cladding, was a semi-continuous line of tungsten particles surrounded by a matrix consisting of γ Ni(Cr, W) solid solution while the foil barrier was a solid, continuous tungsten phase. The cyclic oxidation test demonstrated that the configuration of the slurry applied tungsten diffusion barrier effectively alleviated expansion problems associated with a continuous tungsten barrier and reduced the oxidation rate of the barrier in an oxidizing atmosphere.

3.3.6 Selection of Optimum Diffusion Barrier

Based on its effectiveness in limiting aluminum diffusion from the Ni-Cr-Al clad into TD-Ni and TD-NiCr substrates, a slurry applied tungsten diffusion barrier was selected for use in the coating systems to be developed in the program. The exact composition chosen was W-10Ni-3Cr. The additive level - 13 weight percent - is identical to that of the W-13Ni barrier tested in the diffusion anneal and found to be very effective. The 3Cr composition was selected because of the beneficial effects on barrier-to-substrate bonding which chromium additions had previously demonstrated and because of the oxidation resistance of the Ni-Cr composition. The more effective continuous tungsten foil barrier was not selected because of the lack of a practical application process and because of the thermal expansion and oxidation problems discussed above.

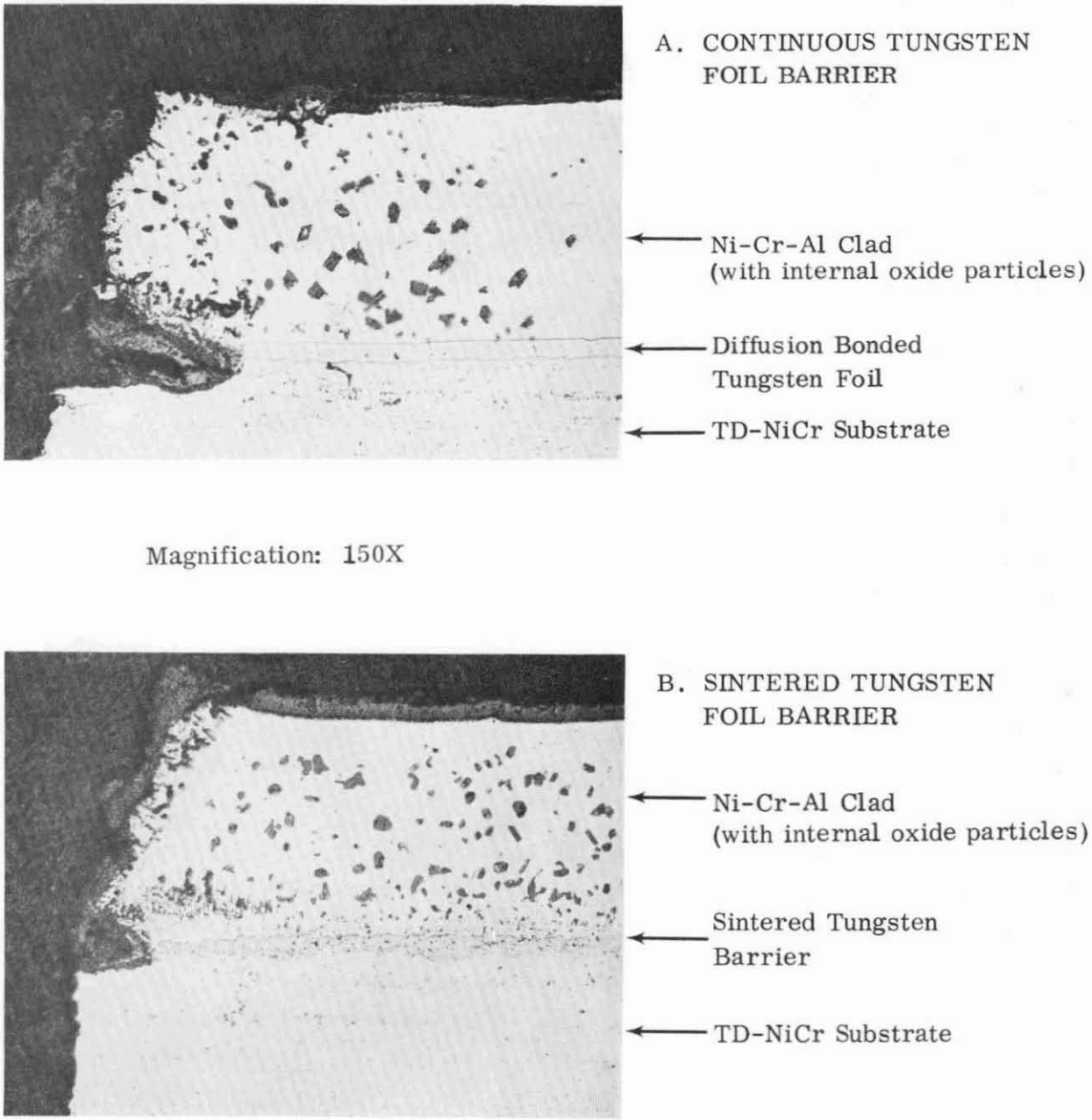

FIGURE 21. INTERFACIAL OXIDATION ON TD-NiCr WITH TUNGSTEN DIFFUSION BARRIERS AND Ni-Cr-Al CLAD; 100 Hours Exposure at 2100°F in Air

3.4 COATING DEVELOPMENT

The coating development activities were aimed at producing a composite coating system consisting of the slurry applied tungsten diffusion barrier and an oxidation resistant gamma Ni(Cr, Al) overcoating. The goal was a 0.004 to 0.006-inch (1.0×10^{-4} to 1.5×10^{-4} m) thick coating, with the inner 0.0005 to 0.001 inch (1.3×10^{-5} to 2.5×10^{-5} m) being the diffusion barrier. Test specimens used in coating development were 1/2 x 1/2-inch (0.013 x 0.013 m) coupons.

3.4.1 Selection of Coating Compositions

Two types of coatings have most successfully provided oxidation protection for TD-Ni and TD-NiCr at high temperatures (2000°F (1366°K) or higher). These are an aluminide coating (Cr-Al) and a solid-solution coating (NiCrAl). The Cr-Al coating, which has been the most extensively investigated system (Refs. 1 through 4), is applied by a duplex process consisting of a chromizing step and a subsequent aluminizing step (both normally utilizing pack techniques). Typically, the resulting coating consists of an outer layer of nickel aluminide, an intermediate layer of alpha chromium, and an aluminum and chromium enriched surface layer in the gamma nickel substrate. The Ni-Cr-Al coating consists of a single phase, a gamma nickel solid solution. It has been applied as a cladding alloy by diffusion bonding (Ref. 5) and by a duplex process in which Ni-Cr-Si and then aluminum are applied by fusion slurries (Ref. 6). Solid-solution coatings were selected for use in this program for two reasons: they are more ductile than aluminides and, having less aluminum, they have less potential for extensive Kirkendall void formation which can cause spalling.

The compositions originally selected were based on the alloy development work of Hill, et al (Ref. 5), who found that Fe-25Cr-4Al and Ni-20Cr-5Al alloys (modified with minor additions) had oxidation lifetimes in excess of 500 hours (1.8×10^6 sec) at 2300°F (1533°K). A total of ten coating compositions, five iron-base and five nickel-base, had been proposed for development and evaluation. However, the lack of success in inhibiting the diffusion of aluminum from the Fe-Cr-Al clad into the TD-alloy substrates with even the best diffusion barrier dictated that the iron-base compositions be dropped from the program. It was, therefore, decided (with concurrence of the NASA Program Manager) to investigate ten nickel-base coating compositions rather than five nickel- and five iron-base compositions. The ten compositions selected are shown in Table V. They provided a range of chromium and aluminum concentrations as well as major oxide additions (Al_2O_3 and MgO) and minor additions of thorium and hafnium.

3.4.2 Modifier Development

A duplex coating process had been proposed for applying the coatings: the first step to consist of the vacuum sintering of a Ni-Cr (plus additives) slurry applied bisque; the second a fusion slurry aluminizing process. The vacuum sintering technique was later changed to a fusion technique which proved to be more promising. In

this section, the development of application techniques for the first step coating, or modifier, is described.

Vacuum Sintering Study

In order to establish a time-temperature cycle which was optimum in terms of maximum modifier density and minimum weight loss, a preliminary vacuum sintering study was made.

TABLE V

COATING COMPOSITIONS

Coating Number	Composition (wt%)					
	Ni	Cr	Al	Al_2O_3	MgO	Other
1	80.0	15	5	-	-	-
2	77.0	15	8	-	-	-
3	73.0	22	5	-	-	-
4	70.0	22	8	-	-	-
5	65.0	30	5	-	-	-
6	62.0	30	8	-	-	-
7	60.0	22	8	10	-	-
8	60.0	22	8	-	10	-
9	69.5	22	8	-	-	0.5Th
10	69.5	22	8	-	-	0.5Hf

Two representative modifier slurry compositions (see Table VI), Ni-20Cr (NC-1) and Ni-30Cr (NC-2), were prepared by mixing -325 mesh elemental powders in an ethyl cellulose-xylene vehicle and milling for 8 hours. TD-Ni and TD-NiCr specimens were prepared by application of the W-8 (W-13Ni) diffusion barrier. The Ni-20Cr and Ni-30Cr modifiers were then applied to both substrates by spraying and they firing in vacuum at $<10^{-4}$ torr (<0.013 N/m^2) for 4 hours. Three firing temperatures were used: 2100, 2200 and 2300° F (1422, 1477 and 1533° K). The primary points of interest in the sintering study were the effects of temperature on the density of the fired modifier and on the weight loss of the modifier during firing. Weight loss measurements revealed that an excessive amount of the bisque was vaporized at 2300° F

(1533° K) (~50 percent) and at 2200° F (1477° K) (~25 percent). At 2100° F (1422° K), the total weight loss was not too great, but approximately 30 percent of the chromium was lost, thereby significantly changing the modifier composition (Ni-30Cr had gone to Ni-23Cr during the firing cycle). Metallographic examination of the modifiers sintered at the three different temperatures (Fig. 22) showed very little difference in density between the three. These results indicated that a 2000° F (1366° K), 4-hour (1.4×10^4 sec) sintering cycle would probably eliminate the significant compositional changes caused by preferential chromium vaporization without significantly reducing the fired density of the modifier. Subsequent sintering runs were thus made at the 2000° F (1366° K) temperature.

TABLE VI

MODIFIER (FIRST-STEP COATING) COMPOSITIONS

Modifier Designation	Composition (wt%)					
	Ni	Cr	Al_2O_3	MgO	Si	Other
NC-1	80.0	20.0	-	-	-	-
NC-2	70.0	30.0	-	-	-	-
NC-3	84.0	16.0	-	-	-	-
NC-4	77.0	23.0	-	-	-	-
NC-5	68.0	32.0	-	-	-	-
NC-6	66.0	24.0	10.0	-	-	-
NC-8*	74.5	22.0	-	-	3	0.5Th
NC-9*	74.5	22.0	-	-	3	0.5Hf
NC-10	83.0	16.0	-	-	1	-
NC-11	67.0	32.0	-	-	1	-
NC-12	65.0	23.5	9.5	-	2	-
NC-13	68.0	25.0	5.0	-	3	-
NC-14	68.0	25.0	-	5	3	-
NC-15*	82.0	15.0	-	-	3	-
NC-16*	75.0	22.0	-	-	3	-
NC-17*	66.0	31.0	-	-	3	-
NC-18	77.0	22.0	-	-	1	-

*These compositions were used to coat tensile specimens which were then aluminized and subsequently tested in cyclic oxidation.

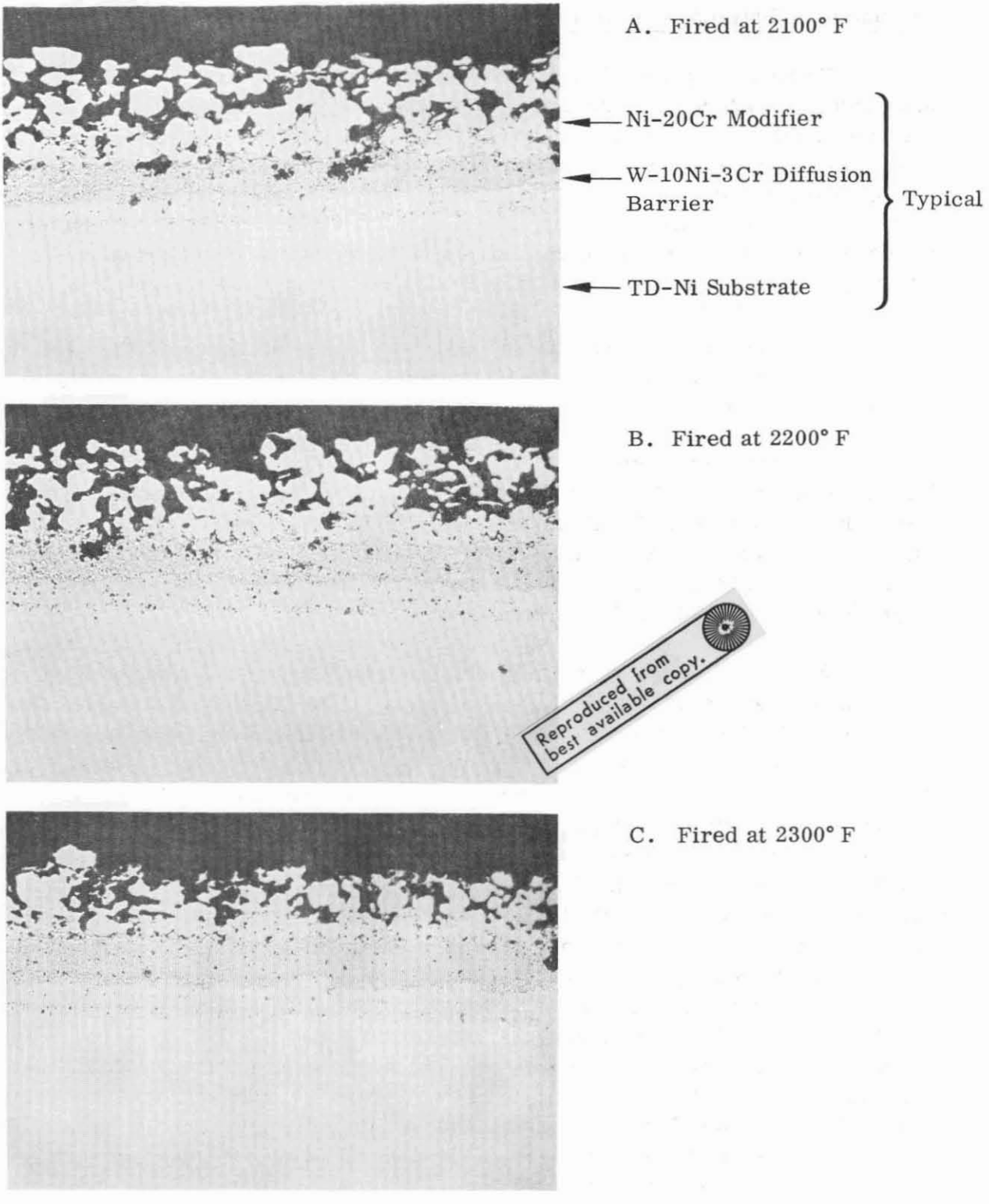

FIGURE 22. SLURRY APPLIED Ni-20Cr MODIFIER ON W-11 COATED TD-Ni; Fired in Vacuum for 4 Hours at Temperature Indicated (Magnification: 150X)

Evaluation of Sintered Modifiers

To effectively provide protection from oxidation, a coating must be uniform and dense. To determine if the sintered modifiers would be dense after aluminizing, a series of TD-Ni and TD-NiCr specimens were prepared with sintered modifiers applied over the W-11 tungsten barrier and then aluminized. The modifiers NC-3, NC-5, NC-6, NC-10, NC-11, and NC-12 (see Table VI) were prepared. They represent a range of Ni-Cr compositions, an oxide addition and an addition (silicon) designed to accelerate sintering by the formation of a small amount of liquid phase (Ni-Si eutectic). After spray application of the modifiers, the specimens were fired in vacuum at 2000°F (1366°K) for 4 hours (1.4×10^4 sec), yielding fired modifier weights from 46 to 60 mg/cm^2 (0.45 to 0.60 kg/m^2). The oxide-containing modifiers exhibited excessively porous surfaces from which oxide particles could be readily removed by light wire brushing.

The modifiers were then aluminized by a fusion slurry technique. A 50Al-50 flux composition in a methyl alcohol vehicle was applied by spraying and fired in a welded Inconel 600 retort for 10 minutes (600 sec) at 1400°F (1033°K) (part temperature) using a titanium gettered argon atmosphere. The bisque weights varied from 8 to 12 mg/cm^2 (0.08 to 0.12 kg/m^2) and the fired coating weights varied from 3 to 6 mg/cm^2 (0.03 to 0.06 kg/m^2).

Figure 23 shows the microstructure of TD-Ni specimens with the W-11 diffusion barrier and modifiers NC-3 (Ni-16Cr) and NC-10 (Ni-16Cr-1Si) after aluminizing, but before diffusion. Three major metallographic features of interest were noted on these specimens. First, the silicon addition significantly increased the density of the fired modifier. Unfortunately, the region of greatest porosity was the outer 20 to 40 percent of the modifier, and there were still many surface connected pores extending well into the modifier. Second, even with the increased density provided by the silicon addition, the coating configuration after aluminizing was poor. The amount of aluminum deposited, as determined by the thickness of the dark aluminide phase, varied greatly from area to area. Also, the small amount of aluminum deposited was not sufficient to yield a dense coating. As a result, many surface connected pores remained after aluminizing, thereby reducing the effective thickness of the coating by as much as 40 percent. The third feature of note was the extensive Kirkendall void formation in the substrate near the substrate/diffusion barrier interface. It is believed that the void formation was caused by the difference in the outward diffusion rate of nickel and the inward diffusion rate of tungsten, with the nickel diffusing more rapidly than the tungsten. The void formation was extensive enough to cause shearing of the barrier/coating layer from the substrate during thermal cycling.

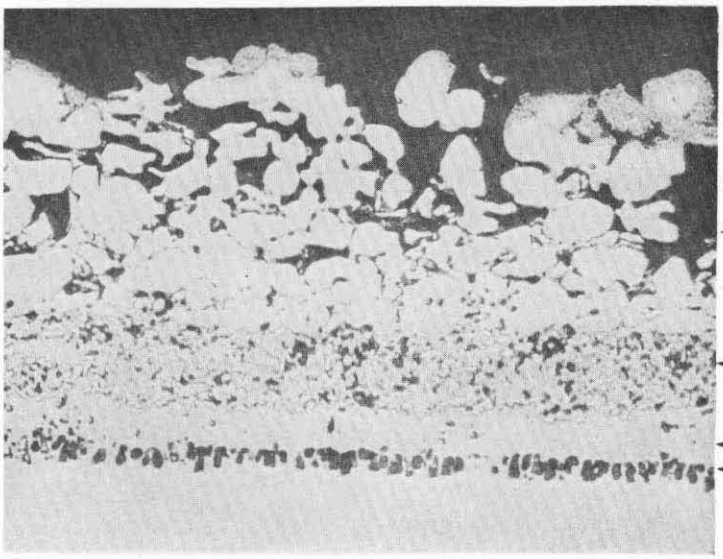

A. Ni-16Cr Modifier Applied by Vacuum Sintering

← Porous Modifier (with nickel aluminide phase on surface)

← Slurry Tungsten Diffusion Barrier

← TD-Ni Substrate
← Substrate Porosity

Magnification: 250X

Note: The dark outer layer is a nickel aluminide phase.

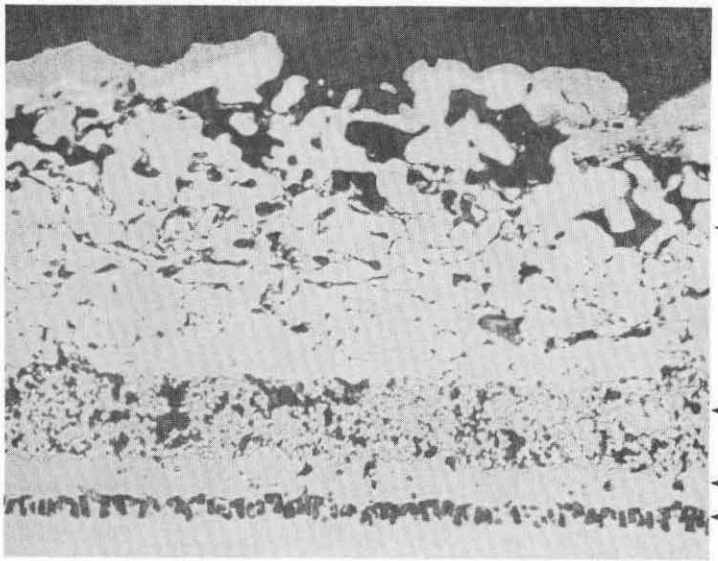

B. Ni-16Cr-1Si Modifier Applied by Vacuum Sintering

← Porous Modifier (with nickel aluminide phase on surface)

← Slurry Tungsten Diffusion Barrier

← TD-Ni Substrate
← Substrate Porosity

FIGURE 23. ALUMINIZED Ni-Cr MODIFIERS ON W-11 COATED TD-Ni

Because of the problems encountered with sintered modifiers, namely, surface connected porosity and a lack of coating density and uniformity, fusion techniques for modifier application were investigated.

Modifier Application by Vacuum Fusion

To determine the fusion temperatures of various Ni-Cr-Si modifier compositions, three firings were made in the Research Laboratory's small vacuum furnace (SVF). The modifiers NC-15, NC-16, and NC-17 (Table VI) were prepared in slurry form, applied to both substrate alloys over the W-11 tungsten diffusion barrier, and fired at 2300 (1533), 2350 (1561), and 2400° F (1589° K) for 10 minutes at $<10^{-4}$ Torr (<0.013 N/m^2). Visual examination revealed that all three modifiers had fused at 2350 and 2400° F (1561 and 1589° K), but none had fused at 2300° F (1533° K). The specimens with fused modifiers were then aluminized by the fusion slurry process previously described and were examined metallographically. Two TD-NiCr specimens with modifiers fired at 2350° F (1561° K) are shown in Figure 24 (after aluminizing). As these photomicrographs clearly show, the as-aluminized coatings were uniform and dense and the substrate was free of Kirkendall voids which were encountered on specimens with the sintered modifier; however, the amount of coating deposited on the specimens in the initial runs, shown in Figure 24, was somewhat low (40 to 50 mg/cm^2), resulting in a coating thickness of about 0.002 inch (5.0×10^{-5} m). Specimens for oxidation testing were to be protected by 0.004 to 0.006 inch (1.0×10^{-4} to 1.5×10^{-4} m) thick coatings.

Based on the visual and metallographic examination of both sintered and fused modifiers, the fusion technique was clearly the superior application process. This process was, therefore, selected for application of the modifiers for oxidation test specimens.

Modifiers With Oxide Additions

A problem was encountered in the application of modifiers containing oxide (Al_2O_3 and MgO) additions. Previously, it had been found that a sintered modifier containing 10 weight percent Al_2O_3 was both porous and non-adherent. As a second attempt at including oxides, the coatings NC-13 and NC-14, with 3 weight percent silicon and 5 weight percent oxide additions, were prepared. They were applied to both substrates and fired at 2400° F (1589° K) for 10 minutes (600 sec) at $<10^{-4}$ torr (<0.013 N/m^2). It appeared that localized fusion of the metallic components had taken place but that little metal-to-oxide bonding had occurred. The result was a modifier with an unacceptably porous surface from which the loose oxide could be removed by light wire brushing with relative ease. To include a significant amount of oxide, it would be necessary to promote wetting of the oxide surface with the metallic phase. One approach could be based on the work of Sutton and Feingold (Ref. 13), who

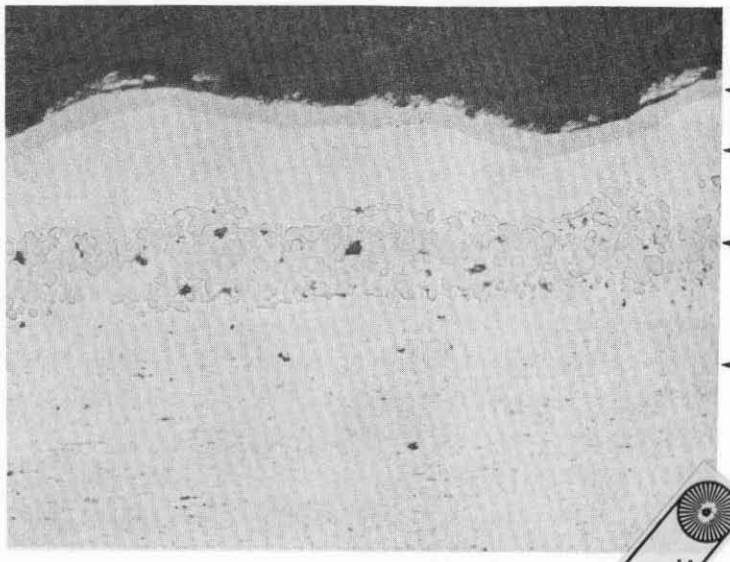

A. Ni-15Cr-3Si (NC-15) Modifier Applied by Vacuum Fusion

←Nickel Aluminide

←Fused Modifier

←Slurry Tungsten Diffusion Barrier

←TD-NiCr Substrate

Magnification: 250X

Note: The dark outer layer is a nickel aluminide phase.

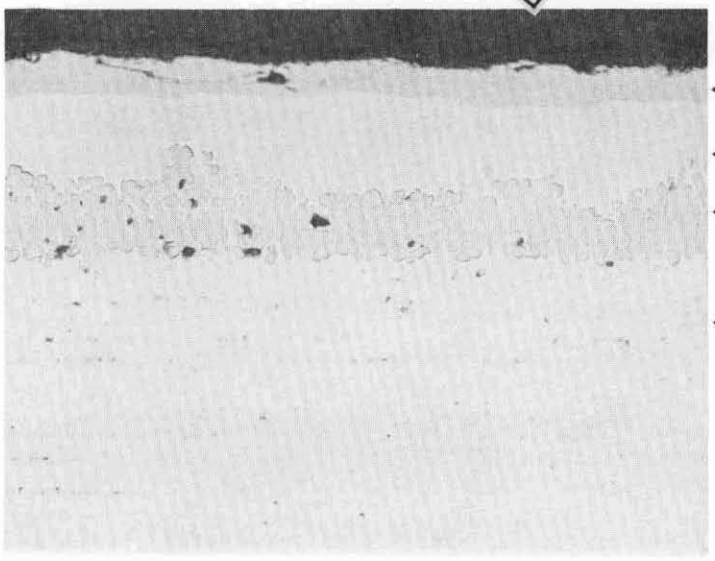

B. Ni-22Cr-3Si (NC-16) Modifier Applied by Vacuum Fusion

←Nickel Aluminide

←Fused Modifier

←Slurry Tungsten Diffusion Barrier

←TD-NiCr Substrate

FIGURE 24. ALUMINIZED Ni-Cr MODIFIERS ON W-11 COATED TD-NiCr

found that addition of a small quantity of either titanium or zirconium to nickel resulted in the wetting of Al_2O_3 by the molten Ni-(Ti or Zr) alloy. Time limitations did not permit further development of oxide containing modifiers, however.

3.4.3 Application of Modifiers to Tensile Specimens

Specimen Preparation

Fifty tensile specimens of each TD-alloy were machined to the configuration shown in Figure 25. The test direction corresponds to the rolling direction. To provide rounded edges for coating, the machined specimens were tumbled for 100 hours in a Sweco vibratory finisher which contained various sizes of ceramic grinding media in a water slurry. Prior to coating, the specimens were pickled to remove all oxide scale. A mixture of $3HNO_3$-$1H_2SO_4$ (by volume) was used for this purpose. Forty specimens of each alloy were coated with the W-11 tungsten diffusion barrier and fired in vacuum for 3 hours (1.1×10^4 sec) at 2300° F (1533° K). The range of weight gains on these specimens was 44 ± 8 mg/cm^2 (0.44 ± 0.08 kg/m^2), as shown later in Table IX. There was no additional surface treatment after barrier coating.

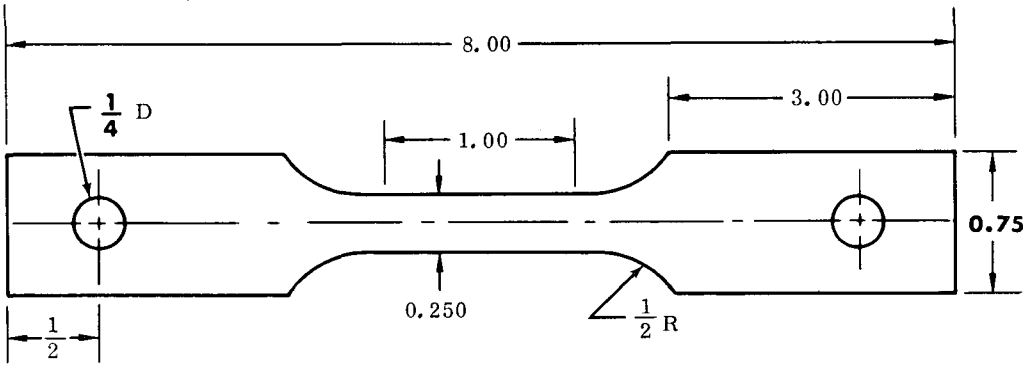

FIGURE 25. OXIDATION AND TENSILE TEST SPECIMEN

Modifier Firings

Before coating the program tensile specimens, additional modifier firings were made to verify firing temperatures and determine reproducibility of results. A problem was encountered when several test coupons of each alloy were fired at 2375° F (1575° K). Increased attack was noted on the W-11 diffusion barrier layer on specimens coated with NC-15, NC-16, and NC-17 modifiers (Figs. 26 and 27). With the NC-15 and NC-17 coatings, the tungsten diffusion barrier was widely dispersed and extended out to the surface of the coating. The outward movement of the diffusion barrier was probably due, at least in part, to the gravity movement of the dense tungsten particles. The specimens shown in Figures 26 and 27 were fired horizontally with the coating in the downward position, whereas the specimens shown previously

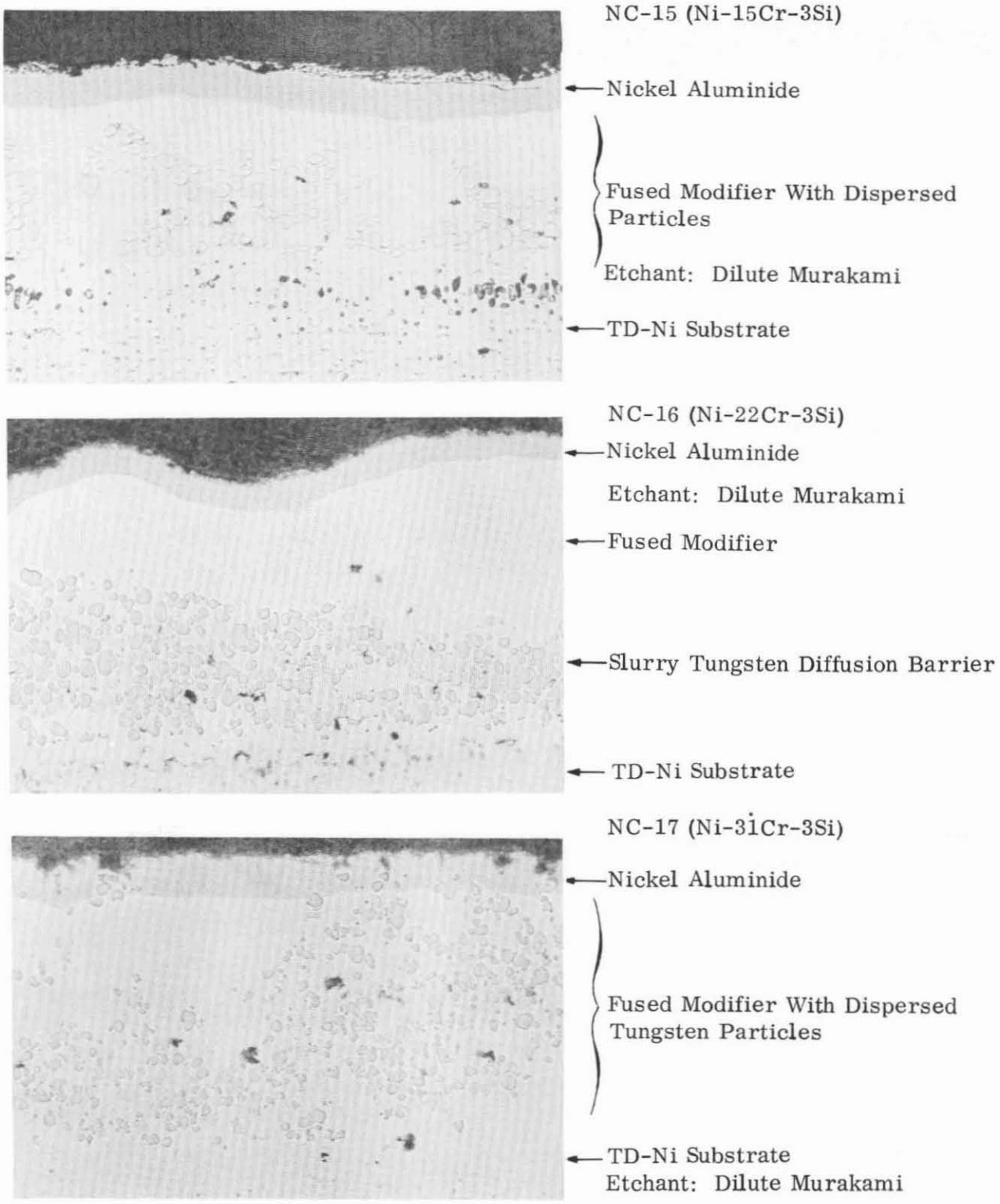

FIGURE 26. ALUMINIZED MODIFIERS NC-15, NC-16 AND NC-17 ON W-11 COATED TD-Ni; Modifier Fired at 2375° F (Magnification: 250X)

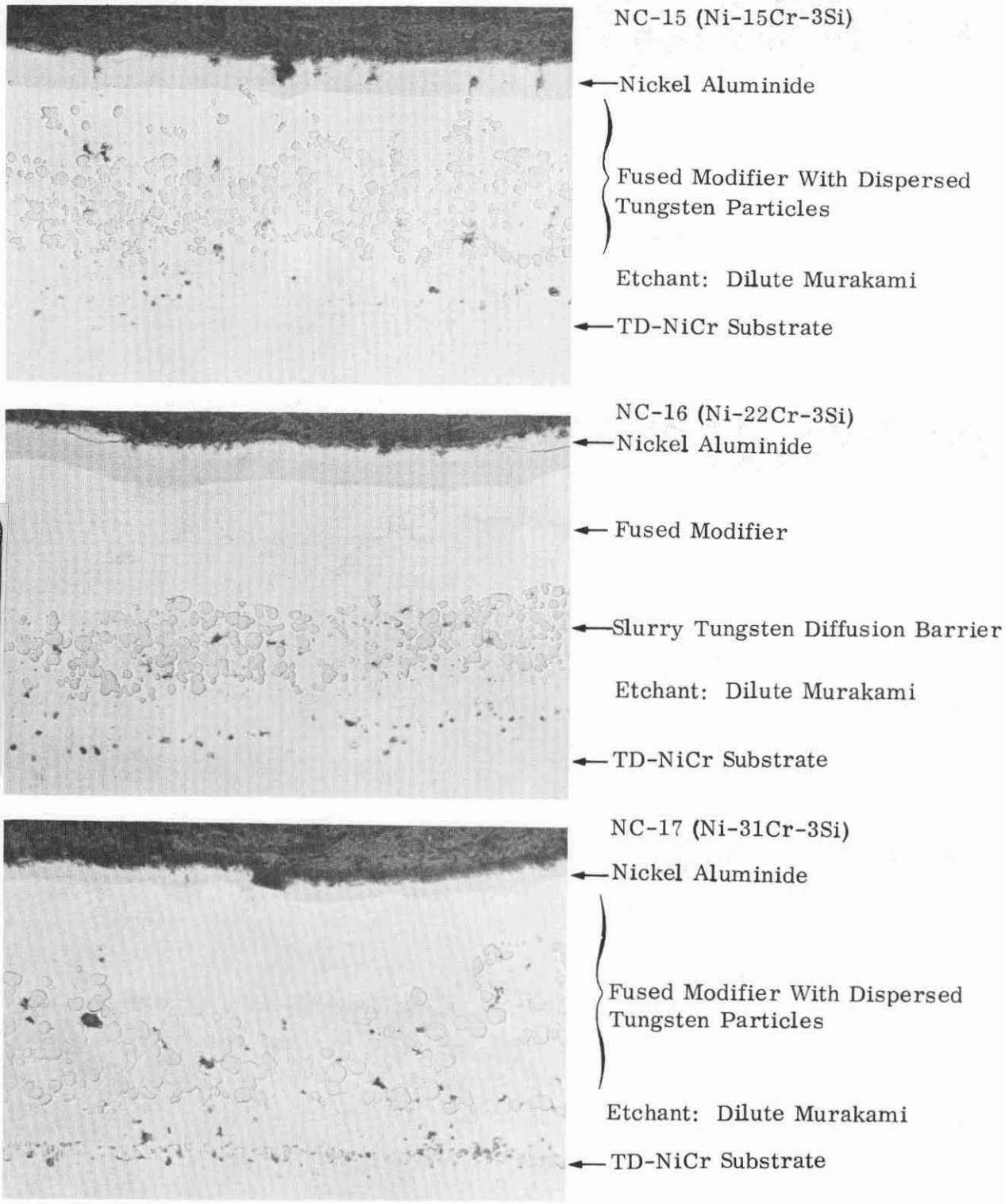

FIGURE 27. ALUMINIZED MODIFIERS NC-15, NC-16 AND NC-17 ON W-11 COATED TD-NiCr; Modifier Fired at 2375° F (Magnification: 250X)

in Figure 24 (without barrier disruption) were fired with the coating facing up. The NC-16 coating retained more of the tungsten at the interface than the other two coatings, indicating slightly less fluidity for this coating.

The problem of dispersion of the tungsten diffusion barrier was considered serious because of the loss of part of the barrier and also because the presence of tungsten particles near the surface of the modifier could lower the oxidation resistance of the coating. Therefore, several experiments were made in order to eliminate the movement of the tungsten particles from the interface:

- Sintering of NC-18 at 2000° F (1366° K) for 4 hours (1.4×10^4 sec) prior to fusion of NC-16 and aluminizing with the S8100 coating.
- Sintering of NC-18 at 2000° F (1366° K) for 4 hours (1.4×10^4 sec) prior to fusion of a nickel-chromium-aluminum composition at 2375° F (1575° K) for 10 minutes (600 sec).
- Sintering of NC-18 at 2000° F (1366° K) for 4 hours (1.4×10^4 sec) prior to application of a pure aluminum coating and fusing in vacuum at 2000 or 2375° F (1366 or 1575° K).
- Sintering of NC-4 at 2050° F (1395° K) for 4 hours (1.4×10^4 sec) prior to aluminizing with the S8100 coating.

None of the above produced an acceptable coating. Significant porosity remained in the NC-18 sintered modifier which made the coating sensitive to shear fracture.

One additional vacuum firing was made at 2260° F (1511° K) with the NC-16 modifier on specimens supported both horizontally and vertically. The surface of the specimens appeared somewhat rough after firing. However, metallographic examination revealed a relatively dense modifier and a virtually undisturbed diffusion barrier (Fig. 28). The results of this run showed that partial fusion was sufficient to yield an acceptably dense modifier without disrupting the barrier layer.

Based on these results, four firing runs were made with various numbers of program tensile specimens in a run (supported vertically). The object was to approach the fusion temperature to promote densification but to remain below it to prevent modifier flow and barrier disruption. The results, summarized in Table VII, led to the following conclusions: (1) vaporization losses in the firing runs with eight or sixteen specimens were only about half as great as in the two-specimen run; (2) chromium and/or silicon vaporized preferentially, so that a higher weight loss caused an increased fusion temperature in the two-specimen run; (3) 2360° F (1566° K) was the approximate upper temperature limit for a multi-specimen run. Figures 29 and 30 are macrophotographs of specimens fired in two of the runs showing a modifier which exhibited severe beading and an acceptable modifier.

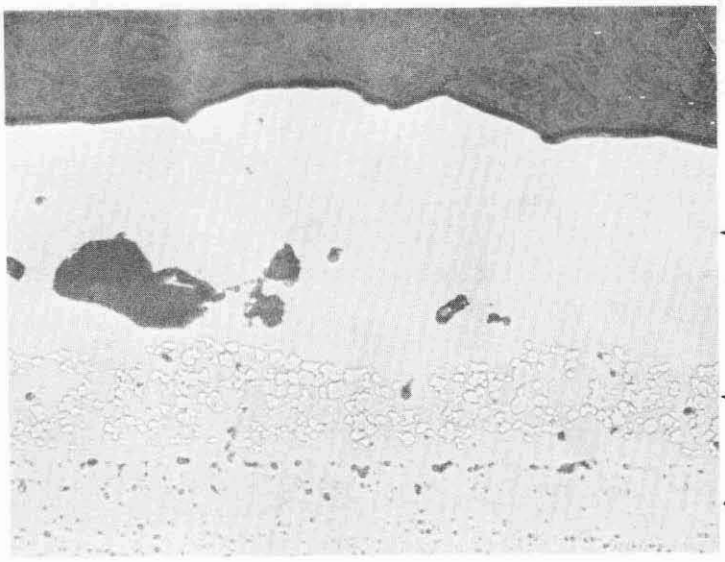

Up Side of Horizontally Fired Specimen

Etchant: Dilute Murakame

←Fused Modifier (with some porosity)

←Slurry Tungsten Diffusion Barrier

←TD-NiCr Substrate

Magnification: 250X

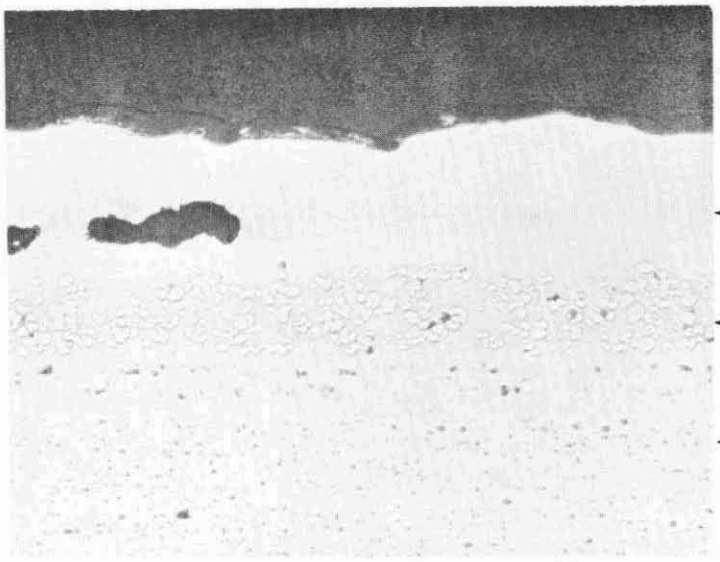

Down Side of Horizontally Fired Specime

Etchant: Dilute Murakami

←Fused Modifier (with some porosity)

←Slurry Tungsten Diffusion Barrier

←TD-NiCr Substrate

FIGURE 28. NC-16 MODIFIER ON W-11 COATED TD-NiCr;
Modifier Fired at 2260° F (Sheet 1 of 2)

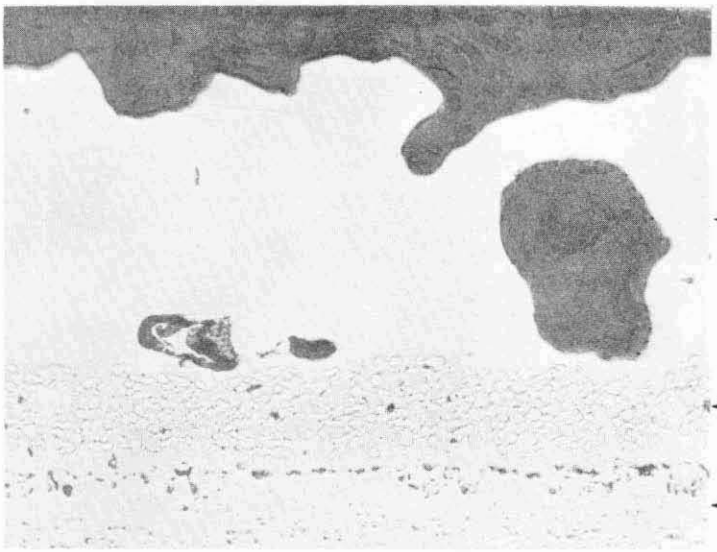

Top End of 3-Inch Long
Vertically Supported Specimen

Etchant: Dilute Murakami

←Fused Modifier (with some porosity)

←Slurry Tungsten Diffusion Barrier

←TD-NiCr Substrate

Magnification: 250X

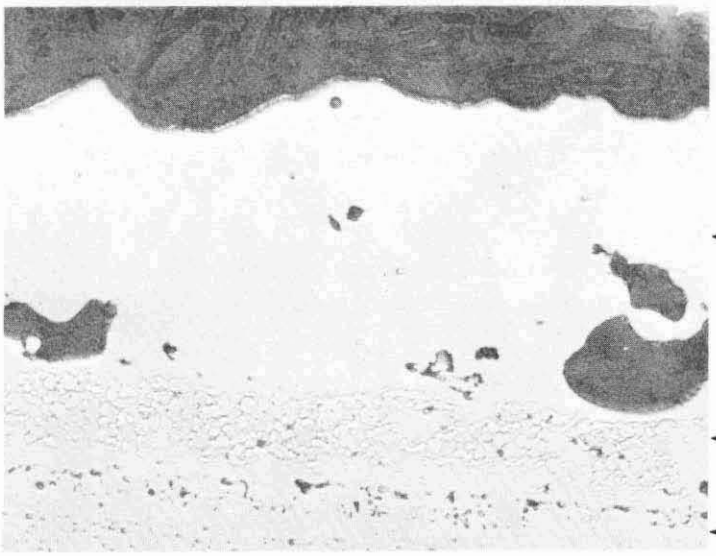

Bottom End of 3-Inch Long
Vertically Supported Specimen

Etchant: Dilute Murakami

←Fused Modifier (with some porosity)

←Slurry Tungsten Diffusion Barrier

←TD-NiCr Substrate

FIGURE 28. NC-16 MODIFIER ON W-11 COATED TD-NiCr;
Modifier Fired at 2260° F (Sheet 2 of 2)

TABLE VII

PRELIMINARY MODIFIER FIRINGS ON PROGRAM TENSILE SPECIMENS

Firing No.	Specimens Fired	Modifier	Firing Temperature (°F)	Firing Temperature (°K)	Average Weight Loss (mg/cm^2)(10^{-2} hg/m^2)	Remarks
A	TD-Ni 51 TD-NiCr C51	NC-16 NC-17	2375	1575	6.0 8.8	Slightly rough surface; no flowdown. Considerable flowdown.
B	TD-Ni 1-8	NC-15	2375	1575	2.8	Considerable flowdown on all specimens.
C	TD-NiCr C1-C8	NC-15	2360	1566	3.6	Slightly rough surface; no flowdown.
D	TD-Ni 9-16	NC-16	2365	1569	3.0	Considerable flowdown on all specimens.

Notes: (1) All specimens had previously been coated with the W-11 diffusion barrier.
(2) Firing time was 10 minutes (600 seconds) for all runs.
(3) Firings B, C and D were 8-specimen runs while Firing A was a 2-specimen run.

Based on the above results, the temperature range 2350 to 2360°F (1561 to 1566°K) was selected for firing of the modifiers on the barrier coated substrates. The remaining tensile specimens were, with a few exceptions, fired successfully in this range. Table VIII summarizes these firing runs. As noted in the table, flowdown occurred with isolated specimens, but for each modifier there was a sufficient number of good specimens for oxidation testing. The typical appearance of the modifiers after firing was as shown in Figure 30, with a slightly rough surface which is characteristic of the partially fused coating. The weight gains for individual specimens are given in Table IX.

At this point, the specimens which would ultimately be oxidation tested were selected. The selection criteria were as follows: first, no obvious coating defects such as blistering, running, or large pinholes; and second, minimum surface porosity.

3.4.4 Aluminizing of Tensile Specimens

The Solar S8100 aluminizing slurry, consisting of 50 weight percent aluminum and 50 weight percent halide flux in a methanol vehicle, was used to aluminize the barrier and modifier coated tensile specimens. Experience had shown that 35 to 45 percent of the bisque was retained as aluminum after firing. Therefore, the slurry was applied (by spraying) in quantities such that the dry bisque weight was approximately 2.5 times the final weight of aluminum desired. Based on the range of modifier weights, the desired aluminum levels in the overall coating (5 and 8 weight percent), and the 2.5 to 1 bisque to deposited aluminum ratio, the applied bisque weights ranged from 10 to 16 mg/cm^2 (0.10 to 0.16 kg/m^2).

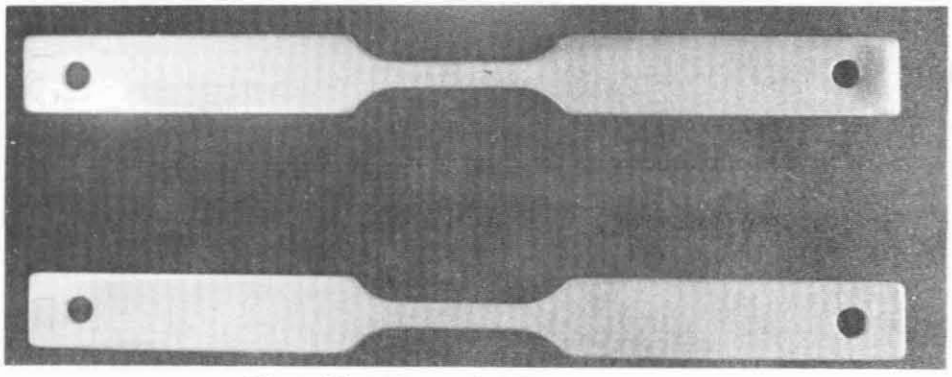

NC-17 Modifier
2375° F, 10 Minutes
Severe Beading

NC-16 Modifier
2375° F, 10 Minutes
Satisfactory Firing

Magnification: 0.7X

NC-17 Modifier
Severe Run Area
of Above Specimen

Magnification: 1.3X

FIGURE 29. TWO-SPECIMEN MODIFIER FIRING RUN

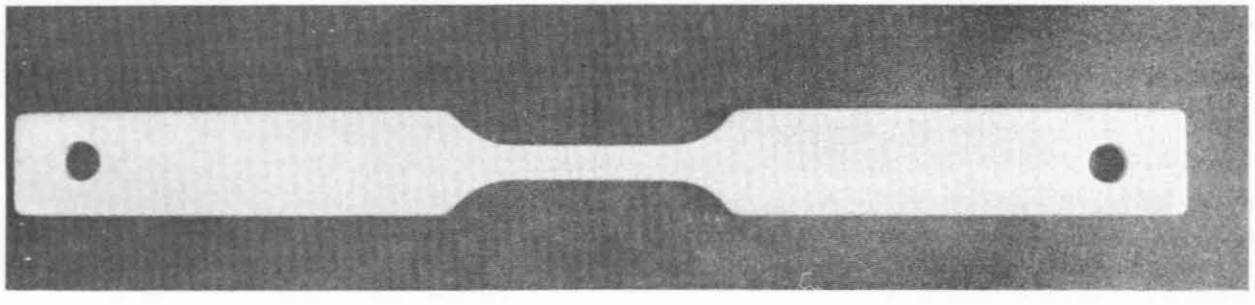

Magnification: 0.9X

FIGURE 30. REPRESENTATIVE SPECIMEN FROM AN EIGHT-SPECIMEN MODIFIER FIRING RUN AT 2360° F

TABLE VIII

MODIFIER FIRINGS ON PROGRAM TENSILE SPECIMENS

Firing No.	Specimens Fired	Modifier	Firing Temperature (°F)	Firing Temperature (°K)	Average Weight Loss (mg/cm^2)($10^{-2} kg/m^2$)	Remarks
1	TD-Ni 17-20	NC-17	2350	1561	4.3	Slightly rough surface; no flowdown.
2	TD-Ni 21-24	NC-17	2350	1561	4.0	Slightly rough surface; no flowdown.
3	TD-NiCr C17-C20	NC-17	2350	1561	5.6	Slightly rough surface; no flowdown.
4	TD-NiCr C21-C24	NC-17	2350	1561	5.4	Slightly rough surface; no flowdown.
5	TD-Ni 25-32	NC-15	2360	1566	1.7	Slightly rough surface; flowdown on 26 only.
6	TD-Ni 33-38	NC-16	2355	1564	3.3	Slightly rough surface; flowdown on 38 only.
7	TD-NiCr C25-C31	NC-16	2350	1561	4.6	Slightly rough surface; flowdown on C28 only.
8	TD-Ni 39-42 TD-Ni 43-46	NC-8 NC-9	2350	1561	3.4 4.0	Slightly rough surface; flowdown on 40, 44, and 46.
9	TD-NiCr C32-C35 TD-NiCr C36-C39	NC-8	2350	1561	3.6 3.9	Slightly rough surface; no flowdown.

Notes: (1) All specimens had been previously coated with the W-11 diffusion barrier.
(2) Firing time was 10 minutes (600 seconds) for all runs.

The specimens were fusion fired at 1400°F (1033°K) for 10 minutes (600 sec) in an argon atmosphere (fusion cycle). An Inconel 600 retort with a welded lid was used, and the argon gas was dried and gettered with hot (1350°F (1005°K)) titanium chips. After firing, the specimens were cleaned in hot water and lightly brushed to remove all remaining flux, then vacuum dried and weighed. The weight changes showed that the percent of bisque retained after firing was greater for the low aluminum level than for the higher level. As a result, the actual composition ranged from 4.5 to 6 percent for the low level (versus a target of 5 percent) and from 6.5 to 8.5 percent for the higher level (versus a target of 8 percent). The amount of aluminum deposited on each specimen is given in Table IX. The range was from 3.5 to 7.3 mg/cm^2 (0.035 to 0.073 kg/m^2).

After flux removal and weighing, the aluminized specimens were subjected to a diffusion cycle consisting of 4 hours (1.4×10^4 sec) at 2000°F (1366°K) in an argon atmosphere. The purpose of the diffusion cycle was to convert the nickel aluminide (Ni_xAl_y) surface layer to a homogeneous gamma-nickel solid solution. During the cycle, the dark gray as-fused surface had been changed to a shiny metallic surface. This change in surface appearance indicated that the solid solution or at least a high nickel aluminide had formed.

3.4.5 As-Coated Microstructure

Several tensile specimens which were not to be oxidation tested were examined metallographically in the as-coated condition. Figure 31 shows the coating structure on both TD-Ni and TD-NiCr which was typical for the flat surfaces. The coating

TABLE IX

SUMMARY OF COATING DATA FOR TENSILE SPECIMENS

Alloy	Specimen Number	Diffusion Barrier (W-11) Weight (mg/cm^2) (10^{-2} kg/m^2)	Modifier		Aluminum Weight (mg/cm^2) (10^{-2} kg/m^2)	Approximate Coating Composition (wt %) (Excluding W-11)				
			Designation	Weight (mg/cm^2) (10^{-2} kg/m^2)		Ni	Cr	Al	Si	Other
TD-Ni	25	39	NC-15	83	4.4	78	14	5	3	--
TD-Ni	26	39	NC-15	85	4.3	78	14	5	3	--
TD-Ni	27	39	NC-15	77	5.0	77	14	6	5	--
TD-Ni	28	43	NC-15	78	7.0	75	14	8	3	--
TD-Ni	29	40	NC-15	85	4.8	78	14	5	3	--
TD-Ni	30	42	NC-15	75	5.7	76	14	7	3	--
TD-Ni	31	39	NC-15	73	6.3	75	14	8	3	--
TD-Ni	32	42	NC-15	88	7.3	75	14	8	3	--
TD-NiCr	C1	40	NC-15	93	5.1	78	14	5	3	--
TD-NiCr	C2	45	NC-15	93	6.7	76	14	7	3	--
TD-NiCr	C3	40	NC-15	84	4.0	78	14	5	3	--
TD-NiCr	C4	40	NC-15	67	3.4	78	14	5	3	--
TD-NiCr	C5	41	NC-15	84	5.4	77	14	6	3	--
TD-NiCr	C6	36	NC-15	82	5.8	76	14	7	3	--
TD-NiCr	C7	35	NC-15	79	5.5	76	14	7	3	--
TD-NiCr	C8	37	NC-15	74	5.3	76	14	7	3	--
TD-Ni	33	42	NC-16	72	3.8	71	21	5	3	--
TD-Ni	34	43	NC-16	72	3.3	71	21	5	3	--
TD-Ni	35	41	NC-16	69	4.2	70	21	6	3	--
TD-Ni	36	44	NC-16	68	5.0	70	20	7	3	--
TD-Ni	37	45	NC-16	72	5.4	70	20	7	3	--
TD-Ni	38	45	NC-16	73	4.6	70	21	6	3	--
TD-Ni	51	41	NC-16	67	5.6	69	20	8	3	--
TD-Ni	52	38	NC-16	86	7.2	69	20	8	3	--
TD-NiCr	C25	41	NC-16	72	3.3	71	21	5	3	--
TD-NiCr	C26	37	NC-16	72	3.1	72	21	4	3	--
TD-NiCr	C27	38	NC-16	72	3.5	71	21	5	3	--
TD-NiCr	C28	39	NC-16	74	3.5	71	21	5	3	--
TD-NiCr	C29	39	NC-16	70	4.8	70	21	6	3	--
TD-NiCr	C30	45	NC-16	76	4.6	70	21	6	3	--
TD-NiCr	C31	37	NC-16	71	5.0	70	20	7	3	--
TD-NiCr	C52	42	NC-16	86	6.2	70	20	7	3	--
TD-Ni	17	45	NC-17	71	4.4	62	29	6	3	--
TD-Ni	18	44	NC-17	76	5.3	61	29	7	3	--
TD-Ni	19	50	NC-17	72	3.8	63	29	5	3	--
TD-Ni	20	49	NC-17	84	5.3	62	29	6	3	--
TD-Ni	21	36	NC-17	72	6.3	61	28	8	3	--
TD-Ni	22	42	NC-17	72	6.8	60	28	9	3	--
TD-Ni	23	41	NC-17	68	5.3	61	29	7	3	--
TD-Ni	24	40	NC-17	71	5.9	61	28	8	3	--
TD-NiCr	C17	38	NC-17	80	3.4	63	30	4	3	--
TD-NiCr	C18	39	NC-17	71	4.1	62	29	6	3	--
TD-NiCr	C19	44	NC-17	69	3.6	63	29	5	3	--
TD-NiCr	C20	38	NC-17	80	4.2	63	29	5	3	--
TD-NiCr	C21	39	NC-17	78	5.9	61	29	7	3	--
TD-NiCr	C22	42	NC-17	72	5.6	61	29	7	3	--
TD-NiCr	C23	43	NC-17	76	6.1	61	28	8	3	--
TD-NiCr	C24	41	NC-17	81	6.4	61	29	7	3	--
TD-Ni	39	47	NC-8	73	4.6	70	20.5	6	3	0.5Th
TD-Ni	40	43	NC-8	76	5.1	70	20.5	6	3	0.5Th
TD-Ni	41	44	NC-8	78	5.1	70	20.5	6	3	0.5Th
TD-Ni	42	44	NC-8	77	4.2	70.5	21	5	3	0.5Th
TD-NiCr	C32	38	NC-8	77	5.6	69.5	20	7	3	0.5Th
TD-NiCr	C33	40	NC-8	85	4.4	70.5	21	5	3	0.5Th
TD-NiCr	C34	42	NC-8	74	5.8	69.5	20	7	3	0.5Th
TD-NiCr	C35	41	NC-8	82	5.2	70	20.5	6	3	0.5Th
TD-Ni	43	42	NC-9	74	4.5	70	20.5	6	3	0.5Hf
TD-Ni	44	47	NC-9	78	5.0	70	20.5	6	3	0.5Hf
TD-Ni	45	46	NC-9	71	5.0	69.5	20	7	3	0.5Hf
TD-Ni	46	46	NC-9	75	4.7	70	20.5	6	3	0.5Hf
TD-NiCr	C36	38	NC-9	78	4.6	70	20.5	6	3	0.5Hf
TD-NiCr	C37	41	NC-9	79	5.9	69.5	20	7	3	0.5Hf
TD-NiCr	C38	44	NC-9	75	4.7	70	20.5	6	3	0.5Hf
TD-NiCr	C39	47	NC-9	81	5.9	69.5	20	7	3	0.5Hf

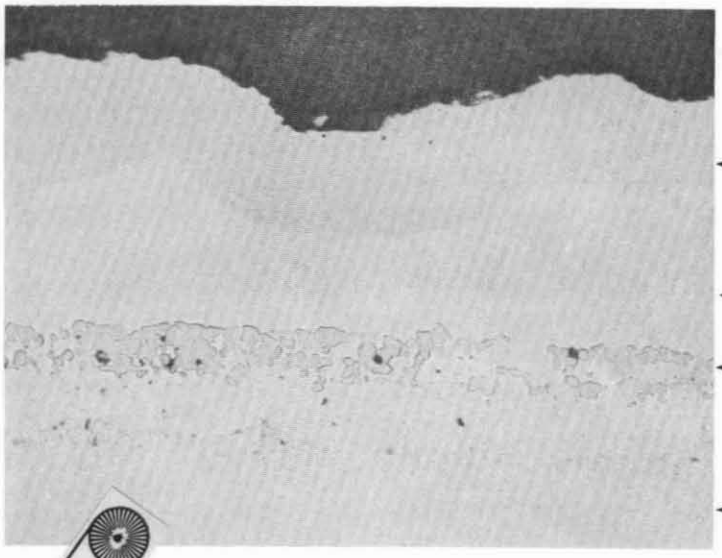

Flat Surface on TD-Ni
Specimen 32
7.3 mg/cm^2 of Al
←Probable β-NiAl Surface Layer
Unetched
←Fused Modifier
←Slurry Tungsten Diffusion Barrier
←TD-NiCr Substrate

Magnification: 250X

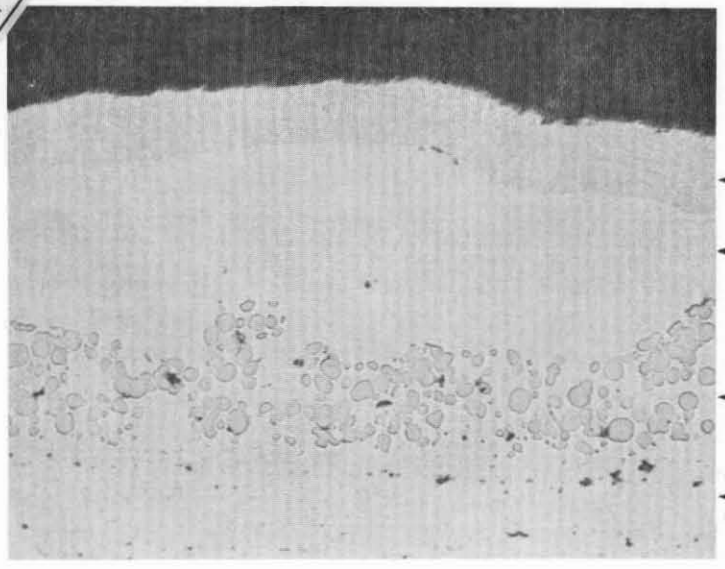

Flat Surface on TD-NiCr
Specimen C4
3.4 mg/cm^2 of Al
←Probable β-NiAl and Ni_3Al Surface Layer
←Fused Modifier
Unetched
←Slurry Tungsten Diffusion Barrier
←TD-NiCr Substrate

FIGURE 31. ALUMINIZED NC-15 MODIFIER ON W-11 COATED TD-Ni AND TD-NiCr

density and uniformity of aluminum distribution were excellent in most areas on these surfaces. The coatings possessed a slightly "wavy" surface, and the thickness varied from 0.004 to 0.007 inch (1.0×10^{-4} to 1.8×10^{-4} m). The separate outer phase indicated that the diffusion cycle had not produced a homogeneous gamma phase. Electron microprobe results showed that essentially all the aluminum remained in the dark outer phase on as-coated specimens. The EMP data and extensive past metallography of aluminide coatings at Solar indicate that the dark etching aluminum diffusion zone (Fig. 31, top) is β-NiAl and the lighter etching phase separating the β-NiAl from the γ-Ni alloy, or within the β-NiAl phase, (Fig. 31, bottom) is γ'-Ni_3Al. Conversion of the entire outer diffusion zone to γ-Ni alloy would have been desirable in the diffusion cycle to reduce aluminum concentration gradients and to slightly improve oxidation resistance, but time at 2000-2100° F to effect this conversion was considered prohibitive (>100 hours, Ref. 9). Both β-NiAl and Ni_3Al are quite oxidation resistant and conversion to γ-NiCrAl is quite rapid at 2300° F (Fig. 38) so that lack of the initial presence of γ-NiCrAl was not considered a serious limitation of the coatings.

The coatings were not entirely free from defects. The most serious defect observed on the as-coated specimens was a consistently thin modifier layer on the edges. In the early modifier development work, both the W-11 barrier and the modifier were found to be thin on the edges. Corrective measures were taken in coating the program tensile specimens, including additional spraying passes to ensure a sufficiently heavy bisque on the edges. The result, as seen in the top photograph of Figure 32, was an acceptable diffusion barrier layer but a modifier which was still too thin. The liquation which took place during modifier firings was sufficient to cause significant shrinkage, pulling the NC coatings from the edges to the flat surfaces.

A second coating defect observed was the occurrence of medium to large pores on the flat surfaces (see bottom photograph, Fig. 32). While not extensive, these pores were observed on every specimen examined. They were considered to be potentially harmful because of the depth in the coating to which they penetrated. Judging by their size and shape, the pores were a result of incomplete modifier densification.

3.5 COATING EVALUATION

The purpose of the coating evaluation phase of the program was twofold: first, to determine the ability of the coatings to provide oxidation protection; and second, to determine the effect of the coatings on the substrate mechanical properties both before and after exposure. To achieve this purpose, cyclic oxidation tests were performed at 2300° F (1533° K) on coated tensile specimens, and tensile tests were performed on both unexposed and exposed specimens, coated and uncoated, at room temperature and 2000° F (1366° K).

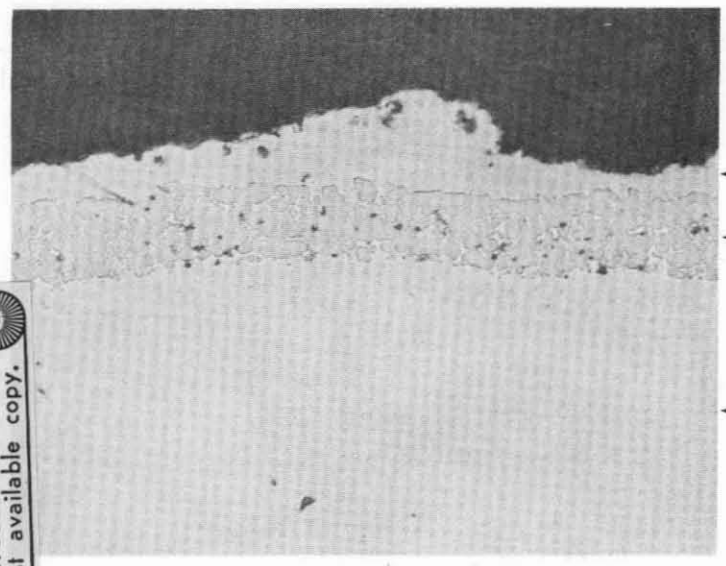

Poor Edge Coverage on TD-Ni
Specimen 32

← Very Thin Aluminized Modifier

← Slurry Tungsten Diffusion Barrier

Unetched

← TD-Ni Substrate

Magnification: 250X

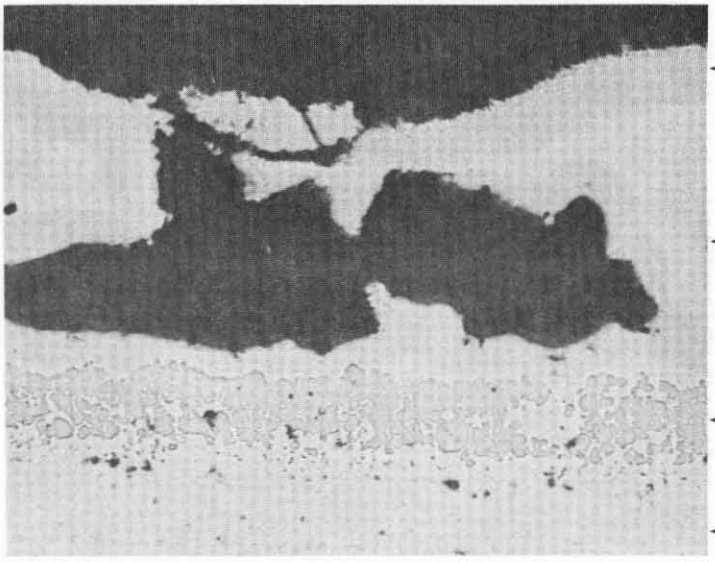

Porosity on TD-NiCr
Specimen C4

← Nickel Aluminide

← Fused Modifier with Very Deep
Surface-Connected Pore

Unetched

← Slurry Tungsten Diffusion Barrier

← TD-NiCr Substrate

FIGURE 32. COATING DEFECTS ON TD-Ni AND TD-NiCr
TENSILE SPECIMENS

3.5.1 Oxidation Test Procedure

The furnace and automatic cycling apparatus which were used in oxidation testing are shown in Figure 33. The furnace was a Lindberg Hevi Duty box type furnace with a 10-inch (0.25 m) high by 12-inch (0.30 m) wide by 24-inch (0.60 m) long heating chamber. It was heated by eight 1-1/2-inch (0.031 m) diameter silicon carbide heating elements, four across the top and four across the bottom of the hot zone. The temperature was proportionally controlled by a saturable core reactor power supply using a shielded Pt-Pt13Rh thermocouple as the temperature sensor.

The specimens were supported in a rack made from 0.1 x 1.0-inch (0.0025 x 0.025 m) Kanthal A-1 strip, as shown in Figure 33. The rack was tied by a connecting rod to an air actuated cylinder mounted beneath the furnace. Automatic cycling was achieved by using a motor driven cam and a system of four microswitches which controlled two double-acting air cylinders, one operating the furnace door and the other connected to the specimen rack. The total time for a cycle was 1 hour, the specimens being in the furnace for 55 minutes (3×10^3 sec) and out for 5 minutes (300 sec). The times in and out of the furnace had been adjusted so that the specimens would cool to about 250°F (394°K). Calibration runs with Inconel 600 "dummy" specimens had shown that a 5-minute fan assisted cooldown was required for specimen temperature to go from 2300 to 250°F (1533 to 394°K). The time versus specimen temperature curve for one cycle is shown in Figure 34 (based on a fully loaded rack of 40 specimens).

During the test, visual observations were made when specimens were on the "out" portion of the cycle, every two or three cycles at the beginning of the test and decreasing in frequency as the test progressed. Approximately every 8 hours the specimens were removed from the rack, brushed with a bristle brush to remove loose oxidation products, examined visually and weighed. The specimens, except those on which coating failure had occurred, were then replaced in the rack and cycling was begun once again.

3.5.2 Oxidation Test Results

Within three cycles, two distinct features were observed. First, it was obvious that there were areas with coating porosity which penetrated to the substrate because small nodules of black, glassy NiO had formed on TD-Ni specimens (see Fig. 35). At the 2300°F (1533°K) test temperature, NiO would be expected to form only by oxidation of the substrate or oxidation of the coating after significant depletion of both aluminum and chromium. And after only three hours, the aluminum and chromium would hardly be depleted from the coating. Second, it was apparent that edge coverage was poor on most specimens. On the flat surfaces, a light gray oxide (Al_2O_3) had formed. However, on the edges of many TD-Ni specimens a light green

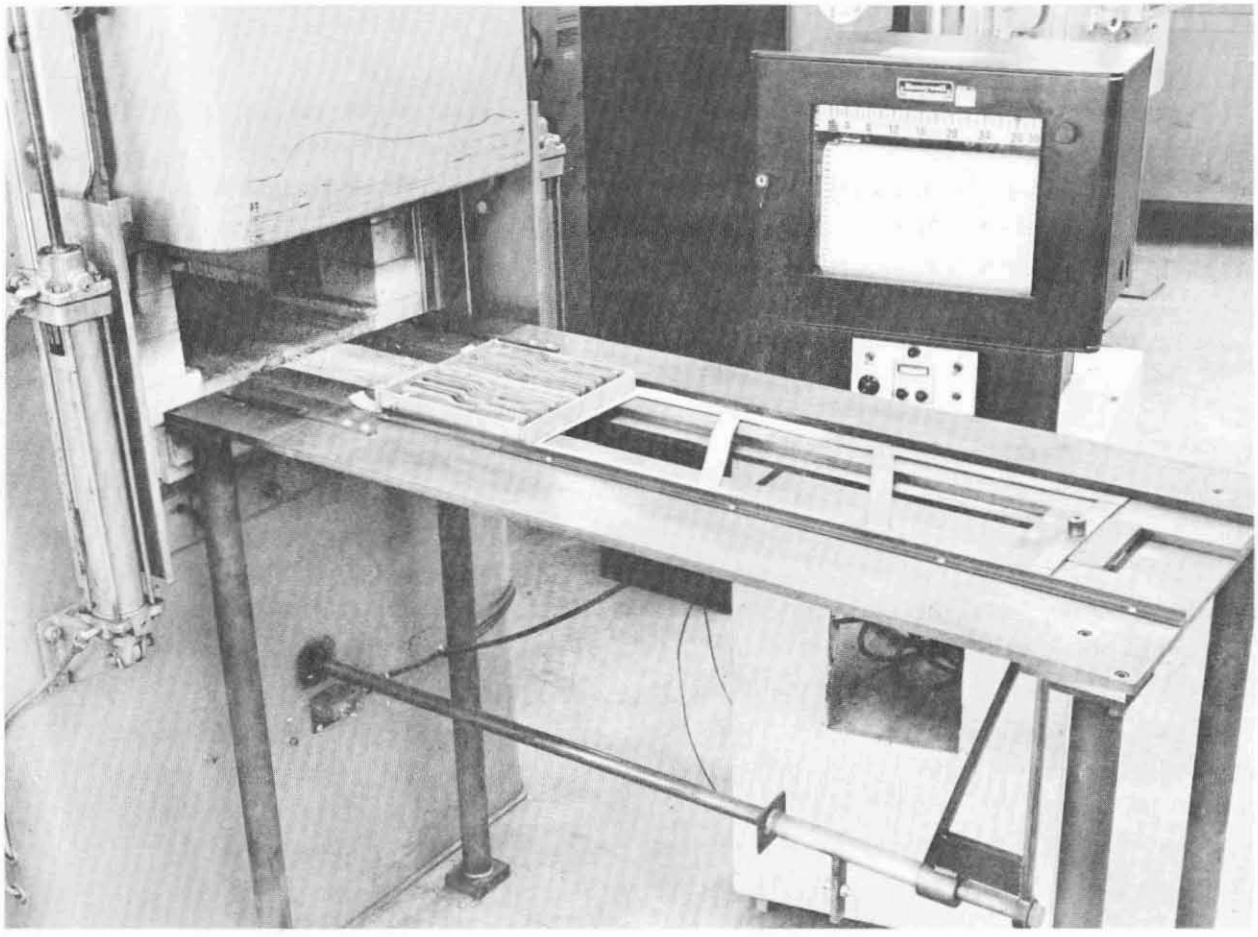

FIGURE 33. AUTOMATIC CYCLIC OXIDATION APPARATUS

NiO had formed, and on the edges of many TD-NiCr specimens a dark green oxide, very likely Cr_2O_3, had formed. The NiO and Cr_2O_3 formed on the edges indicating substrate oxidation resulting from thin coating coverage in these areas. Most TD-Ni specimens and several TD-NiCr specimens were taken out of test after three cycles (see Table X) because of obvious oxidation damage due to coating defects on edges and/or in areas on the flat surfaces.

The remaining specimens were cycled until obvious coating failure had occurred. In each case, the criterion for failure was coating deterioration as determined by visual observation. Weight change measurements were less meaningful because the deteriorated coating areas, while covering only a portion of the total surface area, were probably responsible for most of the weight loss. A summary of the oxidation test results is given in Table X, and Figure 36 gives the weight change versus time plots for the uncoated specimens and typical coated specimens. Specimens with the longest exposure times, 30 hours (1.1×10^5 sec) for TD-Ni, 44 hours (1.6×10^5 sec) for TD-NiCr, exhibited coating failure only in isolated areas, usually at nor near the

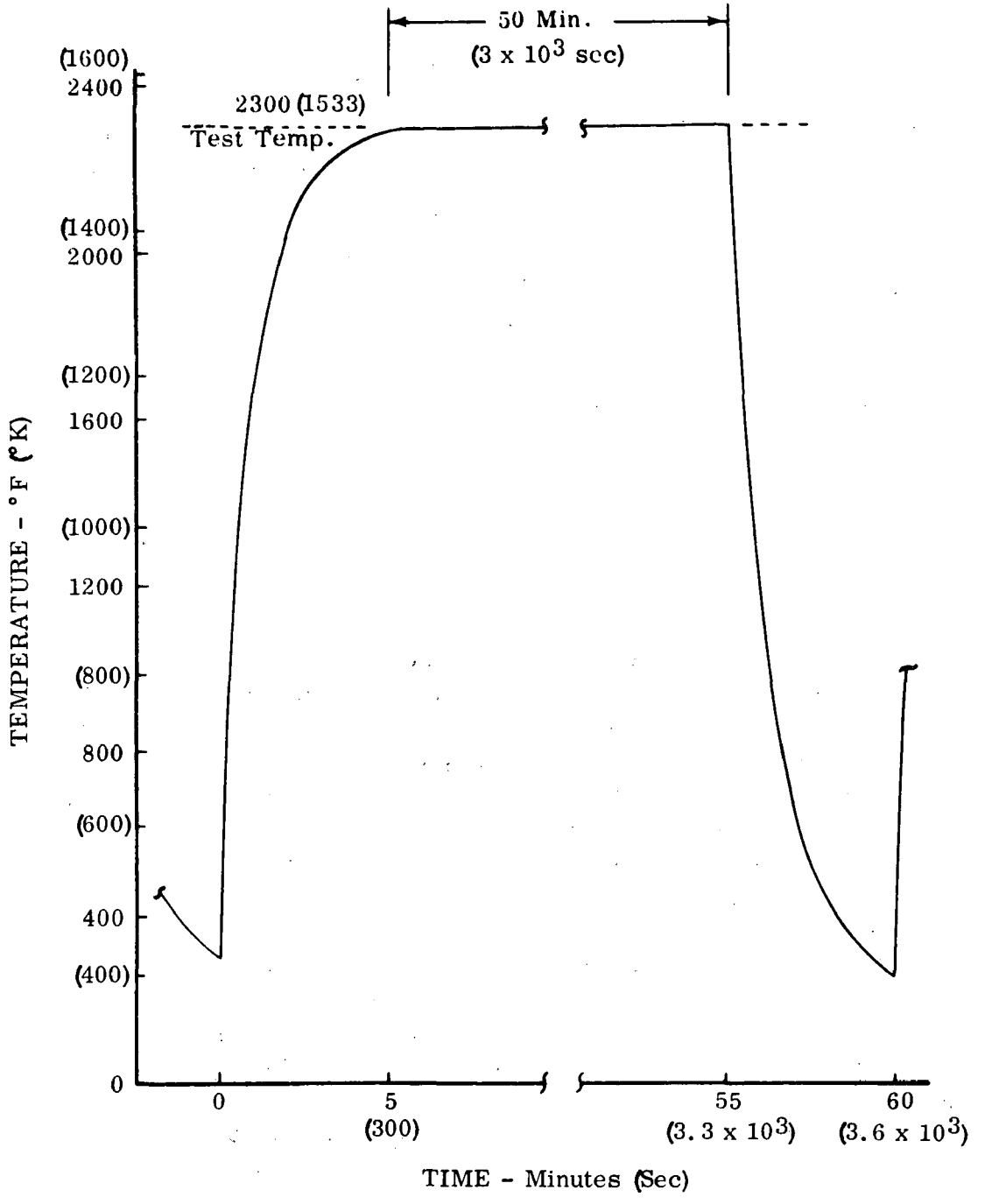

FIGURE 34. SPECIMEN TEMPERATURE VERSUS TIME CURVE DURING ONE OXIDATION CYCLE

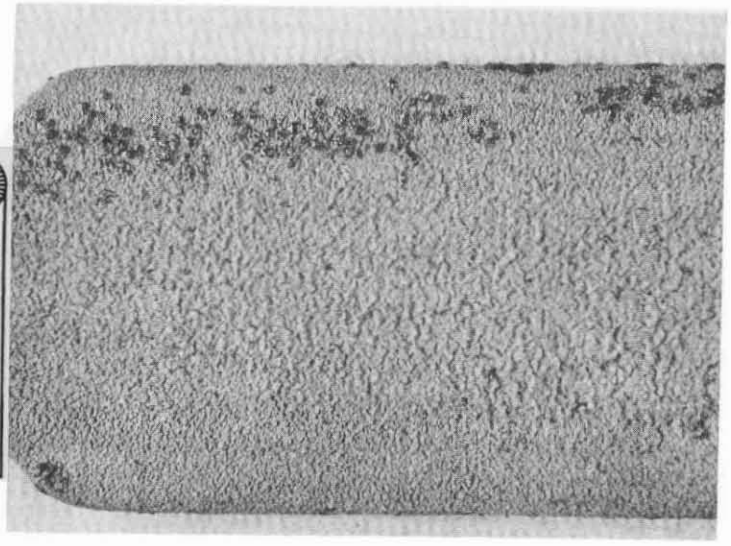

TD-Ni Specimen 28

The black oxide nodules were formed by substrate oxidation in areas of coating porosity.

Magnification: 3X

FIGURE 35. NiO FORMED ON COATED TD-Ni AFTER 3 HOURS AT 2300° F IN AIR

edges (see Fig. 37). Total coating failure had obviously not occurred on any of the specimens. Premature failure caused by defects in the coating appears to be the result of less than fully developed processing techniques. A defect not previously mentioned (one observed only after oxidation testing had begun) was the appearance of areas on the coating where liquation had apparently taken place. This was probably due to insufficient diffusion time and/or temperature which resulted in the presence of phases with melting points at or below the 2300° F (1533° K) test temperature.

The weight change curves in Figure 36 show that TD-Ni oxidizes rapidly at 2300° F (1533° K) but that TD-NiCr is extremely oxidation resistant and, in fact, is superior to the coated specimens. The question naturally arises as to why TD-NiCr should be coated. The answer lies in the fact that while TD-NiCr oxidizes very slowly in a static environment, its protective Cr_2O_3 scale is unstable in a dynamic environment such as that present in a jet engine (Ref. 14). The purpose for coating TD-NiCr, then, is to provide a protective scale such as Al_2O_3 which is much more resistant to combined oxidation-erosion conditions of a dynamic environment.

Metallographic examination of the oxidized specimens confirmed the tentative conclusions which had been based on visual examination of the exposed specimens, namely, that a good, protective coating remained in most areas on any given specimen. Figure 38 shows exposed specimens of both substrate alloys in typical areas on the flat surfaces. A 0.002 to 0.005-inch (5.0×10^{-5} to 1.2×10^{-4} m) coating protective layer remained, as well as at least part of the tungsten diffusion barrier. A very thin oxide scale was found on the coating surfaces. The oxidized surfaces were somewhat

TABLE X

SUMMARY OF OXIDATION TEST RESULTS

Alloy	Specimen No.	Length of Exposure* (cycles)	Weight Change (mg/cm^2)($10^{-2}kg/m^2$)	Observations
TD-Ni	25	30	-17	Edge failure
TD-Ni	27	30	-35	Failure on edges and in areas of porosity.
TD-Ni	28	3	+1.6	Failure on edges and in areas of porosity.
TD-Ni	31	3	+1.4	Failure on edges and in areas of porosity.
TD-Ni	34	3	-3.0	Failure on edges and in areas of porosity.
TD-Ni	35	3	+1.2	Failure on edges and in areas of porosity.
TD-Ni	36	3	-0.2	Failure on edges and in areas of porosity.
TD-Ni	51	3	-7.7	Failure on edges and in areas of porosity.
TD-Ni	17	3	+8.0	Failure on edges and in areas of porosity.
TD-Ni	19	3	-3.7	Failure on edges and in areas of porosity.
TD-Ni	22	3	+3.2	Failure on edges and in areas of porosity.
TD-Ni	23	3	-0.1	Failure on edges and in areas of porosity.
TD-Ni	39	3	-3.8	Failure on edges and in areas of porosity.
TD-Ni	42	3	-0.1	Failure on edges and in areas of porosity.
TD-Ni	43	3	-4.0	Edge failure plus apparent coating liquation.
TD-Ni	44	3	-9.9	Edge failure plus apparent coating liquation.
TD-Ni	47	30	+15	Uncoated; thick, partially spalled NiO.
TD-Ni	48	30	+23	Uncoated; thick black NiO.
TD-NiCr	C1	44	-6.3	Edge failure
TD-NiCr	C2	9	-9.6	Failure on edges and in areas of porosity.
TD-NiCr	C7	44	-3.0	Edge failure
TD-NiCr	C8	3	-1.5	Failure on edges and in areas of porosity.
TD-NiCr	C25	44	-14	Edge failure
TD-NiCr	C26	3	+0.3	Failure on edges and in areas of porosity.
TD-NiCr	C29	3	+0.7	Failure on edges and in areas of porosity.
TD-NiCr	C30	3	-4.1	Failure on edges and in areas of porosity.
TD-NiCr	C19	44	-21	Failure on edges and in areas of porosity.
TD-NiCr	C20	44	-8.7	Failure on edges and in areas of porosity.
TD-NiCr	C22	44	-43	Failure on edges and in areas of porosity.
TD-NiCr	C23	44	-53	Failure on edges and in areas of porosity.
TD-NiCr	C33	3	-1.5	Failure on edges and in areas of porosity.
TD-NiCr	C35	3	-2.8	Failure on edges and in areas of porosity.
TD-NiCr	C36	44	-16	Edge failure
TD-NiCr	C38	3	-2.3	Failure on edges and in areas of porosity.
TD-NiCr	C47	44	-0.2	Uncoated; adherent dark green oxide.
TD-NiCr	C48	44	-0.2	Uncoated; adherent dark green oxide.

*Oxidation Exposure: 1 Hour (3.6×10^3 seconds) cycles at 2300° F (1533° K) in air.

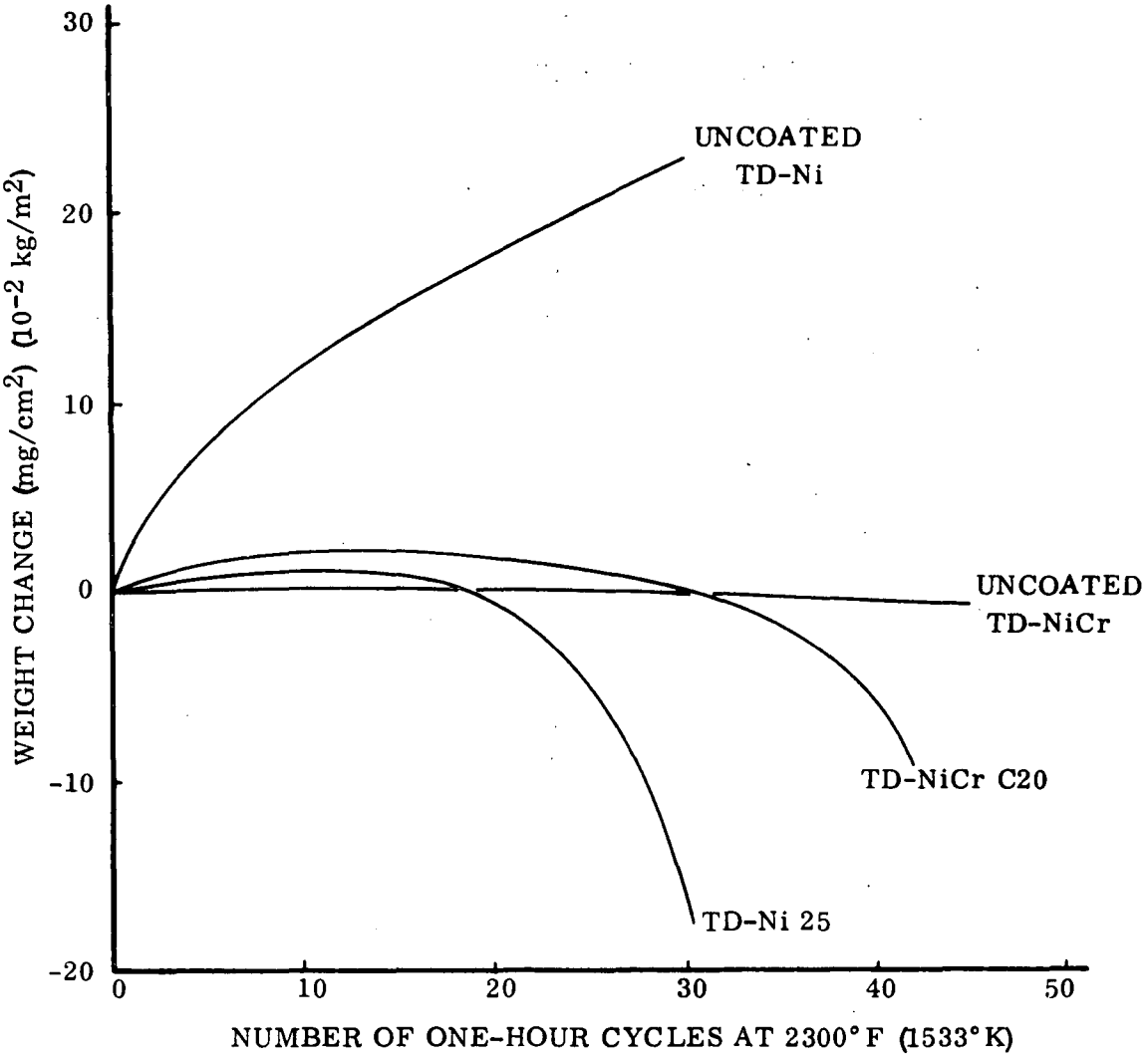

FIGURE 36. WEIGHT LOSS VERSUS EXPOSURE TIME FOR TD-Ni AND TD-NiCr TENSILE SPECIMENS

rougher than the as-coated surfaces, probably as a result of slightly preferential oxidation attack in some areas caused by a lack of compositional homogeneity. Very limited Kirkendall void formation was observed, certainly not sufficient to cause spalling of the coating. The surfaces of internal pores were found to be oxidized.

For comparison, Figure 39 shows uncoated TD-Ni and TD-NiCr after exposure. Metallographic examination confirmed what the weight change data had indicated, namely, that the TD-Ni had oxidized extensively (~0.008-inch (2.0×10^{-4} m) thick scale) while TD-NiCr had shown little attack, forming a thin (~1.5×10^{-4} inch (4×10^{-6} m) thick), adherent layer of dark green Cr_2O_3. It had been previously reported that at 2300° F (1533° K) TD-Ni forms a black outer layer and a light green inner layer of NiO (Ref. 1). However, only the black oxide was found on the uncoated TD-Ni specimens.

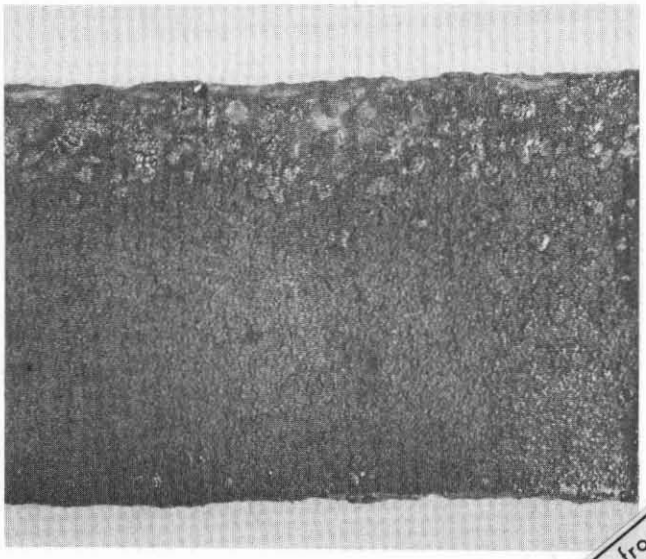

Edge and Adjacent Area Failure on TD-Ni Specimen 25

Exposure Time: 30 Hours

Magnification: 3X

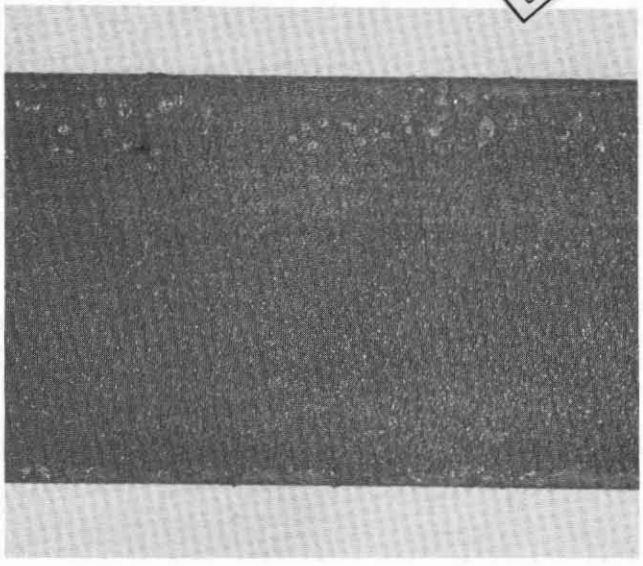

Edge Failure on TD-NiCr Specimen C1

Exposure Time: 44 Hours

FIGURE 37. TYPICAL COATING FAILURES ON TD-Ni AND TD-NiCr AFTER CYCLIC OXIDATION AT 2300° F

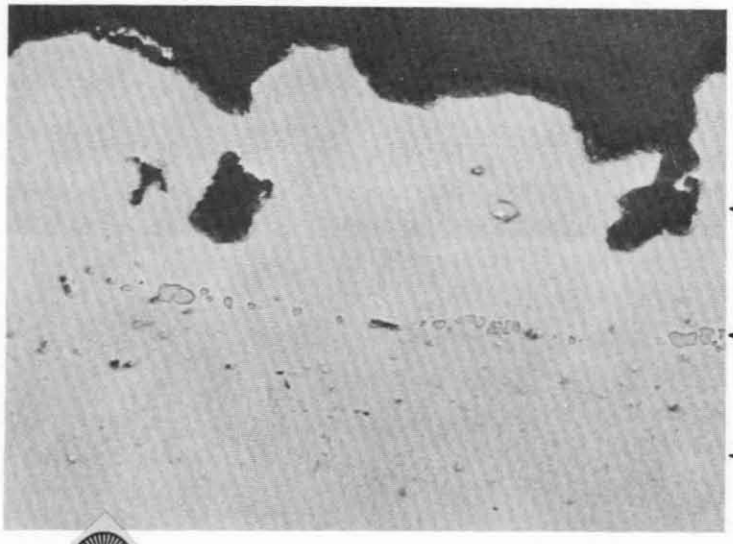

Flat Surface on TD-Ni (NC-15)
Specimen 25

Exposure Time: 30 Hours

←Coating - γ-Ni-Cr-Al Alloy
Unetched

←Remaining Slurry Tungsten Barrier

←TD-Ni Substrate

Magnification: 250X

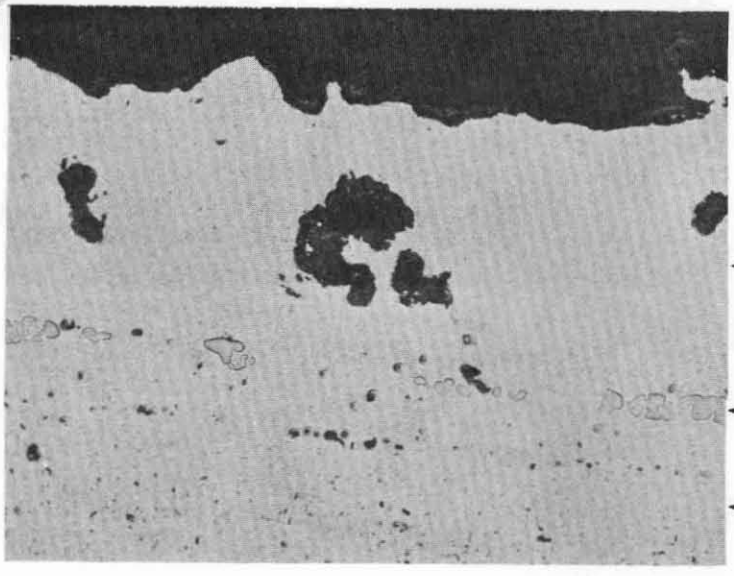

Flat Surface on TD-NiCr (NC-15)
Specimen C1

Exposure Time: 44 Hours

←Coating - γ-Ni-Cr-Al

Unetched

←Remaining Slurry Tungsten Barrier

←TD-NiCr Substrate

FIGURE 38. MICROSTRUCTURE OF COATINGS ON TD-Ni AND TD-NiCr AFTER CYCLIC OXIDATION AT 2300° F

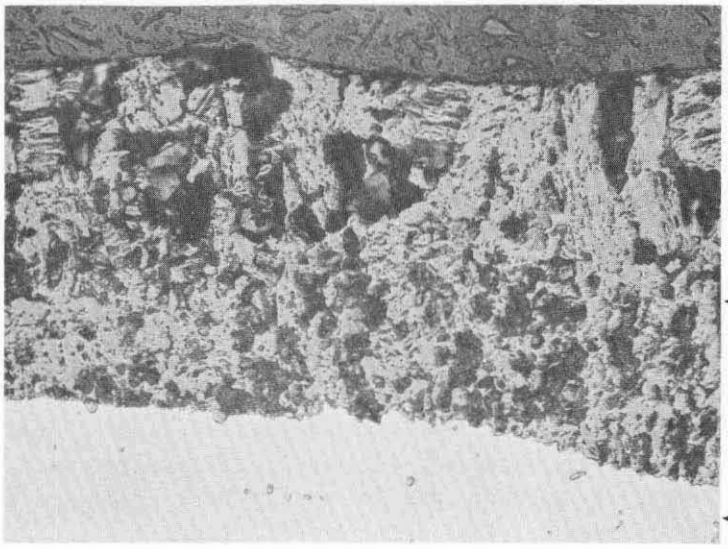

TD-Ni Specimen 47

Exposure Time: 30 Hours

Oxide Thickness: 0.008 Inch
Unetched

←NiO Scale

Magnification: 250X

←TD-Ni Substrate

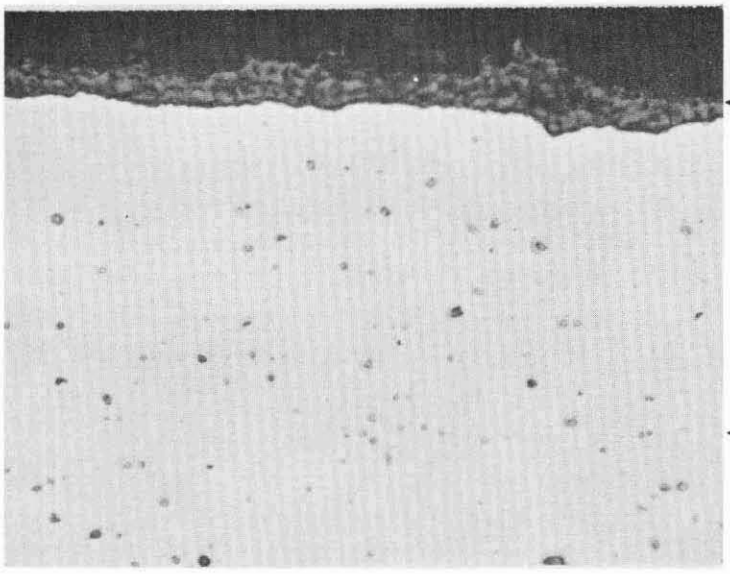

TD-NiCr Specimen C47

←Cr_2O_3 Scale

Exposure Time: 44 Hours

Oxide Thickness: 0.0002 Inch

Unetched

Magnification: 1000X

←TD-NiCr Substrate

FIGURE 39. SURFACE OF UNCOATED TD-Ni AND TD-NiCr AFTER CYCLIC OXIDATION AT 2300° F

Figures 40 and 41 show specimen areas of poor coating coverage after they were exposed. Figure 40 shows the edges on both alloys. Before exposure, the edges were coated with the tungsten diffusion barrier and a very small amount of aluminized modifier. No coating remained on the edges after oxidation. Instead, a 0.002 to 0.003-inch (5.0×10^{-5} to 7.5×10^{-5} m) thick NiO layer was observed on TD-Ni and a very thin Cr_2O_3 layer on TD-NiCr. This behavior was similar to the uncoated alloys, except that the thick inner NiO layer formed on the edges of coated TD-Ni was light green with a thin outer layer of black oxide, while only the black oxide was formed on the uncoated alloy. The presence of tungsten does not seem to have caused accelerated oxidation on either alloy. For example, Figure 41 shows an area on TD-Ni in which extensive coating porosity was probably present before testing. No coating remained in these areas and no evidence of spalling was found. Both points indicated that there had been little, if any, coating coverage in these areas. The lack of preferential lateral oxidation along the tungsten diffusion barrier in the immediately adjacent area showed that the tungsten barrier did not seriously degrade coating performance in damaged areas. The substrate degradation in the uncoated areas observed on both alloys appears to have been caused by internal oxidation which initiated in the stringers of tiny Kirkendall voids which were observed in the substrate running perpendicular to the surface. Figure 41 shows this void formation in a coating protected area on the same specimen but at high magnification. The depth of substrate disruption was greater for TD-Ni than for TD-NiCr, as was the depth of void formation. On both alloys the depth of oxide formation corresponded closely to the depth of void penetration.

Because of the nature of the coating failures, it is difficult to say with much certainty which coating composition was the best. Based on visual observation, weight loss measurements and metallography, the best performing coatings on both alloys had an approximate overall composition of (76 to 78)Ni-14Cr-(5 to 7)Al-3Si. The superior performance may have been due to composition; however it is more likely that the NC-15 modifier was more uniform and free of defects than the other modifiers. During the modifier firing cycle the final coating configuration is determined. The NC-15 modifier, with the lowest chromium content, sintered (with fusion) more uniformly than the other compositions.

Electron microprobe scans were made to determine the aluminum distribution on one exposed TD-Ni specimen (25) and two TD-NiCr specimens (C1 and C22). Figure 42 shows the actual and ideal aluminum distribution in unexposed specimens and the distribution in TD-NiCr specimen C1 after 44 exposure cycles. The curve shown for the exposed specimen was very close to the curves for the other specimens tested. The most notable result of the microprobe scans was the very small amount of aluminum remaining in solution in the coating after exposure. On TD-Ni, only 25 to 30 percent of the aluminum initially present was found after exposure, the remainder having been consumed by formation of the surface oxide scale. On TD-NiCr, the amount of aluminum remaining was even less, 15 to 20 percent. Additional aluminum had been

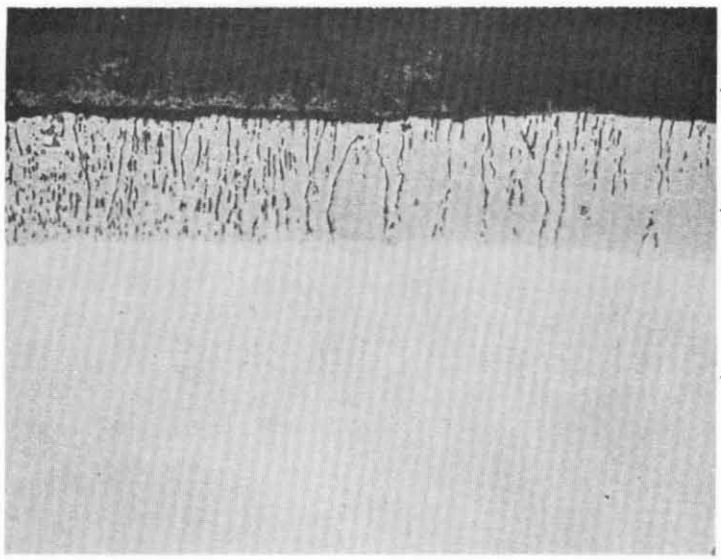

Edge on TD-Ni Specimen 25

←Outer (Black) NiO Layer

Exposure Time: 30 Hours

←Inner (Light Green) NiO Layer

Unetched

←TD-Ni Substrate

Magnification: 250X

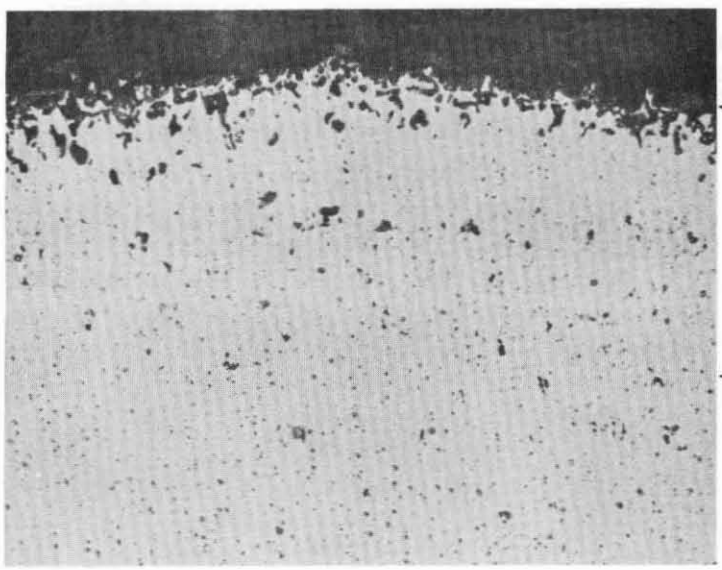

Edge on TD-NiCr Specimen C1

←Thin Cr_2O_3 Scale

Exposure Time: 44 Hours

Unetched

←TD-NiCr Substrate (with commonly observed Cr_2O_3 particles)

FIGURE 40. COATED TD-Ni AND TD-NiCr SPECIMEN EDGES AFTER CYCLIC OXIDATION AT 2300° F

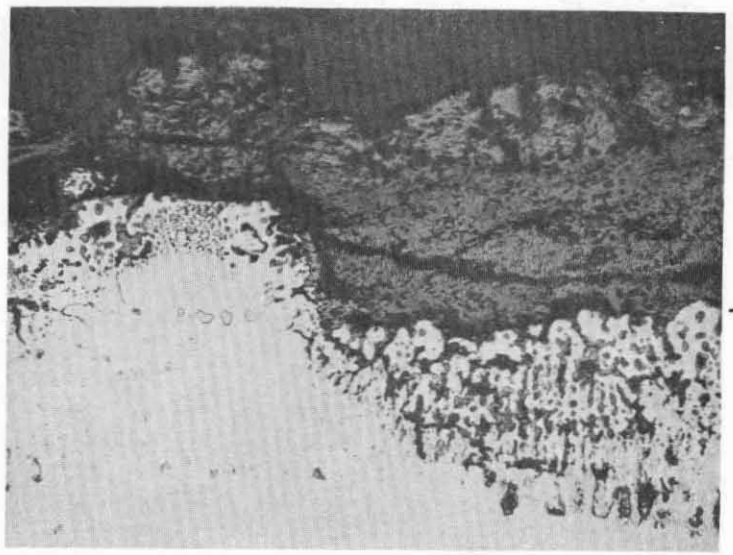

TD-Ni Specimen 25

NiO

Original Diffusion Barrier Location

Zone of Substrate Oxidation and Kirkendall Void Formation

Magnification: 250X

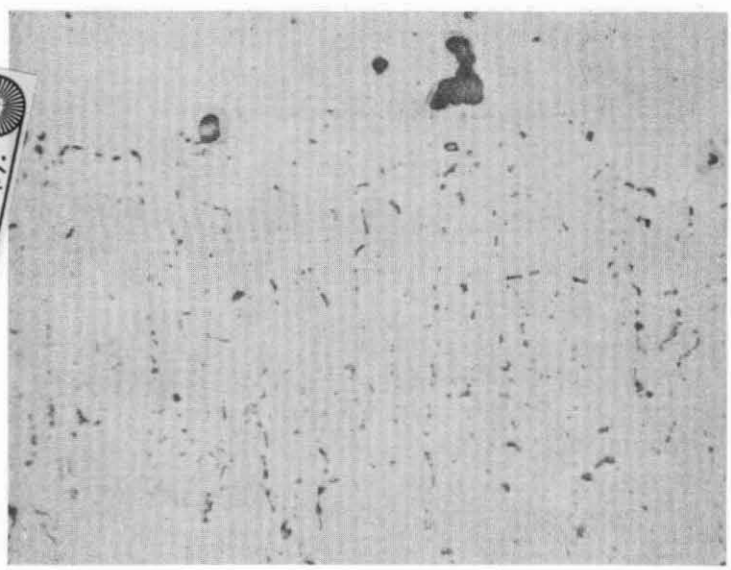

Zone of Kirkendall Void Formation in Coated Area on the Same Specimen

Unetched

Magnification: 1000X

FIGURE 41. SUBSTRATE OXIDATION IN KIRKENDALL VOID SITES IN UNPROTECTED AREA ON TD-Ni; After Cyclic Oxidation Exposure of 30 Hours at 2300° F

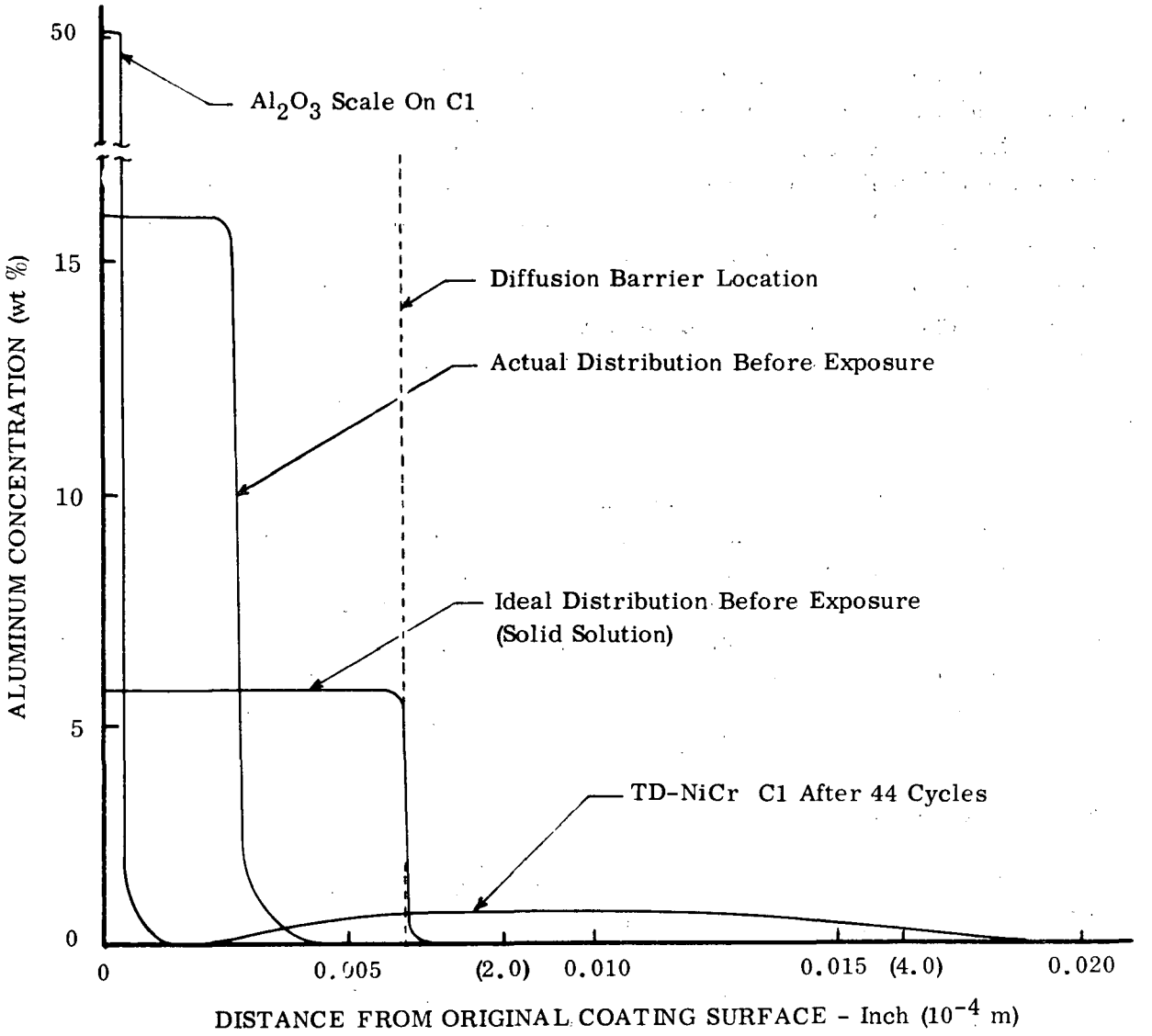

FIGURE 42. ALUMINUM DISTRIBUTION IN TD-NiCr BEFORE AND AFTER OXIDATION EXPOSURE

consumed in the reduction of substrate Cr_2O_3 particles to form Al_2O_3. The remaining aluminum would not be able to provide protection by Al_2O_3 formation for much longer and could not be expected to result in a coating life comparable to the oxidation lives of the Ni-Cr-Al alloys of similar composition tested by Hill, et al (Ref. 5). The reason for this discrepancy, particularly in light of the low aluminum losses by diffusion (less than 20 percent of the original aluminum), is not known. The presence of tungsten was not a factor; microprobe traces after exposure showed that the tungsten concentration at the coating surface was nil. It may be that inhomogeneities in the coating significantly increased the oxidation rate or promoted spalling of the oxide. Possible solutions to the problem are adjusting processing parameters or simply increasing the amount of aluminum initially deposited.

The effectiveness of the tungsten diffusion barrier during the oxidation exposure could not be determined with much certainty. The flat shape of the distribution curve at the diffusion barrier location, i.e., the lack of an aluminum concentration gradient, would at first glance seem to indicate a lack of barrier effectiveness. However, the shape of the curve in this region was determined by the oxidation process rather than by inward diffusion. Oxidation was the dominant factor in depleting aluminum from the coating, consuming it four times as fast as inward diffusion and thus obscuring the effect of the diffusion barrier. Judging by the presence of tungsten particles after oxidation exposure and the results of the previously run diffusion anneal (Figs. 16 and 17), the inward diffusion of aluminum was probably limited by the tungsten diffusion barrier.

To summarize the oxidation results, areas of porosity in the Ni-Cr-Al coating and thin edge coverage with this coating, defects caused by lack of fully developed processing techniques, caused premature failure of the coatings in cyclic exposure at 2300° F (1533° K). Furthermore, in areas with good coating coverage, the aluminum reservoir had been essentially depleted in less than 50 hours (1.8×10^5 sec) by surface oxidation. Less than 20 percent of the original aluminum had diffused into the substrate during exposure. The effort to prolong the potential of the coating to form Al_2O_3 was thus thwarted by the rapid consumption of aluminum by oxidation.

3.5.3 Tensile Tests

A total of 22 specimens were tensile tested, 11 at room temperature and 11 at 2000° F (1366° K) (5 TD-Ni, 6 TD-NiCr at each temperature). The tests were performed using an Instron model TTD screw type testing machine with a 20,000 pound maximum load capacity. At room temperature, a strain rate of 0.005 inch/inch/minute (8.3×10^{-5} m/m/sec) was used to the 0.2 percent offset, and 0.05 inch/inch/minute (8.3×10^{-4} m/m/sec) until specimen failure. At 2000° F (1366° K), a strain rate of 0.05 inch/inch/minute (8.3×10^{-4} m/m/sec) was used during the entire test. A 6-inch (0.15 m) high furnace with Pt-20Rh resistance wire was used for the elevated temperature tests. It was determined by measurements on a dummy specimen with thermocouples welded to the surface that, at the 2000° F (1366° K) mean test temperature, the top of the 1-inch (0.025 m) reduced section was 10° F (5.5° K) hotter than the bottom of the reduced section.

The tensile test results are presented in Table XI. To provide a common basis for comparison, the yield and ultimate strengths were calculated using the cross-sectional areas determined before coating and/or exposure. At room temperature, coated specimens of both alloys were less ductile than uncoated specimens, both before and after exposure. Coated TD-Ni was significantly stronger than uncoated TD-Ni after exposure because of the significant reduction in metal cross section of the uncoated material due to oxidation. The strength and ductility of TD-NiCr as-coated and after exposure did not vary greatly. At the 2000° F (1366° K) test temperature,

TABLE XI

SUMMARY OF TENSILE TEST RESULTS

Alloy	Specimen No.	Condition*	Test Temperature (°F)	Test Temperature (°K)	Yield Strength (ksi)	Yield Strength (N/m^2)	Tensile Strength (ksi)	Tensile Strength (N/m^2)	Elongation (%)
TD-Ni	18	Coated, no exposure	70	294	47	3.2×10^8	65	4.5×10^8	9
TD-Ni	29	Coated, no exposure	70	294	49	3.4×10^8	72	5.0×10^8	15
TD-Ni	49	Uncoated, no exposure	70	294	38	2.6×10^8	60	4.1×10^8	14
TD-Ni	25	Coated, 30-cycle exposure	70	294	41	2.8×10^8	72	5.0×10^8	10
TD-Ni	47	Uncoated, 30-cycle exposure	70	294	29	2.0×10^8	47	3.2×10^8	16
TD-Ni	20	Coated, no exposure	2000	1366	14.1	9.7×10^7	14.1	9.7×10^7	13
TD-Ni	30	Coated, no exposure	2000	1366	13.3	9.2×10^7	13.3	9.2×10^7	14
TD-Ni	50	Uncoated, no exposure	2000	1366	12.6	8.7×10^7	12.6	8.7×10^7	13
TD-Ni	27	Coated, 30-cycle exposure	2000	1366	13.7	9.4×10^7	13.7	9.4×10^7	10
TD-Ni	48	Uncoated, 30-cycle exposure	2000	1366	11.0	7.6×10^7	11.0	7.6×10^7	6
TD-NiCr	C3	Coated, no exposure	70	294	86	5.9×10^8	129	8.9×10^8	13
TD-NiCr	C18	Coated, no exposure	70	294	81	5.6×10^8	120	8.3×10^8	13
TD-NiCr	C49	Uncoated, no exposure	70	294	80	5.5×10^8	129	8.9×10^8	17
TD-NiCr	C1	Coated, 44-cycle exposure	70	294	80	5.5×10^8	126	8.7×10^8	13
TD-NiCr	C19	Coated, 44-cycle exposure	70	294	81	5.6×10^8	116	8.0×10^8	12
TD-NiCr	C47	Uncoated, 44-cycle exposure	70	294	78	5.4×10^8	120	8.3×10^8	18
TD-NiCr	C5	Coated, no exposure	2000	1366	17.7	1.22×10^8	17.7	1.22×10^8	4
TD-NiCr	C21	Coated, no exposure	2000	1366	17.8	1.23×10^8	17.8	1.23×10^8	5
TD-NiCr	C50	Uncoated, no exposure	2000	1366	16.9	1.16×10^8	16.9	1.16×10^8	4
TD-NiCr	C7	Coated, 44-cycle exposure	2000	1366	17.4	1.20×10^8	17.4	1.20×10^8	4
TD-NiCr	C20	Coated, 44-cycle exposure	2000	1366	17.8	1.23×10^8	17.8	1.22×10^8	5
TD-NiCr	C48	Uncoated, 44-cycle exposure	2000	1366	17.7	1.22×10^8	17.7	1.22×10^8	3

*Oxidation Exposure: 1-hour (3.6×10^3 seconds) cycles at 2300° F (1533° K) in air.

the only significant effect of coating or exposure on either alloy was the reduction in both strength and ductility of uncoated TD-Ni after exposure.

The principal effects of the coatings on the substrate alloys' tensile properties were thus to improve the strength of exposed TD-Ni and to reduce the room temperature ductility of both alloys. With elevated temperatures being the range of interest for the potential application of these alloys, the program coatings were judged to have had a beneficial effect on TD-Ni and no significant effect on TD-NiCr.

4

CONCLUSIONS

Several coatings, each consisting of a slurry tungsten diffusion barrier and a Ni-Cr-Al protective layer, were developed and evaluated for use on TD-Ni and TD-NiCr. The premature failure of the coatings in oxidation was caused by defects resulting from processing problems rather than by exhausting the protective ability of the coatings. Based on the experimental results obtained in the program, the following conclusions are made:

- The 2300° F (1533°K) cyclic oxidation life of the slurry applied Ni-(15 to 30)Cr-(5 to 8)Al-3Si coatings (applied over the tungsten barrier) was limited to 30 hours (1.1×10^5 sec) on TD-Ni and 44 hours (1.4×10^5 sec) on TD-NiCr by thin edge coverage and areas of porosity.

- Approximately 80 percent of the original aluminum in the coatings had been consumed by oxidation during the exposure described above. The coatings were thus less oxidation resistant than previously developed cladding alloys with similar compositions.

- The tungsten diffusion barrier, applied by slurry techniques and sintered in vacuum, showed the potential to effectively inhibit the diffusion of aluminum from Ni-Cr-Al coatings into the TD-Ni and TD-NiCr substrates.

- The slurry tungsten diffusion barrier did not appear to adversely affect the oxidation resistance of the coatings or cause accelerated substrate oxidation in areas where the barrier was exposed directly to an oxidizing atmosphere by an intentional defect through both coating and barrier.

- The coatings did not significantly degrade the tensile properties of the substrate alloys (compared to the uncoated alloys) either as coated or after exposure. In fact, the coated and exposed TD-Ni was significantly stronger than the uncoated and exposed TD-Ni. (All strength measurements were based on the original cross sectional area of the substrate.)

- The use of the Fe-Cr-Al coating compositions for protection of the TD alloys is not considered practical at present because of the extremely rapid Fe-Cr-Al clad/substrate interdiffusion which took place even with the use of the most effective diffusion barrier.

5

RECOMMENDATIONS

The premature failure of the coatings was caused by defects which resulted from processing problems rather than by exhausting the protective ability of the coating. In light of this result, and in view of the fact that the aluminum had been consumed so rapidly by oxidation, the following recommendations are made:

- Further development work on processing techniques should be performed, with the goal being to deposit a uniformly pore-free and homogeneous coating with adequate coverage on edges and corners.

- The use of higher aluminum levels, pre-alloyed Ni-Cr powders, and sintered modifiers (no fusion) are possible ways to achieve this goal.

- Assuming that the processing problems can be solved, tests which more closely simulate actual use conditions, e.g., oxidation-erosion "rig" tests, should be performed.

REFERENCES

1. Monson, L. A. and Pollack, W. I., "Development of Coatings for Protection of Dispersion Strengthened Nickel From Oxidation, Part I - Oxidation Studies, Coatings Development and Coating Analysis", E. I. duPont de Nemours & Co., Inc., Technical Report AFML-TR-66-47, Part I (March 1966).

2. Gadd, J. D., "Development of Cr-Al Coatings by Vacuum Pack Techniques", Thompson Ramo Wooldridge, Inc., Technical Report AFML-TR-66-47, Part II (March 1966).

3. Baker, F. R., et al, "Further Development of Coatings for Protection of Dispersion Strengthened Nickel From Oxidation", E. I. duPont de Nemours & Co., and Thompson Ramo Wooldridge, Inc., Technical Report AFML-TR-67-230 (August 1967).

4. Peck, J. V., Bublick, A. V., and Berkley, S. G., "Development of Production Manufacturing Techniques for Application of Protective Coatings to Thoria Dispersion Strengthened Alloys", TRW, Inc., and Pratt & Whitney Aircraft Division of United Aircraft Corp., Contract F33615-70-C-1084, Third Interim Report (August 1970).

5. Hill, U. L., Misra, S. K., and Wheaton, H. L., "Development of Ductile Claddings for Dispersion Strengthened Nickel-Base Alloys", IIT Research Institute, Sylvania Electric Products, Inc., Contract NAS3-10489 (December 1968).

6. Sama, L., et al, "Development of Ductile Claddings for TD-Nickel Turbine Vane Applications", Sylvania Electric Products, Inc., Contract NAS3-10489 (December 1968).

7. Walitt, A. L. and Bolger, J. C., "Development of Diffusion Bonded Ceramic Coatings", Amicon Corp., Technical Report AFML-TR-66-47, Part III (March 1966).

8. Grehila, R. B., et al, "Development and Evaluation of Controlled Viscosity Coatings for Superalloys", Westinghouse Research Laboratory, Contract NAS3-10486 (August 1969).

9. Moore, V.S., Brentnall, W.D., and Stetson, A.R., "Evaluation of Coatings for Cobalt- and Nickel-Base Superalloys", Solar Division of International Harvester, NASA CR-72714, Contract NAS3-9401 (July 1970).

10. Hansen, M., Constitution of Binary Alloys, McGraw-Hill, New York p. 380 (1958).

11. Brophy, J.M., et al, "Nickel-Activated Sintering of Tungsten", Powder Metallurgy, Ed. W. Leszynski, Interscience, New York (1961).

12. English, J.J., "Binary and Ternary Phase Diagrams of Columbium, Molybdenum, Tantalum, and Tungsten", Battelle Memorial Institute, DMIC Report No. 183 (February 1963).

13. Sutton, W.H. and Feingold, E., "Role of Interfacially Active Metals in the Apparent Adherence of Nickel to Sapphire", Materials Science Research, Vol. 3, pp. 577-611, Plenum, New York (1966).

14. Ohnysty, B. and Stetson, A.R., "Evaluation of Composite Materials for Gas Turbine Engines," AFML-TR-66-156, Part II (December 1967).

DISTRIBUTION

NASA Headquarters
600 Independence Avenue, S.W.
Washington, D.C. 20546
Attn: Mr. G. Deutsch (RW)
Mr. N. Rekos (RLC)
Mr. J. Gangler (RWM)
Mr. J. Maltz (RWM)

National Technical Information Service
Springfield, VA 22151 (40 copies)

NASA-Lewis Research Center
21000 Brookpark Road
Cleveland, OH 44135
Attn: Aeronautics Procurement Section (MS 77-3)
Technology Utilization Office (MS 3-19)
Library (MS 60-3) (2 copies)
Patent Counsel (MS 500-311)
Report Control Office (MS 5-5)
Technological Util. Off. (MS 3-19)
Mr. G. M. Ault (MS 3-13)
Mr. S. S. Manson (MS 49-1)
Mr. R. W. Hall (MS 105-1)
Mr. N. T. Saunders (MS 105-1)
Mr. J. C. Freche (MS 49-1)
Mr. S. J. Grisaffe (MS 49-1)
Mr. J. P. Merutka (MS 49-1)
Mr. R. L. Ashbrook (MS 49-1)
Mr. Jack B. Esgar (MS 60-4)

Library
NASA-Marshall Space Flight Center
Huntsville, AL 35812

Mr. J. R. Williamson
AFML/LTF
Headquarters
Wright-Patterson AFB, OH 45433

Mr. B. Stein, MS 206
NASA-Langley Research Center
Hampton, VA 23365

Dr. J. Buckley, MS 206
NASA-Langley Research Center
Hampton, VA 23365

Library
NASA-Ames Research Center
Moffett Field, CA 94035

Library
NASA-Goddard Space Flight Center
Greenbelt, MD 20771

Library
NASA Flight Research Center
P. O. Box 273
Edwards, CA 93523

Library
Jet Propulsion Laboratory
4800 Oak Grove Drive
Pasadena, CA 91102

Library
NASA-Langley Research Center
Langley Field, VA 23365

Library
NASA-Manned Space Flight Center
Houston, TX 77058

Mr. N. Geyer
AFML/LLP, Headquarters
Wright-Patterson AFB, OH 45433

Mr. A. E. Wright, SANEPJ
U. S. Air Force
San Antonio Air Materiel Area
Kelly AFB, TX 78241

DISTRIBUTION (Cont)

Mr. M. Levy
Army Materials Res. Agency
Watertown Arsenal
Watertown, MA 02172

Mr. I. Machlin, Code AIR-52031B
Department of the Navy
Naval Air Systems Command
Washington, D.C. 20360

Mr. P. Goodwin, AIR-5203
Naval Air Systems Command
Navy Department
Washington, D.C. 20360

Mr. H. Rosenthal, MRL
Metallurgy Research Lab
Frankfort Arsenal
Philadelphia PA 19137

Mr. Y. Telang
Ford Motor Company
2000 Rotunda Drive
P.O. Box 2053
Dearborn, MI 48123

Mr. L. P. Jahnke, Manager
Materials Dev. Lab. Oper.
General Electric Company
Cincinnati, OH 45215

Mr. M. Levinstein
General Electric Company
Materials Dev. Lab. Oper.
Adv. Engine & Tech. Dept.
Cincinnati, OH 45215

Mr. D. Hanink, Manager
Materials Laboratory
Allison Division
General Motors Corp.
Indianapolis, IN 46206

Mr. V. Hill
IIT Research Institute
Technology Center
Chicago, IL 60616

Mr. J. Wurst
University of Dayton Res. Inst.
Dayton, OH 45409

Dr. J. Berkowitz
Arthur D. Little, Inc.
20 Acorn Park
Cambridge, MA 02140

Mr. R. Perkins
Lockheed Palo Alto
Materials and Science Lab
3251 Hanover Street
Palo Alto, CA 94304

Reports Acquisition
Aerospace Corporation
P. O. Box 95085
Los Angeles, CA 90045

Supervisor, Materials Engineering
AiResearch Company
402 East 36th Street
Phoenix, AZ 85034

Mr. G. Cook
Alloy Surfaces, Inc.
100 S. Justison Street
Wilmington, DE 19899

Mr. W. H. Freeman
Lycoming Division
AVCO Manufacturing Company
505 South Main Street
Stratford, CT 06497

Mr. E. Bartlett
Battelle Memorial Institute
505 King Street
Columbus, OH 43201

Dr. R. I. Jaffee
Battelle Memorial Institute
505 King Street
Columbus, OH 43201

DISTRIBUTION (Cont)

Mr. M. Negrin
Chromalloy Corporation
169 Western Highway
West Nyack, NY 10994

DMIC
Battelle Memorial Institute
Columbus Laboratories
505 King Avenue
Columbus, OH 43201

Mr. H. E. Marsh, Manager
Information Services
Stellite Division
Cabot Corporation
1020 West Park Avenue
Kokomo, IN 46901

Mr. G. J. Wile
Polymet Corporation
11 West Sharon Road
Cincinnati, OH 45246

Mr. W. D. Lang
Kaman Sciences Corporation
Garden of the Gods Road
Colorado Springs, CO 80907

Mr. L. Sama
Sylvania Electric Products, Inc.
Chem. and Met. Division
Cantiague Road
Hicksville, NY 11802

Mr. Gene Wakefield
Texas Instruments, Inc.
M. and C. Division
P.O. Box 5474
Dallas, TX 75222

Dr. J. Gadd
TRW, Inc.
1400 N. Cameron Street
Harrisburg, PA 17105

Dr. E. Steigerwald T/M 3296
TRW Equipment
TRW, Inc.
23555 Euclid Avenue
Cleveland, OH 44117

Dr. W. Goward
Advanced Materials R&D Labs
Pratt & Whitney Aircraft
Middletown Plant
Middletown, CT 06158

Mr. E. F. Bradley
Pratt & Whitney Aircraft
United Aircraft Corporation
400 Main Street
East Hartford, CT 06108

Mr. D. Maxwell
Pratt & Whitney Aircraft
United Aircraft Corporation
West Palm Beach, FL 33402

Mr. D. Goldberg
Westinghouse Electric
Astronuclear Laboratory
Pittsburgh, PA 15236

Mr. R. Grekila
Westinghouse Electric
Research Laboratories
Beulah Road, Churchill Bur.
Pittsburgh, PA 15235

Mr. G. R. Sippel, Supervisor
Applied Materials Research
Materials Science Laboratory, W5
Allison Div. of General Motors
Indianapolis, IN 46206

Library
University of Dayton
Research Institute
300 College Park Avenue
Dayton, OH 45409

Prof. R. A. Rapp
Dept. of Metallurgical Engineering
Ohio State University
Columbus, OH 43210

Dr. J. Wert
Materials Engineering Dept.
Box 1621
Vanderbilt University
Nashville, TN 37203

Dr. J. Mueller
University of Washington
Ceramics Department
Seattle, WA 98101